THE EFFECT OF ACTIVE SCREEN PLASMA NITRIDING ON THE CELLULAR COMPATIBILITY OF POLYMERIC BIOMATERIALS

By

GEORGIA KAKLAMANI

A thesis submitted to The University of Birmingham

for the degree of

DOCTOR OF PHILOSOPHY

School of Metallurgy and Materials

College of Engineering and Physical Sciences

The University of Birmingham

February 2012

UNIVERSITY OF
BIRMINGHAM

University of Birmingham Research Archive

e-theses repository

This unpublished thesis/dissertation is copyright of the author and/or third parties. The intellectual property rights of the author or third parties in respect of this work are as defined by The Copyright Designs and Patents Act 1988 or as modified by any successor legislation.

Any use made of information contained in this thesis/dissertation must be in accordance with that legislation and must be properly acknowledged. Further distribution or reproduction in any format is prohibited without the permission of the copyright holder.

To the memory of my grandfathers

Miltiadi Kaklamani

Nikiforo Kallergi

Στη μνήμη των παππούδων μου

Μιλτιάδη Κακλαμάνη

Νικηφόρο Καλλέργη

ABSTRACT

Active Screen Plasma Nitriding (ASPN) is a novel surface engineering technique, the main advantage of which is the capacity to treat homogeneously all kind of materials surfaces of any shape. ASPN has been used mainly for hardening of metals. In this project ASPN, for the first time, is used to modify the surface properties of ionomer glasses and polymers in order to improve the surface cellular compatibility of these materials.

A conventional direct current (DC) nitriding unit (Klockner Ionan, 40 kW) has been used together with an active screen (AS) experimental arrangement. The materials that were treated were an ionomer glass (IG) of the composition $4.5SiO_2$-$3Al_2O_3$-$1.5P_2O_5$-3CaO-$2CaF_2$ of ca 0.3 cm thickness and an UHMWPE (M.W = 9.2 x 10^6 g/mol) sheet of 0.2 cm of thickness. The treatment was conducted for different time intervals, temperatures and gas mixture. The glass was treated for 1 hr at a temperature of 400^{o}C, for 60 mins using a gas mixture of 25% N_2/ 75% H_2. The UHMWPE samples were treated for 10, 30 and 60 mins, at 90^{o}C using two different gas mixtures, 25% N_2/ 75% H_2 and 80% N_2/ 20% H_2. After the treatment, all treated and untreated samples were seeded with the 3T3 fibroblasts cell line for 28 days.

In order to identify the nature of the film on the surface of all treated materials, chemical and mechanical properties characterisation was conducted. An additional decay study was carried out in order to examine the effectiveness of the surface modification in a period of 30 days, in different environmental conditions (Air, PBS and S-DMEM). FT-IR, XPS and Raman spectroscopy were used to examine the changes that the ASPN treatment caused on materials surface. Nanoindentation and interferometry were conducted to determine hardness, modulus and roughness, respectively. For the cellular samples, a qualitative study using SEM was

initially conducted in order to observe cells' behaviour on the untreated and plasma treated materials. MTT assays, Interferometry and AFM were also performed providing information about the approximate number of cells, the thickness of the biofilm formed, the topography of surfaces as well as the modulus of cells and cell adhesion forces.

The inert surface of the untreated glass showed good interaction with fibroblasts only after the ASPN treatment which resulted in enhanced fibroblasts attachment and proliferation. The treatment temperature, the length of treatment and the presence of nitrogen had an influence on the surface properties of glass. An increase in hardness, elastic modulus and surface roughness was observed. Raman spectroscopy showed that nitrogen containing groups were present on the glass surface evidenced by peaks observed in the range between 700 and 1300 cm^{-1}, associated with the presence of Si-N bonds. Finally, SEM was used for the observation of the cellular behaviour, which showed that fibroblasts did not attach themselves to the untreated glass surface while the treated glass surface attracted the cells, and their adhesion and proliferation was significantly enhanced.

UHMWPE (Ultra High Molecular Weight Polyethylene) that was treated in the gas mixture 25% N_2/ 75% H_2 showed an increase of hardness and elastic modulus. FTIR and XPS showed the formation of C-N and N-H groups resulting in an increase of the functionality of treated surfaces. Possible cross-linking on the surfaces might occur due to free radicals formed because of the plasma treatment at 120^{o}C and subsequent exposure of the treated surfaces in air as well as formation of chemical structures involving -C=C- structures. The roughness of the treated surfaces did not change significantly by the treatment. 3T3 fibroblasts cell culture studies showed that the ASPN treatment had a positive effect on the adhesion and proliferation of cells according to the time of treatment.

In the case of UHMWPE teated in the gas mixture 80% N_2/ 20% H_2 the mechanical properties such as hardness, modulus and surface roughness did not show any differences for untreated and plasma treated materials. SEM imaging of cellular samples showed that only the treated surfaces attracted cells and the treatment was beneficial for the cell attachment and proliferation. Different periods of cell seeding showed that at day 7 the metabolic activity was significantly increased compared to days 0, 14 and 28. AFM tests showed that the adhesion forces between the SiO_2 AFM cantilever tip and the surface of a fibroblast cell was higher in day 14 of the cell seeding period and reduced in day 28. Interferometry measurements showed that the thickness of the cells layer was larger in day 0 and smaller in day 28 which is consistent with some of the factors that often affect the number of cells on the materials surfaces during the experiment.

As a conclusion ASPN treatment can be a very effective method to modify inorganic and organic polymeric surfaces in order to improve cellular compatibility.

ACKNOWLEDGEMENTS

I would like to express my sincere thanks to my supervisor **Dr Artemis Stamboulis**, for helping and supporting me at any difficulty though the 3 years of my PhD study, being my mentor, advisor and friend. Without her excellent supervision, experience, suggestions and innovative ideas, this project would never reach completion.

I would also like to express my thanks to my co-supervisors **Dr Liam Grover** and **Prof Hanshan Dong** who gave their best to our collaboration and were present every time that I needed them.

A special thank to **Dr Nazia Mehrban** and **Dr James Bowen** for their significant contribution to my PhD work, for teaching, supervising and helping me to complete my research study.

I would also like to thank all my friends who shared my difficulties and my stress, who advised and helped me, each with a unique and different way.

Finally, inspiration, motivation and mentoring throughout all these years are attributed to my *Butterfly Effect* **Dr George Deligeorgis**. Many Thanks!

TABLE OF CONTENTS

LIST OF FIGURES

LIST OF TABLES

LIST OF ABBREVIATIONS

AC	Alternative current
AFM	Atomic force microscopy
ASPN	Active screen plasma nitriding
BG	Bioactive glasses
DC	Direct current
DCPN	Direct current plasma nitriding
DMEM	Dulbecco's modified eagle's medium
ECM	Extracellular matrix
FEP	Fluorinated ethylene propylene copolymer
FIB	Focused ion beam
Fn	Fibronectin
FTIR	Fourier transform infrared spectroscopy
GICs	Glass ionomer cement
HA	Hydroxyapatite
HDPE	High density poly (ethylene)
IG	Ionomer glass
LDPE	Low density poly (ethylene)
MTT	3-(4, 5-Dimethylthiazol-2-yl)-2,5-diphenyltetrazolium bromide
MW	Molecular weight
PBS	Phosphate buffered saline
PC	Poly carbonate
PCL	Poly (caprolactone)
PE	Poly (ethylene)
PEO	Poly (ethylene oxide)
PTFE	Poly (tetrafluorethylene)

PET	Poly (ethylene terephthalate)
PLA	Poly (lactic acid)
PLGA	Poly (lactic-co-glycolic acid
PP	Poly (propylene)
PS	Polystyrene
PSM	Plasma surface modification
PU	Polyurethane
SEM	Scanning electron microscopy
TCP	Tricalcium phosphate
UHMWE	Ultra high molecular weight poly (ethylene)
UV	Ultraviolet
Vn	Vitronectin
XPS	X-Ray photoelectron spectroscopy
XRD	X-Ray diffraction

CHAPTER 1 INTRODUCTION

1.1 Surface modification of biomaterials

Surface modification is very often required to alter the surface characteristics of all kind of materials. The scope of the materials surface modification is to change the surface properties while maintaining the bulk properties of the material. In the literature so far, various methods have been proposed to modify the surface of metals, polymers and glasses in order to achieve the desirable surface characteristics. Plasma immersion ion implantation (PIII) and high power lasers have been used to change the surface characteristics of metals and metal alloys [1, 2]. Oerh *et al.* and Hoffman *et al.* suggest techniques such as plasma, radio frequency gas discharge, UV radiation, laser ablation and microlithography to change the surface characteristics of polymers [3, 4]. Finally, Theppakuttai *et al.* used pulsed laser to modify glass surface [5]. The same concept applies to biomaterials. Biomaterials surface characteristics often need to be changed in order to exhibit rapid and precise interaction with cells and proteins in a biological environment while their bulk properties must be maintained the same [6].

In the past 30 years the interest in biomaterials has led to the development of a great number of different types of materials such as hydrogels, biosensors and piezoelectric biomaterials for use in various biomedical applications (implants, surgery, diagnostics) with the requirement that they must be biocompatible in the physiological environment [7, 8]. In tissue engineering the main interest focuses on the use of biomaterials in order to promote new tissue formation *in vitro* or *in vivo* [9]. According to Hench *et al*. the materials surface chemistry is very important and should meet the requirements of the new tissue. Generally,

apart from the biocompatibility and bioactivity, the ideal implant replacing the host tissue should satisfy the requirements set by the host tissue, there must be an interfacial bond between the material and the tissue, the tissue at the interface should be equivalent to the host tissue and the implant response to different stimuli should be similar to the response of the replaced tissue [10]. The bulk properties eg: mechanical properties of a biomaterial, determine its biological performance; however, the biological response to a biomaterial is determined by its surface properties [11]. Therefore, surface modification is very often required in order to enhance the surface characteristics of materials, and improve their properties in clinical applications. It is important to design and modify materials with optimized surface properties because their biological response and cellular events at the cell-material interface are controlled by their surface chemistry and structure [12]. Surface topography, chemistry and mechanics are the three most important parameters that affect the cell shape and consequently the cells ultimate behaviour. Thus the initial cellular events such as attachment and growth are affected within the first few minutes of the co-existence of cells and materials [13].

The surface modification of biomaterials has been classified in to two groups. The first one has to do with the modification of the already existing surface and the second with covering this surface with a material which has a different composition. Modification of the already existing surface can be achieved with methods such as ion beam etching, ion beam implantation, plasma, ion exchange and UV irradiation. On the other hand, covering the surface can be achieved with non-covalent (e.g. solvent coating, surface active additives, vapour deposition) or covalent coatings (e.g. radiation grafting, plasma, gas deposition, chemical grafting) [14].

The surface characteristics of a biomaterial that need to be changed are dependent on the use of the material and the biological components that will come in contact with. Generally, the most common surface properties to be considered for materials used in biomedical applications are: corrosion properties, surface roughness and morphology, surface crystallinity, wear and friction, surface reactivity, surface free energy, adhesion and adsorption [15].

According to Ratner [14] surface is the part of the materials where the composition and structure differs from the bulk of the material, but the depth of its extension is not always clear. Surface modifications in order to be successful, should fulfil some general requirements. First of all, they should be thin (a few nm). If the depth of the modification is too thick, it may affect the bulk properties of the material such as the mechanical properties. Ideally, a few nm (10-100 nm) are sufficient for the alteration of a surface. Furthermore, modified biomaterials should resist to failure (e.g. rejection from the body) when they come in contact with aqueous environments or protein solutions. One way to achieve such surfaces is to incorporate functional groups that create strong intermolecular adhesion. Moreover, surface chemical stability and precision of the surface functional groups (specific reactions) should be considered as parameters to be controlled, as well as uniformity of the treatment of materials with different shapes and geometries [14-16].

1.1.1 Plasma surface modification

Biomaterials surface modification can be processed by various techniques. Plasma techniques represent a unique way to modify the surface properties of materials used in medicine and biology [17]. Generally, plasma methods in the biomaterials field were introduced in 1960's, and since then are applied to biomaterials and biomedical devices. This is due to the fact that

plasma-modified materials have been proved to have different surface properties compared to the untreated and, therefore, respond better when they come in contact with a biological environment thus they offer possibilities for improving the functionality of already existing materials and devices [18].

Plasma surface modification (PSM) is an effective, quick and economical technique for surface treatment [19]. Some of the most common plasma techniques are: plasma sputtering and etching, plasma deposition, plasma polymerization, plasma implantation and plasma spraying [12]. Various properties of a materials surface can be improved using plasma. Some of them are: wettability, refractive index, chemical inertness, dyeability, hardness, lubricity and biocompatibility [20].

Plasma is a reactive chemical environment in which many plasma-surface reactions occur [12]. This environment contains positive and negative ions, free radicals, electrons, atoms, molecules and protons [18]. The plasma process involves glow discharge plasma which is created by evacuating a quartz vessel which is refilled with a low-pressure gas that can be energized with the use of AC (alternative current), microwaves, radio-frequency energy or DC (direct current). The particles (ions, electrons, atoms) in the gas plasma bombard the material surface transferring their energy to the surface. Other processes are possible to occur in order to modify a surface such as ablation and etching. These processes can cause chemical and morphological changes of the surface, such as the insertion of new functional groups or changes on the surface roughness [21].

Plasma surface modification techniques offer unique advantages compared to other surface modification methods (e.g. laser irradiation, etching, UV radiation). First of all, the treatment can change the very upper surface characteristics starting from a few nanometres to ~10 μm without affecting the bulk properties of the material [22]. Plasma treatment allows treatment

of all free surfaces of objects of any shape that are placed inside the plasma chamber. Another important parameter that can be selectively controlled is the surface chemistry of the materials to be treated. A variety of chemical structures can be provided to the surface [23]. For example, oxygen plasma can provide hydroxyl, carbonyl, carboxyl, ether, ester and carbonate moieties [24], whereas nitrous plasma provides ester, carboxyl, carbonyl, hydroxyl, ether, amide, cyano, urethane and amine moieties. Nitrogen plasma provides amide, amine, and urethane and can incorporate oxygen when the material is exposed to atmosphere [25, 26].

Plasma techniques have been developed in order to enhance specific surface characteristics for biomaterials dependent on their use. Adhesion improvement for example is one of them. The use of plasma techniques helps the creation of functional groups and active sides on the materials surface resulting in improvement of interfacial adhesion e.g. adhesion between Polycarbonate (PC) and SiO_2 has been shown to be improved when PC is plasma treated using O_2 plasma [27]. Plasma surface modification is also used to change the surface energy. The interaction of materials surface with a plasma gas can change the hydrophilic or hydrophobic nature of a surface. Especially the use of oxygen plasma is responsible for the induction of hydroxyl groups increasing the wettability of the treated surface [28]. Biocompatibility can be a result of a successfully plasma treated surface [19]. When biomaterials come in contact with an aqueous environment containing proteins they need to have special surface characteristics in order to attract the appropriate biomolecules. For example, the existence of amine groups on a biomaterials surface can attract heparin and consequently decrease thrombogenicity [29], or the increase of hydrophilicity on a materials surface can attract fibronectin easier [30] Furthermore, during plasma treatment it has been reported that surface crosslinking occurs resulting in hardening and chemical resistance of the surface. Sheu *et al.* reported the crosslinking of low density polyethylene surface by argon

plasma [31]; similar results have also been reported by France *et al.* who used the same gas to induce carbon-oxygen functionalities onto low density poly(ethylene) (LDPE), poly(propylene) (PP) and poly(ethylene terephthalate (PET) surfaces [32].

1.1.2 Active screen plasma nitriding

Nitriding is a surface engineering method used to introduce nitrogen into a surface, in order to improve the surface microhardness, wear and corrosion resistance, microstructure and morphologies of metals such as stainless steel, chromium and titanium [33-36]. Various techniques have been used in nitriding. One of them is gas nitriding where liquid salts containing cyanide and cyanate are used to nitride the surface of metals, these methods result in environmental hazard, problems on the working conditions and also difficulties to control the nitride layer created onto the materials surface [37]. Another method that has been used for nitriding is gas nitriding using ammonia to provide the surface with active species; however this method also creates problems during the treatment with the pollutants emission, difficulties in processing and controlling the nitride layer [38]. Consequently, plasma nitriding is considered a better nitriding method in terms of reduction of gas and energy consumption, the non-emission of pollutants and minimizing the time of treatment. The DCPN (DC plasma nitriding) technique is one of the oldest surface engineering processes, and has been widely used in industry for more than 30 years [39]. This advanced surface modification technology is mainly used to improve physical characteristics of metallic surfaces e.g. steels such as increasing fatigue strength, surface hardness, corrosion and wear resistance [40-42]. More specifically, plasma nitriding has been proved one of the most efficient methods for increasing surface micro hardness, modulus, fatigue strength, wear resistance and protects the materials surface from corrosion. Karakan *et al* have treated the

surface of AISI 5140 steel using plasma nitriding with different gas mixtures of hydrogen, nitrogen and argon. Their results showed that the most effective gas mixture for the increase in materials hardness was 10% N_2 + 90% H_2 [152] Previous work by Li and *et al* showed the ASPN effect on the mechanical properties of different metals. Materials such as low alloy steel (722M24) and austenitic stainless steel (AISI316) were treated with the active screen plasma nitriding technique. After micro hardness tests and hardness profile measurements it was concluded that the compound layer produced on the materials surface led to the increase of hardness and elastic modulus. Moreover, wear and corrosion resistance were found to be improved after the treatment [38, 43].

Despite the fact that the conventional DC plasma technique has been proved efficient to treat simple shapes and small loads, it is associated with many difficulties during the treatment [43] such as difficulties in maintaining a uniform chamber temperature, especially in full work loads of components with different shapes and geometries. Also, damage can be caused to the samples by arcing, edging effect (non uniform appearance of samples) and hollow cathode effect (strong ionization produced by fast electrons in the cathode) due to unstable plasma or overheating of the samples [38-39, 41-42, 44]. Moreover, in DC plasma nitriding technique the materials to be treated are subjected to a high cathodic potential. This means that the plasma heats directly the samples surface in order to provide the nitride species but due to distortions of the electric field around the materials the ion flux distribution is unstable affecting the uniformity, the surface phases of coating and the hardness of the materials [40].

To overcome the problems mentioned above, many efforts have been made in the recent years. The solution to these problems is Active Screen Plasma Nitriding (ASPN) that was invented and patented in 1999 by Georges [45]. ASPN is a novel method to modify the surface of different kind of materials, the main advantage of which is the capacity to

homogeneously treat surfaces of any morphology [45]. In ASPN technique, the entire workload is enclosed by a large metal screen or cage (Active Screen) as shown in Figure. 1.1. A high voltage cathodic potential is applied to the screen (instead of the components) and the worktable together with the materials to be treated are allowed to float (voltage at which the probe collects no current) or subjected to a small negative bias voltage (-100 ~ -200 V) resulting in insulation of the worktable and the components to be treated from the cathodic screen and the anodic chamber walls. Hence, the plasma forms on the Active Screen rather on the components surface. The plasma heats up the screen and radiation from the heated screen pass through and is provided to the components. Then the components are heated and come to the required temperature for the treatment. Also, the plasma that is formed on the screen contains a mixture of ions, electrons and active nitriding species, which pass through the screen and the materials surface via a specially designed gas flow. Thus, the screen plays two roles; to heat up the materials to the required temperature and to provide their surface with active nitriding species [46]. Since the plasma is not formed directly to the components surface, uniform nitride layers can be produced on the materials surface, the arcing damage and the edging effect can be eliminated and complex shapes of different geometries can be homogeneously treated [47-49]. Moreover, the ASPN is less sensitive to contaminations, since the active species generation can be controlled as the electric parameters of the screen and the worktable can be set separately [50]. Finally, the materials are subjected to a floating potential, resulting in no sputtering on the surface [51-52].

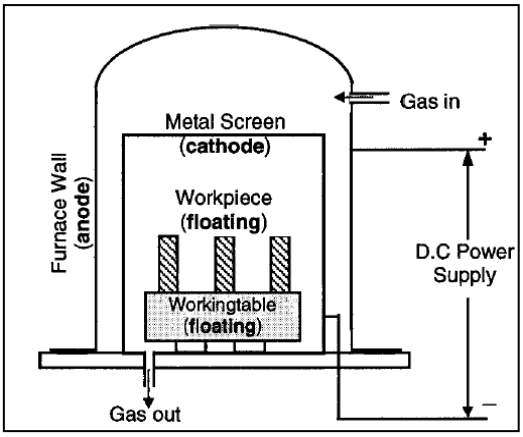

Figure 1.1: Schematic diagram of Active Screen Plasma Nitriding surface modification method [39].

1.1.3 Plasma Surface modification of polymers

Polymers are materials widely used for industrial and medical applications. This is due to their excellent physical and chemical properties, their mechanical characteristics, light weight, easy formation/shaping and inert behaviour in a biological environment. Moreover, they can be easily processed because of their design possibilities and compared to other materials their cost is relatively low [53]. However, despite the fact that polymers offer excellent bulk properties, most of the times the selected polymers have surface characteristics that are not optimal for a specific application, and here the surface modification is required [54].

The purpose of modifying the surface of polymers is the introduction of new functional groups on polymer surfaces. The methods used generally to modify the surface of polymers include roughening, oxidation, coating, blending and ion implantation [55]. More specifically the techniques used for the introduction of polar groups on the polymeric surfaces include plasma treatments, particle beam irradiation, corona discharge treatment, exposure to energy radiation and wet chemical treatments [56-61].

The surface characteristics of polymers that often need to be changed include: surface wettability, adhesive bonding, surface hardness, wear resistance, electrical and optical properties, friction, and scratch resistance [62]. Concerning polymers used for biomedical applications, biointeraction, biocompatibility, biorecognisability and biofunctionality are some of very important characteristics that can be achieved by surface modification [12].

Plasma surface modification of polymers can result in the increase of the surface roughness [63], the formation of new functional groups (e.g. $–NH_2$, -OH, -COOH) depending on the gas used [64] and enhancement of the surface hardness due to cross linking occurring on the surface of polymeric materials [65]. When polymeric surfaces are subjected to plasma treatment, the modification of the surface occurs during the exposure of the material to the plasma; however, post-plasma reactions may occur. For example, free radicals that are still active after the plasma treatment may result in oxidation reactions or post plasma functionalization after the exposure to air, showing that plasma affects are not permanent and lead to aging processes [66]. The type of surface changes due to plasma treatment depends highly on the treatment conditions. For example: the gas composition, temperature, duration of treatment, type of ions present, electrons and radicals present in the plasma chamber are some important factors [67].

Surface modification of polymers has been extensively applied for various applications. For example oxygen and argon plasmas have been used to improve the wettability of polystyrene and polyethylene [68] whereas argon plasma has been used in the surface modification of polysulfone films in order to improve specific enzyme immobilization due to the introduction of oxygen-bearing functional groups onto the polymers surface, these functionalities served as anchoring-sites for immobilization of enzymes [69]. On the other hand, polycaprolactone films have been treated with ion beam in order to enhance protein adsorption on the polymer

surface [70] and a silicon elastomer was treated by microwave plasma surface modification in order to improve its biocompatibility [71].

A polymer widely used in biomedical applications is UHMWPE. UHMWPE is a linear homopolymer, formed from ethylene (C_2H_4) and its general formula is -$(C_2H_4)_n$-. The chemical structure of UHMWPE is shown in Figure 1.2 and some of the physical and mechanical properties are shown in Table.1.1. UHMWPE is a unique polymer due to its very good mechanical and physical properties, such as chemical inertness, lubricity, impact resistance and abrasion resistance. The main difference between UHMWPE and HDPE (High Density Polyethylene) and LDPE (Low Density Polyethylene) is that UHMWPE has significantly higher abrasion and wear resistance which make it more suitable for biomedical applications.

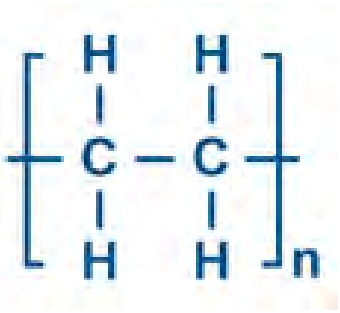

Figure 1.2: Chemical structure of UHMWPE.

Table 1.1: Physical and mechanical properties of UHMWPE [72].

Property	**UHMWPE**
Molecular Weight	2-6 x 10^6 g/mol
Glass Transition Temperature	-160 ^oC
Melting Temperature	125-138 ^oC
Tensile modulus of elasticity	0.8-1.6 GPa
Tensile yield strength	21-28 MPa
Tensile ultimate strength	39-48 MPa
Degree of crystallinity	39-75 %

In order for UHMWPE to be used in biomedical applications, a three-step procedure takes place. First, UHMWPE is polymerized from ethylene gas, second in the form of resin powder is it consolidated in shapes such as rods or sheet and finally it is machined in to the desired for the implant shape. UHMWPE is mainly used for total joint replacement prostheses as an acetabular cup (Figure 1.3) [72].

One of the major problems concerning UHMWPE used in hip implantation is the wear of the polymer and consequently its wear debris which can cause osteolysis and finally failure of the implant [73]. Thus, improvement of wear resistance and the volume of wear debris as well as the polymers surface mechanical properties is a challenging task indicating that surface modification of UHMWPE is required [74].

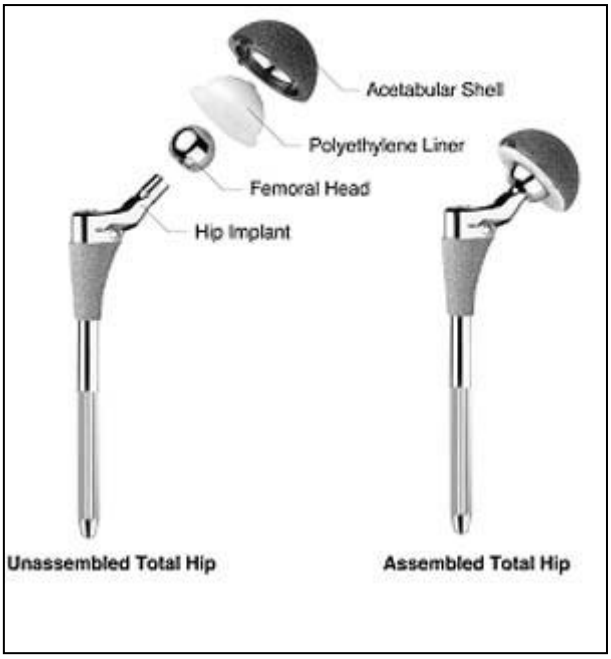

Figure 1.3: Hip replacement implant.

Studies on UHMWPE surface modification with plasma methods show an improvement of the polymer surface properties. Li *et al*. treated UHMWPE with the ASPN technique. They used a medical grade UHMWPE of MW= $3.6x10^6$ and the treatment was carried out in a gas mixture of 25% N_2 and 75% H_2, at 400Pa for 5 hours and for two different temperatures (100^{o}C and 120 ^{o}C). The treatment resulted in improvement of the materials mechanical properties such as, hardness and elastic modulus. The hardness was increased from 42 MPa (untreated material) to 70 MPa for the material treated at 100 ^{o}C and to 84 MPa for the material treated at 120 ^{o}C. Similar results were obtained from the measurement of elastic modulus, it was increased from 90 MPa (untreated UHMWPE) to 160 MPa (100 ^{o}C treated UHMWPE) and 168 MPa (100 ^{o}C treated UHMWPE); also it was found that the nitrided material exhibited higher wear resistance compared to the untreated [75]. Nitrogen plasma-based ion implantation has also been employed to modify UHMWPE surface, resulting in changes on the surface chemistry of the material, the chain structure was damaged due to the

ion bombardment and a layer of hydrogenated amorphous carbon was formed on the surface, also XPS measurements showed that nitrogen ions implanted on the surface formed new chemical bonds with the polymer [76]. Shi *et al*. used different dosages of nitrogen to modify the polymers surface. They used the plasma immersion ion implantation technique (PIII) and the treatment parameters were V = 20kV, voltage pulse repetition rate = 100Hz, the pulse length = 60μs and the different nitrogen ion dosages were $1x10^{17}$, $2\ x10^{17}$ and $3\ x10^{17}$ N^+ ions/cm^2. The experimental results showed that UHMWPE's hardness increased from 50 MPa to 110 MPa and the elastic modulus from 782 MPa to 1435 MPa for the highest ion dose treated polymer, also the improvements of the surface's mechanical properties are proportional to the ion dose [73].

In conclusion, polymer modified surfaces by plasma or ion beam surface modification techniques, offer enhanced surface properties, which make the polymer surfaces more effective and appropriate for biomedical applications.

1.1.4 Surface modification of ionomer glasses

Ceramics, glasses and glass-ceramics are inorganic non-metallic compositions. The basic components of these materials are SiO_2, Na_2O, CaO and P_2O_5. They are widely used in the biomedical industry, for example, insoluble porous glasses as carriers for enzymes and antigens [77]. The use of these materials in such applications has many advantages having to do with resistance to microbial attack, pH changes, solvent conditions and temperature [77]. A 3rd generation biomaterial that belongs in this category is Bioglass. Bioglass has been used in clinical applications since 1985 for tissue regeneration and repair due to its gene activation properties [78].

In dentistry, ionomer glasses are used as the glass component in glass ionomer cement systems. Recent developments in ionomer glasses led to glass compositions that offer radiopacity, translucency, controlled setting reaction of glass ionomer cements and release of therapeutic ions such as fluorine and strontium [79-80]. The microstructure and crystallization of ionomer glass compositions has been extensively studied by advanced techniques such as MAS-NMR spectroscopy, X-ray diffraction and real time neutron diffraction and scattering [81- 82] The glass composition $4.5SiO_2$-$3Al_2O_3$-$1.5P_2O_5$-3CaO-$2CaF_2$ crystallises into an apatite and mullite phase at two different crystallization temperatures. Real time neutron diffraction and scattering showed that apatite crystallizes first, at the first crystallization temperature followed by mullite and apatite at the second crystallization temperature. It was reported, that the glass undergoes spinodal decomposition prior to amorphous phase separation evidenced also by the presence of two different glass transition temperatures. Apatite nano-crystallisation was observed and the glass appeared clear [83-85]. Freeman *et al.* reported an animal study implanting amorphous and crystalline glasses of a similar composition in the femur of a rat and showed that only the crystalline glass with a high fraction of apatite phase and the apatite stoichiometric glass ceramic were able to show a good bone response. This indicated, that a crystalline surface containing a large proportion of fluorapatite is more likely to favour bone bonding. It was clear, however, that the amorphous glass did not interact with the bone tissue and the glass was classified as completely inert [86].

So far plasma surface modification without the addition of coatings on the ionomer glass surface has not been reported. However, other methods for surface modification of glasses and ceramics have been used. Qin *et al*. have treated simple glass cover slides with two methods (silanization and hydrophobin coating) and manage to achieve protein immobilization [87]. Also, helical coupling plasma has been used for the surface modification

of glass fiber/polyester composite systems to improve shear strength of the composite material [88].

In this study the composition of ionomer glass used was $4.5SiO_2$-$3Al_2O_3$-$1.5P_2O_5$-3CaO-$2CaF_2$. This glass composition has been previously extensively studied [80-81, 84]. This type of glasses has been used as the glass component in two component glass ionomer cements in dentistry. The glass was designed so that all aluminium in the glass network remains in four fold coordination (network former) (AlO_4^-). The role of aluminium and silicon in the structure of glass has been extensively discussed in the literature [83, 149-150]. It has been recognised that both silicon and aluminium act as network formers. In the case of aluminium it has been observed that it also acts as network modifier in situations where the network modifiers such as calcium and phosphorus are consumed. The network modifiers charge balance non bridging oxygens in silicon and aluminium as well as non-bridging fluorines. Fluorine can replace oxygen and become both bridging and non-bridging. It also acts generally as glass network disrupter (forming non bridging fluorines) reducing the melting point of the glass. Generally, it has been recognised that the following species are present in the glass network: Al-F-Ca, F-Ca, Si-O-Al, Si-O-Si and Al-O-P. The glass crystallises to a fluorapatite and a mullite phase and the glass-ceramic has been proved to be osteoconductive if used in bone repair [86].

1.2 Biological behaviour of biomaterials

1.2.1 Cell – Biomaterials interaction

Biomaterials play a very important role in the tissue engineering field especially when used as matrices to guide tissue regeneration in vitro or in vivo [89]. Thus cell-surface interactions are crucial in order for new tissue to be developed since cells behaviour is determined by the substrate surface properties [90]. The surface properties influence the initial cellular events at the cell-material interface and consequently the formation rate and the quality of the new tissue [91].

Referring to cell-material interactions it is generally considered that interactions occur at the interface between a solid material surface and a biological environment. Research shows that all organized biological systems have the ability to recognize foreign objects to molecular dimensions [92]. The initial events occurring at cell-material interface include the oriented adsorption of different molecules. This procedure creates a conditioned environment to which cells respond. The nature of the adsorbed biomolecules affects cell recruitment, attachment and differentiation [9].

Cell adhesion is a very complicated process and it takes place in different steps. The first and short-term events involve ionic and Van der Waals forces which link the cells to the surface with physicochemical linkages, the second and long term events involve bio-molecules such as ECM (extracellular matrix), cell membrane proteins and cytoskeleton proteins, which determine the quality of adhesion between the cells and the substrate [93]. As soon as a biomaterial is exposed to the biological environment proteins (present in the aqueous culture medium) are absorbed immediately on its surface. The sequence of events occurring after the protein absorption is highly dependent on the type, composition and amount of the absorbed

proteins. When the proteins are successfully absorbed they recruit the cells which are in contact with the substrate. The cells then attach, spread, migrate, proliferate and some kind of cells differentiate on the surface [94, 95].

In a micro-molecular scale the situation is more complicated. When cells are placed in an external environment, the receptors in the cell membrane are covered with the ECM proteins such as fibronectin (Fn) and vitronectin (Vn), and interact with the proteins and ligands that have already been absorbed on the substrate. These receptors transduce biochemical signals to the nucleus by activating the same intracellular signalling pathways used by growth factor receptors (Figure 1.4) [93]. The adhesion molecules determine the cell-material interactions and they have the capacity to interact with a specific ligand and with each other. Generally, since cell membrane, its coating of biomolecules and the material surface are dynamic; they can exchange many different substances and form a complex and dynamic interface [96].

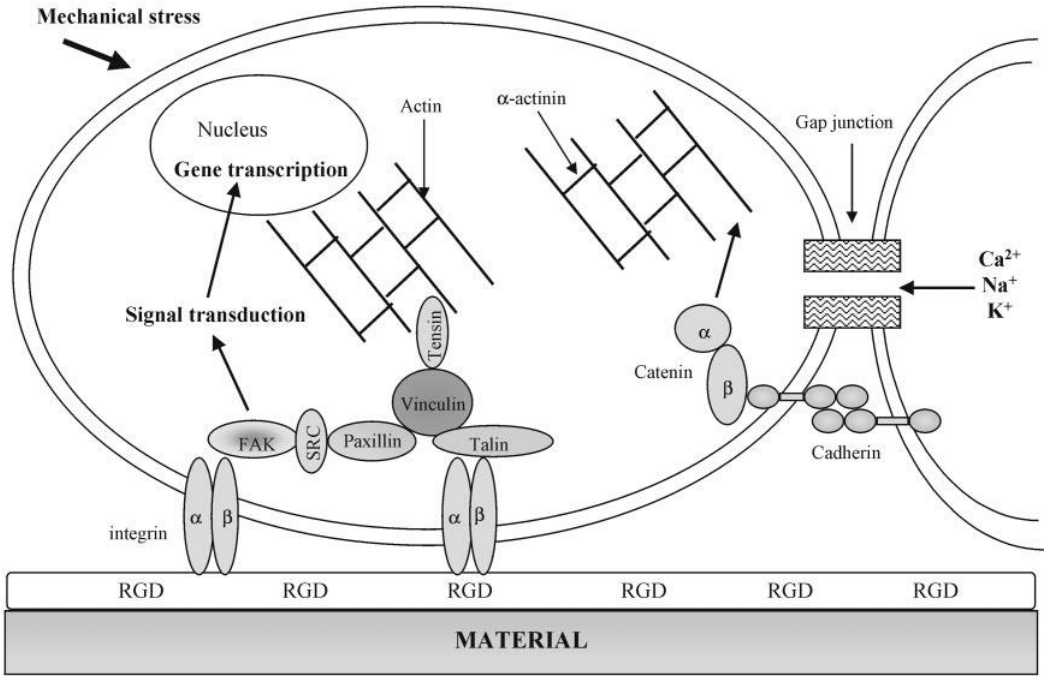

Figure 1.4: Representation of cell proteins involved in cell adhesion on biomaterial [93]

Cells are very sensitive to the physical and chemical characteristics of the material that they interact with. The surface characteristics influence the cell adhesion, proliferation and growth. The surface chemistry, topography, energy, 3D morphology, wettability and mechanics are the most important surface properties that affect the cellular behaviour.

The changes of the surface functional groups, surface wettability and surface energy are associated with changes of the surface chemistry of a biomaterial. Altering the surface chemistry has been proved beneficial for cells behaviour [97]. It has been shown, that the introduction of different chemical groups such as sulfonic groups on polymeric surfaces enhanced the spreading and adhesion of fibroblasts [98]. Zhu *et al.* reported that argon plasma modification of chitosan membranes improved the surface hydrophilicity and resulted in an increase in the surface energy. As a consequence, better attachment, adhesion and proliferation of human skin derived fibroblasts was observed [99]. Similar plasma treatments of polymers using different kind of gas mixtures of nitrogen and oxygen have been reported. Pu *et al.* treated polyethylene terephthalate (PET) and polytetrafluorethylene (PTFE) with ammonia plasma showing that human endothelial cells had an efficient attachment due to the increase in expression of adhesion molecules on the plasma treated surfaces [100]. Ammonia plasma treatment of polymer surfaces was also tested by Greisser *et al*. they examined the effect of plasma on Fluorinated Ethylene Propylene copolymer (FEP) and found that the introduction of amine and amide groups on to the polymers surface after the treatment supported fibroblasts and human endothelial cells attachment [101].

Apart from the surface chemistry, the surface morphology and topography affect cellular reactions when they come in contact with a substrate enhancing cell attachment and proliferation. Research has shown that cells are very sensitive to the substrates with specific nano- and micro-scale topography, for example cellular interactions with nano-micro-scale

features result in alteration of cell adhesion, morphology, orientation and phagocytotic activity [102-103]. Cliffs, groves, ridges, hills, pits, tubes and tunnels, fibres, spikes or even random roughness are some of the most known surface structures that have been proved to influence various cells behaviour such as fibroblasts, macrophages, osteocytes, endothelial and muscle cells [104]. So far methods such as photolithography, microstamping or microfluidic patterning have been used to create micro-patterns on a biomaterials surface [105]. Condie *et al.* have shown that titanium surfaces textured with 100 μm cavities, favour osteoblast attachment and growth [106]; it has also been shown that osteoblasts viability on carbon fibres is highly dependent on the fibres size, smaller diameter favours cell growth [107]. Rosa *et al*. reported that osteoblasts proliferation and protein synthesis were favoured by the smaller pore size of HA substrate [108]. Finally, epithelial cells shape and spreading was proved to increase with the increase of protrusions on silicon wafers [109], and osteoprogenitor cells proliferation and morphology seem to be improved on electrospun polymeric fibres compared to smooth surfaces [110].

Cells are able not only to react to the surface chemistry and topography but also to the surface mechanical properties. This is because a mechanical balance should be maintained between the cells and the environment they grow in, since it is very important for the tissue formation, cohesion, homeostasis and signalling between the cells and the substrate [111]. Cells behaviour is dependent on the rigidity and elastic nature of the tissue substrate they are attached to [112]. Choquet *et al*. have shown that cells have the ability to feel and respond to forces as low as 5 pN [113].

Cell adhesion on different material surfaces is very important for tissue engineering. All the parameters that influence cell behaviour must be taken into account before cell seeding on the substrate. Different cells, attach to different surfaces in different ways. Therefore, their

reactions, most of the times, are unpredictable. However, there are basic rules to follow in order to succeed in having a good cell response on various substrates. The understanding and systematic approach of the cell-material interaction domain, will enable scientists to design and test the balance of substrate chemistry, topography and mechanical properties in engineering the cell-material interface to control cellular response. Finally, by manipulating the surface of a material it may be possible to improve both in vivo and in vitro tissue engineering applications, which are very important for medicine.

1.2.2 Cell attachment on polymer and glass surfaces

Different types of scaffolds have been used so far in tissue engineering. They include metals, polymers, ceramics and glasses. The first materials used were metals [114]. Their use in orthopaedic surgeries as implants was forced by their ability to carry significant loads, withstand fatigue loading and sustain plastic deformation. Stainless steels, cobalt-chromium-molybdenum alloys, commercial pure titanium and titanium alloys are the most widely used metals for this purpose [115]. However metals appeared to create problems because of metal ion release, which in some cases is toxic and the bonds created between the bone and the implant which are not strong enough thus slow fixation and gradual loosening of the implant is very possible [116]. Consequently, alternative type of materials such as polymers, ceramics and glasses has been investigated [117].

Polymers have been used extensively in tissue engineering. In order to repair or reconstruct damaged tissues, the use of polymer scaffolds is due to their ability to act as supports for tissue regeneration. Thus, many degradable polymeric materials, natural or synthetic are used for medical applications [118]. Synthetic or natural polymeric scaffolds provide a good basis for cells to attach, proliferate and form ECM; also they are used as carriers for cells, growth

factors and biomolecular signals [102]. Polymer scaffolds must fulfil some very important requirements. Firstly, it is essential that they are biocompatible and biodegradable. Hence they should biodegrade at the same rate with the regeneration process. A second parameter is that they must be very porous with the correct pore size and highly permeable to allow diffusion procedures. Furthermore, they should have such mechanical properties in order to provide the appropriate microstress environment to the cells. Finally, their surface should be conductive for cells to attach, encourage ECM formation and carry biomolecular signals [119, 120].

Polycaprolactone (PCL), polylactic acid (PLA), polyethylene oxide (PEO), poly(lactic-co-glycolic acid) (PLGA), polystyrene (PS) and polyethylene (PE) are some of the most common synthetic polymers used as scaffolds to support tissue formation [121-125]. Apart from them, natural polymers such as collagen are also used in tissue engineering [126]. Due to the fact that these materials do not often meet the requirements for new tissue formation, blends of natural and/or synthetic polymers have also been investigated in order to favour cell behaviour [127]. Yoon *et al*. reported the fabrication of poly(lactic-co-glycolic acid) (PLGA) scaffolds using the particulate leaching technique and identified the pore size and structure suitable for skin fibroblast cells. They reported that anhydrous ammonia plasma treatment improved the surface energy and hydrophobicity of the polymer and that the pores with size smaller than 160 μm were suitable for fibroblast cell growth [128]. Kooten *et al.* examined the plasma treatment with oxygen of polystyrene (PS) scaffolds. They reported that increasing the oxygen incorporation on the surface, the water contact angle decreases. Epithelial cells reportedly adhered and spread on these surface showing well developed focal adhesion on stress fibres and higher proliferation rates with the increased oxygen incorporation [129]. Another example are Polycaprolactone (PCL) macromers that were crosslinked with photopolymerization resulting in changes on the polymers crystallinity,

modulus and degradation rate, human osteoblast culture showed that the modified materials was biocompatible since it favours cell growth compared to PCL itself [130]. Generally polymeric materials can be a good choice for tissue engineering as they can support both cell regeneration and tissue formation. In addition, there are still many unknown factors that need to be studied.

Apart from polymers, glasses and ceramics are used as substrates for cell attachment especially in bone tissue engineering. Synthetic grafts such as hydroxyapatite (HA), tricalcium phosphate (TCP), bioactive glasses (BG) and glass-ceramics are of great importance in biomedical applications, such as orthopaedic, dental and maxillofacial surgery because of their ability to chemically bond with the bone after implantation [131, 132].

Bioactive materials, in tissue engineering have many advantages compared to other materials. First of all, they permit the prosthesis adaption to the bone cavity. Moreover, they prevent fibrous tissue formation at the interface of prosthesis-bone. Finally, they can create a strong chemical bond between the bone tissue and the implant [133].

So far, a lot of work has been published on osteoblasts attachment on bioactive materials surface, showing that bioactive materials exhibit good cellular compatibility. For example, Price *et al*. reported that Bioglass® can support cell proliferation and maintain the cell phenotype of human osteoblasts-like cells [134]. It has also been reported that when bioactive glasses are subjected to surface reaction modification, two kind of layers can be formed on their surface, amorphous calcium phosphate or carbonated HA layer. This layer can enhance fibronectin-mediated cell adhesion and consequently proliferation and spreading [135]. Matsuda *et al*. compared the Bioglass® cellular compatibility with a non-bone-bonding quartz glass. It was shown that osteoblasts migrated on the Bioglass® surface forming ECM, also the interface that was developed on the Bioglass® was characterised as collagen of type I

and II. None of these results was observed on the quartz glass surface showing that osteoblasts react better on calcium phosphate-rich surfaces [136]. Finally, osteoblast adhesion seems to be increased on nanophase ceramic surfaces such as alumina, titania and HA. Their surface properties can control protein interactions and consequently osteoblast attachment, proliferation and differentiation. Bioactive ceramics are able to absorb a protein that enhances osteoblast adhesion (vitronectin). Research conducted on nanoceramic substrates, which were prepared without further chemical modification, showed that these surfaces facilitate cell adhesion [137].

1.2.3 Fibroblasts interaction with biomaterials

Different types of cells have been used in tissue engineering research including cell types like osteoblasts, chondrocytes, hepatocytes, fibroblasts and smooth muscle cells. The initial sequences of events that take place when cells interact with different surfaces in vitro are similar to those in vivo processes of cell adhesion and spreading. Studies conducted in fibroblasts showed that these initial steps can be easily observed. This explains why fibroblasts are widely used in this types of experiments. Fibroblasts are responsible for synthesizing and maintaining the ECM of most of the animal tissues. Consequently, they are the most common cells in connective animal tissues and their importance in wound healing is crucial [138].

The behaviour of different types of cells when in contact with metals, polymers and glasses has been the subject of a large number of published work. Pecheva *et al.* looked at human fibroblast behaviour on silica glass, silicon and stainless steel. They also looked at the behaviour of the cells when the above surfaces were coated with natural ECM. The cell attachment was found to be enhanced in the case of the ECM coated surfaces because of the

presence of ECM proteins [138]. Geurtsen *et al*. reported that Fuji II LC (FLC), Vitrebond (VB), Compoglass (CG), Dyract (DY) and Dyract Cem (DYC) light-cured glass ionomer cements (GICs) are cytotoxic preventing cell growth when 3T3 fibroblasts were seeded on their surface, and proposed that these materials are not appropriate for cell culture [139]. Furthermore, Meryon *et al.* examined the cytotoxicity of two other commercial glass-ionomer cements ASPA and ChemBond. These two materials were proved to be cytotoxic for BHK-21 fibroblasts [140]. On the other hand, polymer materials interact differently with fibroblasts. For example 3T3 cells seeded on sulfonated styrene copolymer showed that the higher the surface density of sulfonic groups the higher the number of cells attached on the substrate. It has been suggested, that this behaviour was due to the nature of the polymer surface and specifically the presence of sulfonic groups which accelerated the Fibronectin and Vitronectin recognition by the fibroblast integrin receptors [97]. Another approach for better results of fibroblast adhesion on polymer substrates is the use of polymeric blends. Blends composed of both synthetic and natural polymers show improved cell adhesion. Mouse embryonic fibroblast interactions with scaffolds made of hydrophilic chitosan and hydrophobic PCL blends were studied by Sarasam *et al*. It was found that the cell activity was superior compared to unblended materials [121]. As mentioned previously, modified surfaces are able to enhance cell activity. Plasma Surface Modification is a way to treat substrates for cell culture. Mouse fibroblast-like cells (L929) have been seeded on chitosan membranes which were plasma modified with nitrogen and argon plasma. The surface roughness and energy were increased and nitrogen and oxygen groups were incorporated into the scaffolds after the plasma treatment on which L929 cells proved to be more viable. Adhesion and proliferation proved to be better on treated chitosan membranes compared to untreated [141].

1.3 Aims and objectives

The aim of this project was to investigate the effect of Active Screen Plasma Nitriding treatment on biomaterials' surfaces and how the changes due to the treatment, influenced cell attachment and proliferation on the materials' surfaces. This research focused into biomaterials such as Ultra High Molecular Weight Polyethylene, and an ionomer glass-composition ($4.5SiO_2$-$3Al_2O_3$-$1.5P_2O_5$-$3CaO$-$2CaF_2$). The cells used for the purpose of this research were 3T3 Fibroblasts.

The objectives of this project were the following:

1. To study the effect of ASPN on biomaterials hardness and elastic modulus.
2. To study the effect of ASPN on biomaterials surface chemical composition.
3. To study the effect of ASPN on biomaterials surface roughness.
4. To study the effect of ASPN on biomaterials crystallographic features.
5. To study the effect of ASPN on biomaterials adhesion forces.
6. To study cell attachment, adhesion and proliferation on ASPN treated and untreated surfaces.
7. To study how plasma treatment affects the cellular compatibility of the polymer and the glass.

The Ionomer glass was treated a temperature of 400^{o}C in a gas mixture of 25% N_2 and 75% H_2 for 1 h. The reasons that these parameters were chosen was: 1. The gas mixture of the equipment was set to be 25% N_2 and 75% H_2 at the time and thus it could not be changed for technical reasons, 2) the temperature 400^{o}C because it is a temperature much lower from the

T_m of the material (as it is described in Chapter 2) and thus it would not affect the material and 3) the duration of the treatment was chosen to 1h since for technical reasons again only one treatment was allowed to be conducted and also the production of more glass samples was impossible. After the treatment, the mechanical properties of the ionomer glass surface were tested, in order to identify if the plasma treatment affected the hardness and elastic modulus of the material. Following, the surface roughness was tested via white light Interferometry, to identify if the nitride treatment induced any changes to the topography of the surface. Surface structure was tested using XRD to examine the effect of the treatment on the amorphous structure of the glass. Surface chemistry was also tested using Raman spectroscopy and XPS in order to check if the surface chemistry changes due to the ASPN. Continuing, focused ion beam together with EDS analysis were conducted to examine the changes on the upper part of the materials surface and examine the depth of the nitrogen that was embedded into the material. Finally, the fibroblasts seeded surfaces were visualised using SEM to qualitatively analyse the cells' behaviour on the plasma treated and untreated glass after four days of seeding. Following to the results a discussion and analysis is presented.

The rest of this research project focuses on the analysis of UHMWPE where we extensively investigated the effect of plasma treatment with two different gas mixtures of UHMWPE. Initially, some general introductory comments concerning UHMWPE are presented. UHMWPE is a polymer used as part of joint replacement, here the specific polymer was chosen in order to examine if the ASPN treatment can induce cell compatibility on to the otherwise inert material. Thus it was not used as a material connected with the role of an implant part but as a widely used polymer which is known to be inert. For the UHMWPE treatment the freedom on the parameters choice was limited. For technical reasons and limitations on the use of the ASPN equipment only two gas mixtures could be used (25% N_2

and 75% H_2 and 80% N_2 and 20% H_2), two treatment temperatures (120 ^oC and 90 ^oC) and three treatment durations (10, 30 and 60 min).

The first treatment involved a gas mixture of 25% N_2 and 75% H_2. Hardness together with elastic modulus data was obtained using nanoindentation. Surface topography was tested with white light interferometry. Following, the changes of the surface chemistry identifying the chemical bonds and the elemental composition were examined using FT-IR and XPS. The cellular compatibility of the treated and untreated UHMWPE was qualitatively tested after four days of seeding with fibroblasts via SEM. A discussion follows the results chapter.

Continuing; the second treatment of UHMWPE involved a gas mixture of 80% N_2 and 20% H_2. Straight after the treatment of the surface using ASPN, the treated and untreated surfaces were seeded with 3T3s. An initial observation using SEM showed that there was significant cell attachment within the first three hours of seeding on the surface of all treated samples. Also the treatment duration seemed not to affect the cell attachment, since cells morphology was similar for all samples. Therefore, the 60 mins treated cellular samples were used for further examination. A 28 days study was conducted and the cell seeded samples were subjected to interferometry, AFM, SEM and MTT assay to test the thickness of the cell layer, the adhesion forces between the cells and the cantilever tip, the cells morphology and to quantify the approximate number of viable cells respectively. Days 0, 7, 14, 21 and 28 were tested. The a-cellular samples subjected to a decay study for 28 days where interferometry, nanoindentation and AFM and XPS were employed. Finally analysis and discussion of the results is given.

At this point it should be clarified that within the text the words cellular and acellular are used to define the cell seeded samples and the non-cell seeded samples respectively.

CHAPTER 2 MATERIALS AND METHODS

2.1 Materials

2.1.1 Ionomer Glass (IG)

The glass composition ($4.5SiO_2$-$3Al_2O_3$-$1.5P_2O_5$-$3CaO$-$2CaF_2$) was produced by a melt quench route previously reported by Stamboulis *et al.* [83]. Following this method appropriate amounts (according to the composition mentioned above) of SiO_2, Al_2O_3, P_2O_5, $CaCO_3$, and CaF_2 were weighed, mixed and transferred to a platinum crucible. $CaCO_3$ is used in order to produce CaO, which is made by the thermal decomposition of $CaCO_3$ above 825^{o}C. The crucible was placed in a furnace (Lenton Thermal design, LTD, Lendon Furnaces) and the mixture was melted at 1475^{o}C for 2h. The melt was rapidly shock quenched into water in order to prevent crystallization and phase separation [79]. The glass was then cast and polished. The casting process was carried out by melting the frit glass at 1475^{o}C for 1h. The melt was poured in a preheated graphite mould at 500^{o}C and annealed at the same temperature for 1h using an Elite Thermal System BSF furnace model. The cast glasses were cylindrical with a diameter of 15 mm and thickness of 20 mm.

The glass surface was treated by ASPN at a temperature of 400^{o}C in a gas mixture of 25% N_2 and 75% H_2 for 1 h. The treated materials were characterised by: Nanoindentation in order to examine the changes that ASPN caused on the materials surface hardness and elastic modulus, white light interferometry in order to test if the plasma treatment affected the surface roughness of IG, X-Ray diffraction to see if the treatment affected the amorphous structure of the glass, Raman spectroscopy to examine the changes induced by the plasma on

the glass chemistry and Focused Ion Beam SEM (FIB-SEM) to verify the thickness of the film that plasma nitride may have created on to the glass surface. After the treatment, the glass surfaces were seeded with fibroblasts for 4 days and after the proper fixation SEM was conducted to visualise the cell behaviour on the treated and untreated glass surface. The cell seeding was conducted in order to examine if the cellular compatibility was improved due to the plasma treatment.

2.1.2 Ultra High Molecular Weight Polyethylene (UHMWPE)

The UHMWPE was supplied in the form of a flat sheet with dimensions 201 x 297 x 20 mm^3 by Oadby Plastics Ltd (Leicester, UK). According to the supplier the molecular weight of the polymer was 9.2 x 10^6 g/mol and the melting temperature of the material was 128^0C. In order to prepare the UHMWPE samples for ASPN treatment, square pieces of 15 x 15 x 20 mm^3 were cut using a diamond wheel. Prior to the plasma treatment, all samples were washed with distilled water and ethanol and were left to dry in air at room temperature.

UHMWPE was subjected to two different treatments. The treatment parameters (time, temperature and gas mixture) were chosen according to the equipment set up at this time. The first treatment was conducted at a temperature of 120^0C, for 10, 30 and 60 min in a gas mixture of 25% N_2 and 75% H_2. After the treatment, the UHMWPE surfaces were characterised by nanoindentation in order to test the effect of the ASPN on the hardness and elastic modulus of the polymer surface, white light Interferometry to examine if the treatment influenced the surface topography and roughness, Fourier Transform Infrared Spectroscopy (FTIR) to test if the nitride treatment induced new chemical bolds on UHMWPE, and X-Ray Photoelectron Spectroscopy (XPS) to examine the elemental composition of the materials surface and to find the bonds that may have been formed on the upper surface layer due to the

treatment. After the treatment all UHMWPE samples were seeded with fibroblasts for 4 days and after the proper fixation (see 2.2.12) SEM was conducted. The fibroblast seeding on the untreated and plasma treated surfaces was carried out in order to examine the materials cellular compatibility, how it was affected by the plasma treatment and if the duration of the treatment influences cells behaviour.

For the second treatment, the gas mixture in the plasma chamber was 80% N_2 and 20% H_2; the temperature of the treatment was 90^{o}C and the duration was 10, 30 and 60 min. Straight after the treatment, all treated and untreated materials were tested by XPS and white light interferometry. Continuing, all samples were subjected to an ageing study for a period of 28 days, in order to identify the exact nature and the environmental degradation of the nitride film and thus to obtain a complete description of the ASPN effect on the materials surface. All samples (untreated and plasma treated) were subjected to nanoindentation tests in order to examine the effect of different environments and the duration of treatment on the materials hardness and elastic modulus, white light interferometry to measure the surface roughness over the period of 28 days, XPS to test if the different environments that the samples were placed had an effect on the surface chemistry and AFM to measure the adhesion forces on the materials surface.

Finally, cell compatibility tests were conducted. Initially, the samples that were treated for all different time points (10, 30 and 60 min) were seeded with fibroblasts straight after the treatment for 24 h and SEM was used for the imaging of the cell seeded surfaces. The reason for this study was to test if fibroblasts attach onto the surface of plasma treated UHMWPE and to examine if the different durations of treatment influence cell attachment. After analysing these results, it was decided that only the 60 min plasma treated sample would be furthered examined. For this reason, a month study was conducted for the specific material.

Fibroblasts were seeded for a period of 28 days on the 60 min UHMWPE. First, SEM was used in order to visualise cell attachment and morphology at different time points of the seeding, white light interferometry was used in order to identify the increase or decrease of the cell layer thickness over 28 days, AFM was conducted while the cells were alive on the substrate so that we could visualise how fibroblasts attach on the treated UHMWPE and finally, an MTT assay was carried out so that the mitochondrial activity of the fibroblasts to be tested.

2.2 Methods

2.2.1 Plasma Treatment of UHMWPE and Ionomer Glass

The method that was applied for the surface treatment of UHMWPE and IG was active screen plasma nitriding (ASPN). The experimental set up of the technique is shown in Figure 2.1. A conventional direct current (DC) nitriding unit (Klockner Ionan, 40 kW) was used together with an active screen (AS) experimental arrangement. The DC plasma nitriding unit includes a sealed chamber, a vacuum system, a DC power supply system, a gas supply system and a temperature measurement and control system. The AS was set inside the nitriding furnace and around the workload. The AS was made out of 700 μm thick (AISI 304) sheet of perforated steel, with a height of 130 mm, a diameter of 120 mm and with holes of 8 mm in diameter. The sample-to-AS distance was kept at a constant distance of 10 mm.

Processing begins by evacuating the chamber, filling the chamber with treatment gas, heating the samples to treatment temperature using the plasma formed on the samples surface, keeping the temperature for a set time and finally cooling down to room temperature in the furnace. A high voltage cathodic potential was applied on the screen, whilst the working table

was electrically insulated with ceramic spacers, thus leaving the specimens at a floating potential. The furnace walls were on an anodic potential. The samples and the working table were insulated from the cathodic (screen) and anodic potential (furnace wall). The plasma that is formed heats the screen (but not the sample surfaces) and then the screen radiation heats the components up to the treatment temperature. The temperature was measured by a thermocouple inserted into a hole of 3 mm diameter in a dummy sample. Before the plasma treatment, all samples were cleaned with distilled water and ethanol. The pressure in the plasma chamber was 2.5 mbar for all treatments. During the treatment, parameters like temperature, gas mixture and time exposure changed according to the material. After the ASPN treatment all samples were put in a desiccator, under a vacuum of 10^{-2} mbar. The materials ID is presented in Table 2.1.

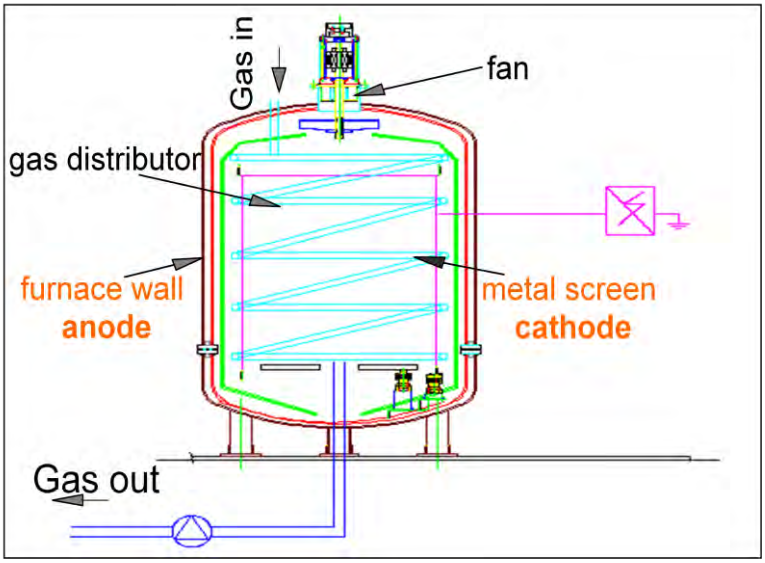

Figure 2.1: Schematic diagram of Active Screen Plasma Nitriding surface modification method.

Table 2.1: Materials coding

Material	**Treatment**	**Gas Mixture**	**Temperature (°C)**	**Sample ID**
Ionomer Glass	untreated	none		IG-0
Ionomer Glass	60min ASPN treated	25% N_2 - 75% H_2	400	IG-PT25
UHMWPE	untreated	none		PE-0
UHMWPE	10min ASPN treated	25% N_2 - 75% H_2	120	PE-PT25-1
UHMWPE	30min ASPN treated	25% N_2 - 75% H_2	120	PE-PT25-2
UHMWPE	60min ASPN treated	25% N_2 - 75% H_2	120	PE-PT25-3
UHMWPE	10min ASPN treated	80% N_2 - 20% H_2	90	PE-PT80-1
UHMWPE	30min ASPN treated	80% N_2 - 20% H_2	90	PE-PT80-2
UHMWPE	60min ASPN treated	80% N_2 - 20% H_2	90	PE-PT80-3

2.2.2 Ageing study of UHMWPE

A study was carried out to examine the ageing of the samples and stability of the plasma treatment on the UHMWPE surface in different environments. The samples were treated in a gas mixture of 80% N_2 and 20% H_2, they were then autoclaved in order to get sterilised and were placed in 12 well-plates exposed in (1) air, (2) 2 ml supplemented Dulbecco's Modified Eagle's Medium (S-DMEM) and (3) 2 ml Phosphate Buffered Saline (PBS). All samples were then stored in an incubator at 37°C at 5% CO_2 and 100% relative humidity. ASPN treated and untreated samples were tested on days 1, 7, 14 and 28 by AFM, white light interferometry and nanoindentation in order to examine the stability of the ASPN treatment measuring the surface electrostatic forces, surface topography and mechanical properties, respectively. Treated and untreated materials were examined using XPS for days 1,7,14 and 28 under ambient conditions only. For the purpose of the XPS study it was not possible to use

PBS and S-DMEM since the current experiment was not possible to complete in Birmingham University.

2.2.3 Nanoindentation: Hardness and Elastic modulus of UHMWPE and IG

Nanoindentation measurements were carried out in order to understand how the plasma treatment affects the hardness and elastic modulus of the surfaces under study. The samples tested with this method are the IG and the UHMWPE that were treated in the gas mixture 25% N_2- 75% H_2. Nanoindentation is one of the most common methods to determine mechanical properties such as hardness and elastic modulus of thin films and surfaces of materials. The nanoindentation measurements are based on a hard small size tip, with known mechanical properties, which is pressed into the surface of a material which mechanical properties are not known; the area that the indentation takes place can be a few square micrometres or nanometres. A small load is applied to the tip and is increased as the tip goes deeper into the material [141, 142]. When the indenter is pressed onto the materials surface both elastic and plastic deformations occur, and result in the formation of a hardness impression conforming to the shape of the indenter. When the indenter is withdrawn only the elastic portion of the displacement is recovered. Nanoindentation hardness is defined as the indentation load divided by the projected contact area. Hardness is obtained by the load displacement curve and is calculated by the equation:

$$H = \frac{Pmax}{A}.$$

Where H is the hardness, P_{max} the maximum load and A the residual indentation area.

The elastic modulus of the material can be measured from the unloading contact stiffness which is the slope of the curve and is calculated by the equation:

$$S = \mathbf{2}\beta \boldsymbol{Er} \frac{\sqrt{A}}{\sqrt{\pi}}$$

Where β is a constant that depends on the geometry of the indenter and E_r is the reduced elastic modulus which accounts from the fact that the elastic deformation occurs in both the sample and the indenter and is calculated for the equation:

$$Er = \frac{1 - \nu^2}{E} + \frac{1 - \nu i^2}{Ei}$$

Where E and ν are the elastic modulus and Poisson's ratio for the sample and E_i and ν_i are the elastic modulus and Poisson's ratio of the indenter [143].

Each sample was tested six times; the hardness and elastic modulus were calculated from the mean of six measurements. The equipment used was a Nano Test 600 machine (Micro Materials UK).

For the decay study the hardness and reduced modulus of the UHMWPE surface were obtained by performing indentation measurements to a depth of 500 nm using a NanoTest (Micro Materials, UK) employing a diamond-coated Berkovich indenter. A minimum of 30 measurements were performed over various locations of the sample surface.

2.2.4 White light Interferometry: Roughness of UHMWPE and IG surfaces

White light Interferometry is a technique used in order to measure the physical geometrical characteristics of an object such as surface roughness and surface profile thickness of thin films [144]. White-light interferometry can obtain intensity data at different positions along the materials surface and thus it can determine their location.

In this study, interferometry was employed to determine the roughness of the surface of samples caused by the plasma treatment and to evaluate the thickness of the cell layers after various time points of seeding of the cell seeded samples. The interferometric measurements were performed using a MicroXAM interferometer (Scantron, UK), using a white light source. The samples were imaged using a 10X objective lens. A scanning Probe Image Processor software (Image Metrology, Denmark) was employed for the analysis of the acquired images, yielding S_a (average roughness) and S_q (root-mean square roughness) and values for the surface roughness. These values were the mean of a minimum of five measurements at separate locations. The average roughness (S_a) and the root-mean-square roughness (S_q) calculated from the surface topographies acquired by interferometry are inherently statistical measures and are obtained from scan areas sufficiently large as to be representative of the overall surface character of the sample.

The same technique that was used for the a-cellular samples was employed also for the cell seeded samples. UHMWPE samples that were treated in a gas mixture of 80% N_2 and 20% H_2 were seeded with 3T3s for a period of 28 days, days 0, 7, 14, 28 were tested by Interferometry following the same procedure of fixation that was used for the cellular samples tested by SEM (see section 3.3.12).

2.2.5 X-Ray diffraction (XRD)

XRD is a technique used to distinguish between single crystal and polycrystalline or powder materials. The XRD diffractometer was used in order to determine the crystal structure of a material by sending X-rays through the sample. X-rays scatter in different directions and produce a diffractogram which gives information about the material structure. The X-ray diffractometer function is based on Bragg's law: $\lambda=2d\sin\theta$ where λ is the wavelength (Cu K_α

radiation, λ= 0.1542 nm), d is the inter-planar spacing of crystal and θ is the diffraction angle [145]

A Phillips Panalytical X-Per 3040 X-Ray diffractometer was used in order to determine the crystal structure of materials. The XRD analysis was carried out in the 2θ angle range of 10^{o}-80^{o} and a step size of $2\theta=0.02^{o}$ using a Cu-radiation and a Ni –filter, with the operating conditions of 40 kV accelerating voltage and a current of 40 mA. XRD was used to examine the possible changes in the surface structure on the plasma treated ionomer glass.

2.2.6 Fourier Transform Infrared Spectroscopy (FT-IR): chemical composition of UHMWPE

FT-IR spectroscopy was used in order to identify the chemical composition of a material, to determine the consistency of a material and the amount of components in a sample. The technique is based on IR radiation, which is passed through the sample. A part of IR radiation is absorbed by the sample and the rest is transmitted. When the two beams are recombined at the detector, an interference pattern is produced. The outcome of an FT-IR measurement is a spectrum that represents the molecular absorption and transmission and is unique for each sample. An infrared spectrum contains bands which represent the frequencies of vibration between the chemical bonds of the atoms present in the material. Therefore, a qualitative analysis of different types of materials can be done [146]

FTIR spectroscopy was conducted in order to study the presence of possibly new chemical groups on the surface of materials caused by the ASPN treatment. A Nicolet Magna 860 spectrophotometer was used for the analysis of untreated and ASPN treated in the gas mixture 25%N_2-75%H_2 UHMWPE surfaces. The measurements were performed in a frequency range between 400 and 4000 cm^{-1} and a resolution of 4 cm^{-1}. 100 scans min^{-1}

were taken. A background scan was conducted prior to measurements and was subtracted from each sample spectra.

2.2.7 Raman Spectroscopy: chemical composition of IG

Raman spectroscopy is a spectroscopic technique which is used in order to study the internal structure of molecules and crystals. Light, of known frequency, and polarization is scattered from the sample, the scattered light is then analyzed for frequency and polarization. [146]

For Micro-Raman analysis a Nicolet Almega XR dispersive Raman spectrometer was used. The spectrometer was equipped with a 785 nm laser accumulating 256 of scans at an exposure time of 1 s and resolution of 8 cm^{-1}. The spectra were collected between 400 and 3600 cm^{-1}. The Raman spectroscopy was conducted for ASPN treated and untreated IG samples in order to identify the changes on the surface chemistry due to the plasma treatment.

2.2.8 X-ray photoelectron spectroscopy (XPS)

The chemical comparison of treated and untreated surfaces was determined using X-ray photoelectron spectroscopy (XPS). XPS was carried out to examine the chemical changes caused on the surface of UHMWPE for both gas mixtures, straight after the plasma treatment. XPS measurements were conducted for untreated, 25% N_2-75% H_2 plasma treated, 80% N_2-20% H_2 plasma treated and also for the ageing study (28 days). First, survey spectra were obtained in order to detect the elements presence on the materials surface and then high resolution spectra of C1s, O1s and N1s were obtained in order to identify the bonds formed after the plasma treatment. All spectra were energy referenced to the C1s spectra whose binding energy was taken at 285 eV.

A bespoke XPS was used for the analysis of both ASPN treated and untreated samples that were treated in gas mixtures 25% N_2-75% H_2 and 80% N_2-20% H_2. The software used was produced by PSP Ltd, UK. The pass energy was 50 eV and the X-ray gun operated at 10 keV. The step size in order to obtain individual peaks was 0.1 eV, whereas 1 eV was used for the acquisition of a full spectrum over the complete range of binding energies. The vacuum pressure in the analysis chamber was less than 10^{-8} mbar.

Apart from the UHMWPE samples that were tested straight after the treatment, XPS was also conducted for the samples that were subjected to the ageing study. For these samples the equipment used was: VG Escalab 250 XPS Monochromated Al Kα source with a spot size 500 nm and a power of 150 W. The XPS testing was performed at Leeds Nanosciencse and Nanotechnology Facility (LENNF) at school of Physics and Astronomy, University of Leeds.

All high resolution spectra were deconvoluted using the XPSPEAK41 software. The curves were fitted using the Gauss-Lorentz functions and the Shirley method for the background subtraction was used.

2.2.9 Atomic Force Microscopy (AFM)

AFM is a high resolution type of a scanning probe microscope. AFM was used here in order to obtain: 1) roughness for the untreated, 25% N_2-75%H_2 plasma treated UHMWPE 2) adhesion data from 80% N_2-20%H_2 ASPN treated UHMWPE a-cellular samples that were subjected to an ageing study and 3) images when cells were still alive on the surface of 80% N_2-20%H_2 ASPN treated UHMWPE at different time points.

Adhesion force measurements and roughness data were performed using a NanoWizard II AFM (JPK, Germany) operating in contact mode under ambient conditions. A scanner with a

maximum lateral range of 100 x 100 μm and a maximum vertical range of 90 μm for adhesion force measurements, employing a CellHesion module (JPK, Germany) was used. Also the images were obtained at the highest possible resolution of 4096 x 4096 pixels which equates to 24.4 nm/pixel. All sample handling was carried out using clean Dumostar tweezers (Agar Scientific, UK) to minimise the risk of sample contamination. Force measurements were performed using triangular 200 μm length Si_3N_4 cantilevers (Veeco, USA). The cantilever spring constant was measured according to the thermal tune method.

For a-cellular samples that were subjected to the aging study, the acquisition of adhesion data was performed using a NanoWizard II AFM (JPK, Germany) employing a CellHesion module (JPK, Germany), operating in contact mode at 18^{o}C and 40% relative humidity. A minimum of 25 adhesion force measurements were performed, employing rectangular 130 μm length Si cantilevers with 6 μm nominal SiO_2 colloid probes at their apex (NovaScan, USA). The cantilever spring constants were on the order of 25-30 N/m, as calibrated according to the method reported by Bowen *et al.* [148].

For the cell seeded samples, the acquisition of topographical, mechanical and adhesion data was performed simultaneously using a NanoWizard II AFM (JPK, Germany) operating in force scan mapping mode under physiological buffer solution. This involved the use of a scanner with a maximum lateral range of 100 × 100 μm and a maximum vertical range of 90 μm in conjunction with a CellHesion module (JPK, Germany). The data acquisition was performed using rectangular 130 μm length Si cantilevers (type NSC36/no Al, Mikro Masch, Estonia) having pyramidal tips with 10 nm nominal radius of curvature. The cantilever spring constants were in the order of 0.2 N/m and were calibrated according to the method reported by Bowen *et al.* [148]. The data were acquired by driving the fixed end of the cantilever at a velocity of 50 μm/s towards the sample surface, whilst monitoring the deflection of the free

end of the cantilever using a laser beam. Upon making contact with a surface feature, the height of the contact point was recorded, representing one pixel in the image, which was converted into a map of surface topography. The force curves acquired on fibroblasts were analysed in order to assess the adhesion properties of the surface, while a Hertzian model was employed to assess the mechanical response of the surface. AFM measurements used a rigid probe, relative to the soft cells, which allowed the use of Hertzian model to estimate the Young's modulus of the fibroblasts. For a rigid indenter and a flat specimen, Hertz proposed a relationship between the indenter radius, elastic modulus of specimen and contact radius:

$$a^3 = \frac{3}{4}\frac{PR}{E^*}$$

Where: a = Contact radius, P = Normal load, R = Indenter radius and E^* = Reduced Modulus

A maximum compressive load of 5 nN was applied to the surface during data acquisition, which corresponded to a small strain during the indentation of a fibroblast.

2.2.10 Focused Ion Beam (FIB-SEM)

The focused ion beam technique was employed only for the plasma treated ionomer glasses in order to identify the nature and the thickness of the nitride film on the glass surface. The equipment used was the Quanta 3D FEG which is a high resolution, low vacuum SEM/FIB for 2D and 3D material characterization and analysis. The field-emission electron source delivers clear and sharp electron images, also the quanta 3D FEG's high-current FIB that enables fast material removal was used to cross section the glass surface together with an EDS elemental analysis of each cross section separately. The specimens were Pt coated by a sputtering method using 25 mA and 1.5 kV and the thickness of sputtered Au was between

10-12 nm. The operating voltage was 20 kV, the working distance was 10 mm and the spot size was 7.

2.2.11 Cell Culture Experiments

All chemicals for cellular studies were purchased from Sigma-Aldrich UK. NIH 3T3 fibroblasts were used to study the cellular compatibility of the treated and untreated UHMWPE and IG surfaces. For the cell culture the standard 3T3 fibroblast cell line was used. Firstly, the cell culture was prepared and afterwards the cells were seeded on the plasma treated and untreated substrates. The fibroblasts used were embryonic murine mouse cells. The cells are called 3T3 because they are transferred (T) and inoculated at the density of $3x10^5$ cells/cm^2 every 3 days (3). The cells were cultured in S-DMEM (supplemented-DMED). The medium was supplemented with 10% foetal bovine serum (FBS), 2.4% L-glutamine, 2.4% 4-(2-hydroxyethyl)-1-piperazineethanesulfonic acid (HEPES) buffer and 1% penicillin/streptomycin. FBS is a type of serum which provides proteins, nutrients hormones and attachment factors to the cell culture; hence it is necessary for in vitro growth. L-glutamine is an essential amino acid for cell growth; this is because it helps in protein and nucleic acid synthesis that is important for cell proliferation. HEPES is important in order to maintain the pH of the medium in the physiological range. Penicillin/streptomycin was added in order to prevent contaminations of the cell culture. PBS is a solution that contains: sodium chloride, sodium phosphate, potassium chloride and potassium phosphate. It is an isotonic and non-toxic solution for the cells. It helps “clean” the flask from the dead cells every time that the medium was changed or the cells were passaged.

Cells were passaged using Trypsin on the 7th day after culture in S-DMEM after they had reached approximately 70% confluency. Trypsin is a proteolytic enzyme that is used in cell

culture processes. The role of this enzyme is to help cells to detach from the cell culture flasks or the dish walls and facilitate cell dissociation. Trypsin is maintained at a low temperature, but in order to be used, it has to be pre-warmed as the enzyme acts better at 37^{o}C. Detached cells were counted using a haemocytometer and trypan blue, to determine live cell number. Every time that the cells were passaged they were counted in order to measure the number of cells in each flask. The cells were diluted together with their medium in 0.5% Trypan Blue (1:1). The dye was used to stain the dead cells. The mixture was placed in both sides of the hemocytometer. The hemocytometer had four squares of 1 mm^2 each. Under a microscope the living cells present within the squares were counted (the dead cells were stained). An average number was obtained, divided by 2 and multiplied by 10^4 giving a number of living cells per 1 ml of medium.

For the cell culture, the 3T3 fibroblasts protocol was followed. The protocol is not standard although there is a general advice in the literature of the processes that needs to be followed. The basic principles are standard; however the amounts and some of the materials and methods differ according to the user. The protocol used is described below:

Frozen cells were used. The frozen cells were preserved in liquid nitrogen under -150^{o}C. The vial used contained 1ml of medium and 2 million cells. The cells were warmed up by placing the vial in a water bath at 37^{o}C. At the same time the medium was warmed up under the same conditions. Next the cells were diluted in 10 ml of medium and were mixed well by pipetting up and down. The mixture was centrifuged at 1000 rpm for 3 min, using an MSE Mistral 2000 centrifuge apparatus, causing the cells to isolate. 2 ml of new medium were added in the vial and the mixture was pipetted up and down. Finally, the cells together with the medium were divided and placed in two flasks (Iwaki, 75 cm^2 canted neck tissue culture flasks) and

13 ml of medium were added in each flask so that 15 ml of mixture was found in every flask. The flasks were stored in an incubator (Sanyo CO_2 MCO-15AC incubator) at 37^{o}C.

Everyday, the cells were observed under the microscope in order to check if they were still alive or infected and whether they were confluent or not. If the cells were confluent in the flask, they were ready for passaging. If passaging was not conducted at the right time, the medium would become acidic and the cells would significantly proliferate and would finally die. All the above process was conducted under the laminar flow and all the equipment used was sprayed with 70% ethanol and cleaned with 1% Vircon in order to prevent contaminations. On the third day of cell culture the medium had to be changed. The old medium was removed and the flasks were cleaned with 10 ml of PBS. After removing PBS, 15 ml of new medium were added in each flask that was stored subsequently in the incubator. On the fifth day when the cells were more confluent (about 50% but not confluent enough for passaging) the same procedure was repeated. In order to passage the cells, they must be confluent about 70%. The seventh day, the cells were ready to be passaged. Briefly the passaging procedure was: first the medium was removed from the flasks. Then the flasks were cleaned with 10 ml of PBS and 4 ml of pre-warmed trypsin were put in each flask. The flasks were placed in the incubator for 3 min so that the trypsin will have the time to act and detach the cells from the flasks walls. Afterwards, 16 ml of medium were added in the flasks so that trypsin's action will stop. The content of the flasks (trypsin and medium) was placed into universals and was centrifuged for 3 min in 1000 rpm. Then the content of the universal was removed with the cells to be left at the bottom and 3.5 ml of medium were added in each universal and mixed with the fibroblasts. 1 ml of the mixture was used for cell counting and the rest was shared in 6 new flasks (1 ml in each). 14ml of fresh medium were put in each flask and all flasks were placed in the incubator.

UHMWPE and glass samples (treated and untreated) and were sterilised in the autoclave for 15 minutes at 121^{o}C prior to seeding. All sterilised samples were placed in a 12 well-plate and the cells together with S-DMEM were added to each well at a seeding density of 1.2x10^{6} cells per sample. The cell seeded surfaces were replenished with an additional 2 mL S-DMEM and incubated at 37°C at 5% CO_2 and 100% relative humidity. The medium in each sample was changed every 3 days. For all cell culture studies day 0 is three hours after the cell seeding.

For the IG samples the seeding was conducted only for four days and afterwards the samples were visualised using SEM. For UHMWPE samples a more detailed study was carried out. First, cell seeding was conducted for four days followed by SEM imaging for the samples that were treated in the gas mixture of 25%N_2-75%H_2. Continuing, further treatment of UHMWPE samples in a gas mixture of 80%N_2-20%H_2 was carried out and cells were seeded initially for 1 day for all different time treated samples. Further investigation of fibroblasts behaviour was examined with seeding only the 60 min treated UHMWPE samples for a month study.

In order to quantify the approximate number of viable cells on the surface of the seeded UHMWPE samples used for the one month study, a tetrazolium assay was used on days 0, 7, 14 and 28. 200 μL yellow MTT (3-(4, 5-Dimethylthiazol-2-yl)-2,5-diphenyltetrazolium bromide) solution was added to each sample and incubated at 37°C at 5% CO_2 and 100% relative humidity for 18 h to allow the tetrazolium ring in the salt to cleave to mitochondrial dehydrogenases and form purple formazan crystals. After incubation, these crystals were dissolved in 2 mL of hydrochloric acid and isopropanol (1 mL HCL to 24 mL isopropanol). The absorbance of the dissolved crystal solution was measured at 620 nm (Cecil, Cambridge, UK) and compared to a standard curve to give an approximate cell number.

2.2.12 Scanning Electron Microscopy to visualise the cell seeded samples

The cell seeded surfaces were visualised using E-SEM (JSM 6060 LV, JEOL, Oxford Instruments Inca, UK) where the SEM mode was selected since the materials used were dried. The operating voltage was 10 kV, the working distance was 10 mm and the spot size was 3. Prior to testing, the cell seeded samples were chemically fixed using 2.5% glutaraldehyde for 24 h and dehydrated with ethanol. Afterwards, the samples were washed in 70, 90 and 100% aqueous ethanol solutions for 30 min followed by 100% dried ethanol for additional 30 min. The samples were then placed in liquid CO_2 at 1070 psi and 31^{o}C for 60 min. Finally, the specimens were Pt coated by a sputtering method using 25 mA and 1.5 kV and the thickness of sputtered Au was between 10-12 nm. SEM was performed for all treated and untreated samples. For the UHMWPE that was treated in the gas mixture of 80% N_2 and 20% H_2 SEM was performed for all treated (10, 30 and 60 min ASPN) and untreated samples after 24 h of seeding and afterwards only for the 60 min treated samples (PE-PT3) on days 0, 14 and 28 after cell seeding.

CHAPTER 3 RESULTS AND DISCUSSION

3.1 ASPN treatment of the Ionomer glass (IG)

3.1.1 Results: Materials characterization and cellular compatibility of IG

3.1.1.1 Mechanical properties of untreated and plasma treated glass

Table 3.1 shows the nano-indentation results for the glass samples IG-0 and IG-PT25. The hardness and elastic modulus were calculated according to the equations described in materials and methods chapter. The values represent the mean value of 6 measurements. As it can be observed, the hardness of the glass was almost doubled after the plasma treatment. An increase in the value of elastic modulus can also be observed. Figure 3.1 shows the change in the hardness and elastic modulus for IG-PT25 compared to the untreated glass sample IG-0. IG-PT25 showed clearly an improvement in hardness and stiffness by ca 50% compared to the untreated sample.

Table 3.1: Hardness and elastic modulus for untreated (IG-0) and ASPN treated (IG-PT25) ionomer glass.

Material	Hardness (GPa)	Elastic modulus (GPa)
IG-0	8.2 (±0.3)	106.5 (±1.9)
IG-PT25	16.5 (±2.4)	177.8 (±5.9)

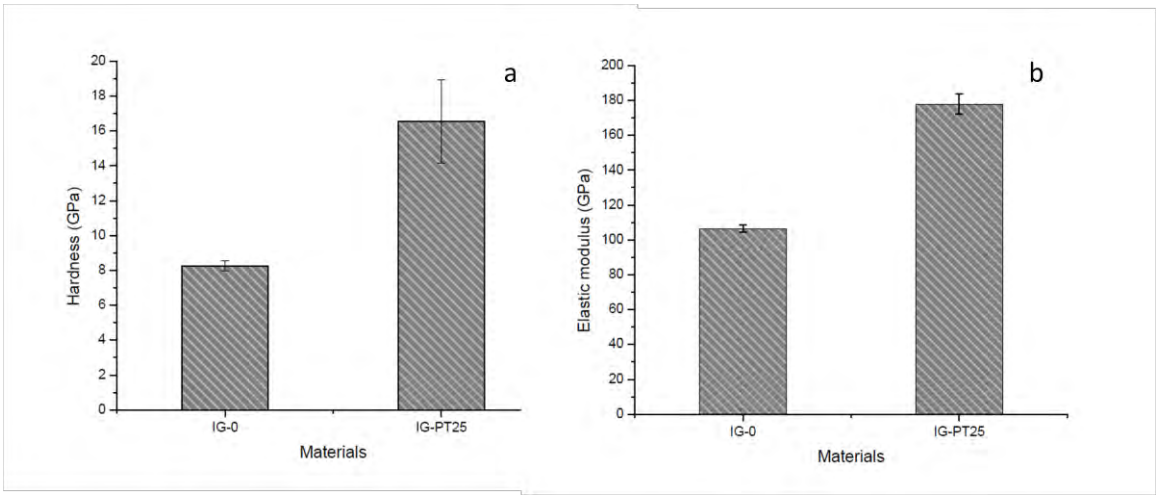

Figure 3.1: (a) Hardness of untreated and plasma treated ionomer glass and (b) Elastic modulus of untreated and plasma treated ionomer glass.

3.1.1.2 Roughness tests of untreated and ASPN treated ionomer glass

Figure 3.2a and b shows the surface topography of both treated and untreated IG samples. Table 3.2 shows the numerical values of both S_a (average roughness) and S_q (root-mean-square roughness). S_a and S_q are by definition statistical values. It is important to report both values as there is no significant difference between the two terms. As it can be observed the values of S_a and S_q of the untreated IG-0 are almost 50% higher compared to the plasma treated glass suggesting that the treatment resulted in a decrease of the surface roughness. From Figure 3.2 the difference of the surface roughness between the two materials is very clear. The plasma treated exhibits a smother surface compared to the untreated glass. Furthermore, the surface of IG-PT25 seems to be porous with pores having an average depth of approximately 400 nm as shown in Figure 3.2c

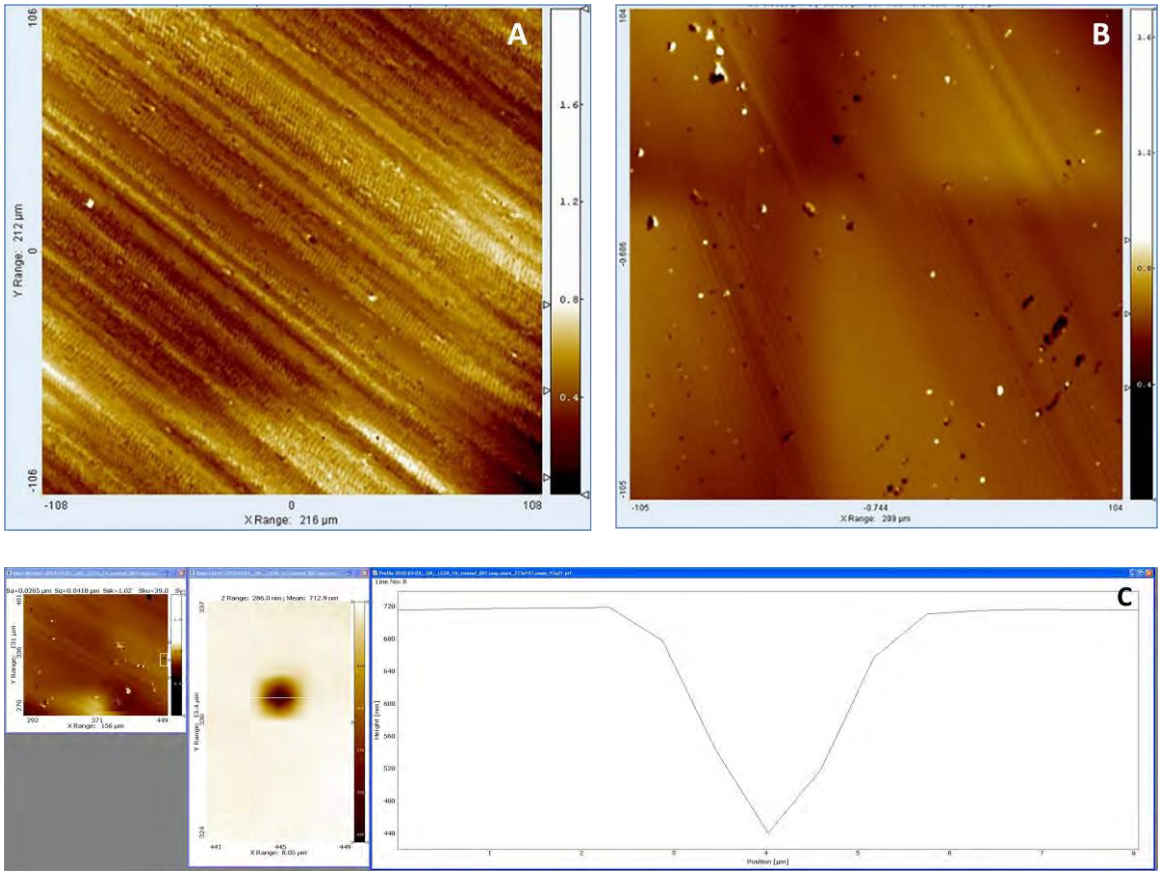

Figure 3.2: 2D topography of a) untreated b) plasma treated ionomer glass and c) pore size on the treated glass surface.

Table 3.2: Numerical values of both Sa and Sq.

Material	Sa (nm)	Sq (nm)
IG-0	79	98
IG-PT25	34	50

3.1.1.3 Structure of ASPN treated IG

The X-ray diffraction analysis of treated glasses is represented in Figure 3.3 and it shows clearly, that the treatment did not induce any change in the structure of the glass. The X-ray diffractogram shows clearly the characteristic chalos that amorphous structures exhibit.

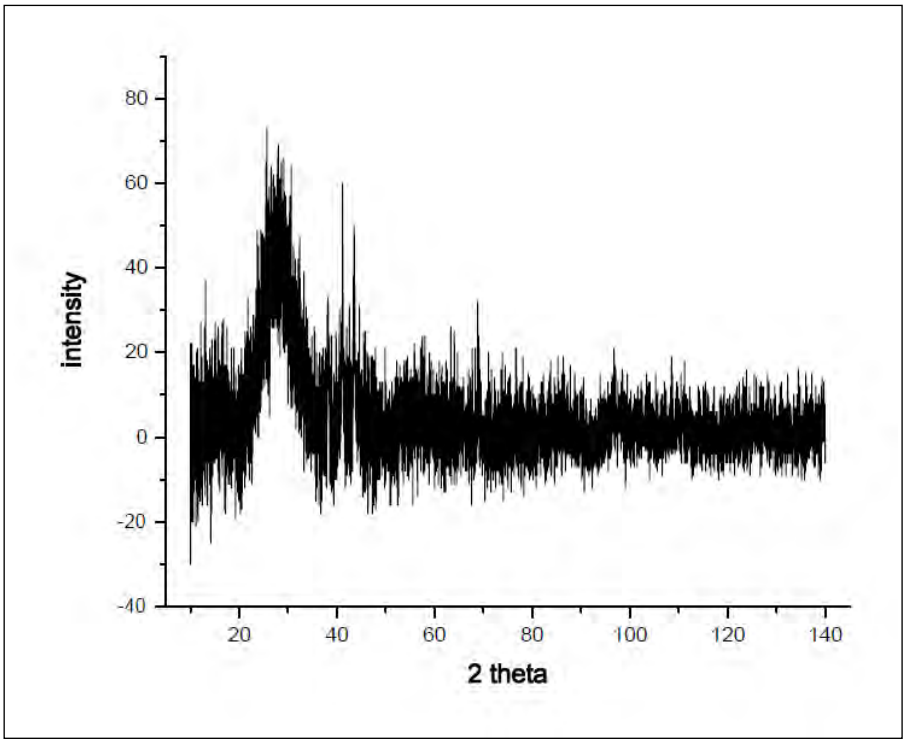

Figure 3.3: X-Ray Diffraction graph of the ASPN treated ionomer glass.

3.1.1.4 Raman and X-ray photoelectron spectroscopy

Figures 3.4 (a) and (b) represent the Raman spectra of IG-0 and IG-PT25, respectively. For both IG-0 and IG-PT25, two similar bands were observed at 1304 and 1314 cm^{-1}, respectively assigned to the presence of Si-O-Si bonds in the glass network. An additional peak at 799 cm^{-1} was present in the spectrum of IG-PT25 most likely attributed to the presence of a Si-N group. Better resolution of spectra could not be achieved for the IG samples with Raman spectroscopy and therefore, it was not possible to receive more information about the structure of the glass surface and particularly the chemical nature of the layer formed on the surface of the glass after the treatment. For this reason X-ray photoelectron spectroscopy (XPS) analysis was also conducted.

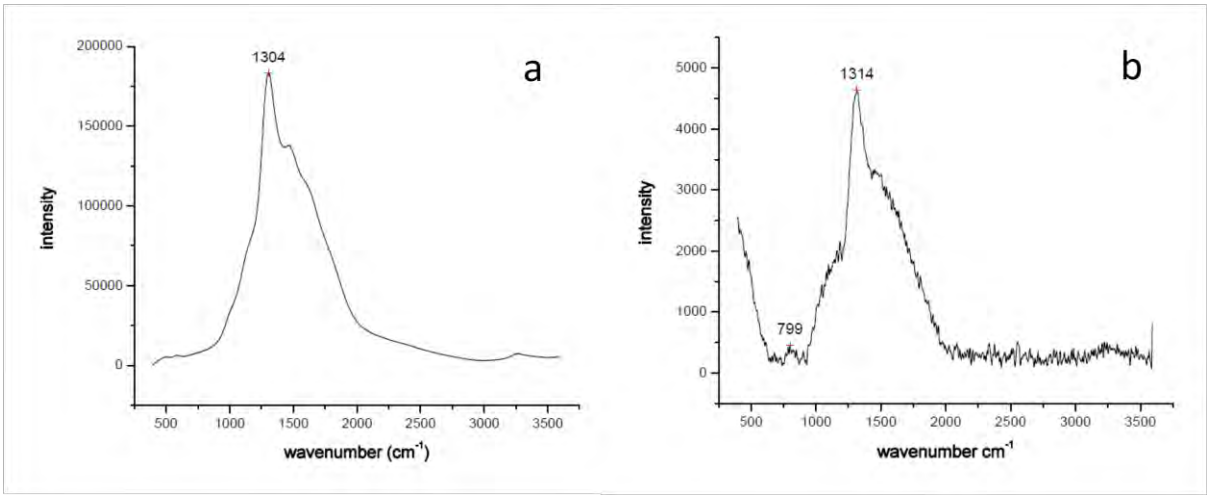

Figure 3.4: Raman spectrum of (a) IG-0 and (b) IG-PT25.

XPS measurements of treated and untreated IG samples revealed the presence of all elements existing in the glass surface with the exception of fluorine and calcium. The presence of iron and carbon is attributed to the impurities that plasma treatment can induce due to the active screen composition; iron presence can also be attributed to the steel specimen stub. Also, from the spectra the presence of nitrogen was very clear on the plasma treated glass. Figures 3.5-3.9 show the XPS spectra with the peaks that represent each element found according to the measurements, for a binding energy varying between 50-550 eV. Table 3.3 shows the assignment of each peak for both IG-0 and IG-PT25. The nitrogen peak is present only on the plasma treated glass and is found at 403 eV. The nitrogen content of the treated glass surface was found to be 1.5% of the total elemental composition.

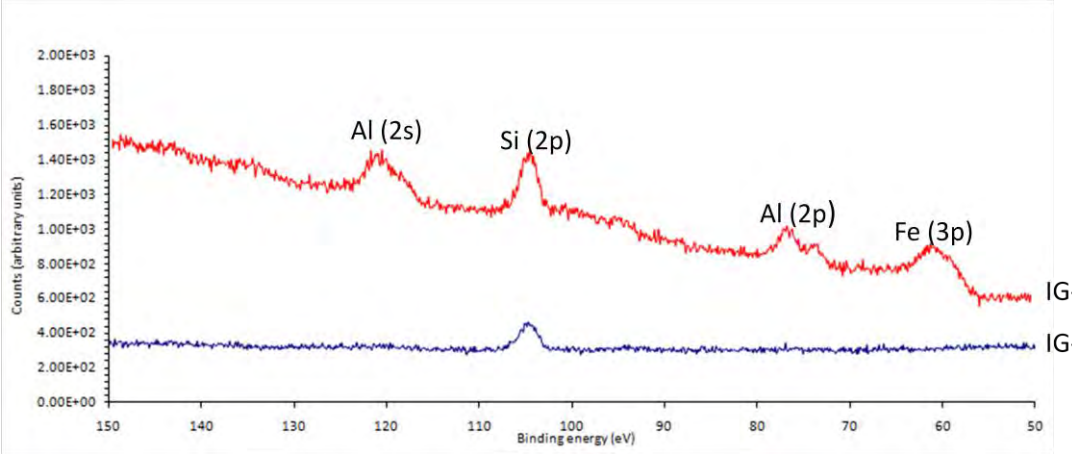

Figure 3.5: XPS spectra for untreated and plasma treated ionomer glass for BE 50 -150 eV.

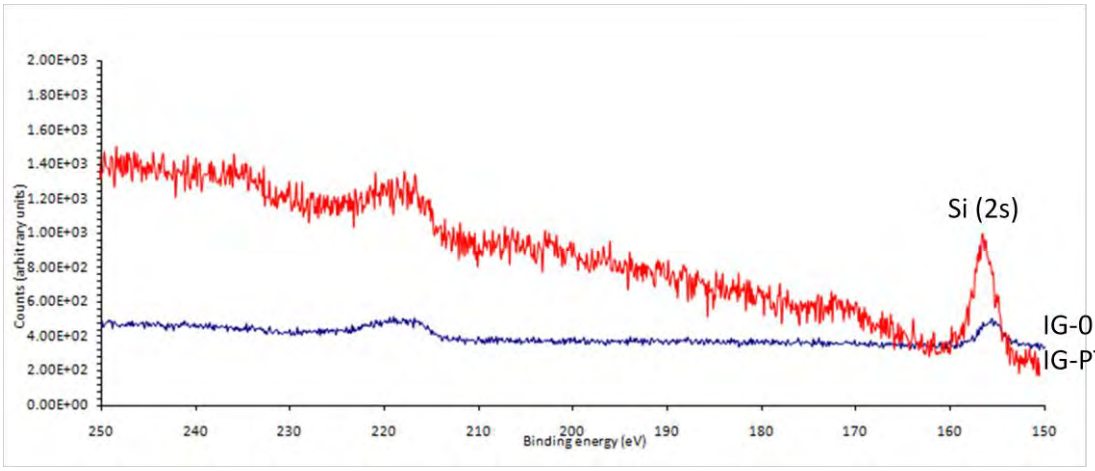

Figure 3.6: XPS spectra for untreated and plasma treated ionomer glass for BE 150 -250 eV.

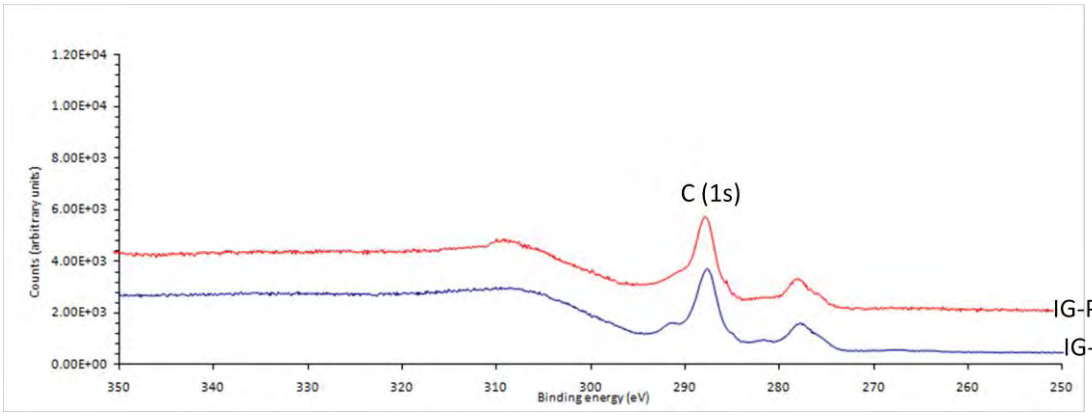

Figure 3.7: XPS spectra for untreated and plasma treated ionomer glass for BE 250 -350 eV.

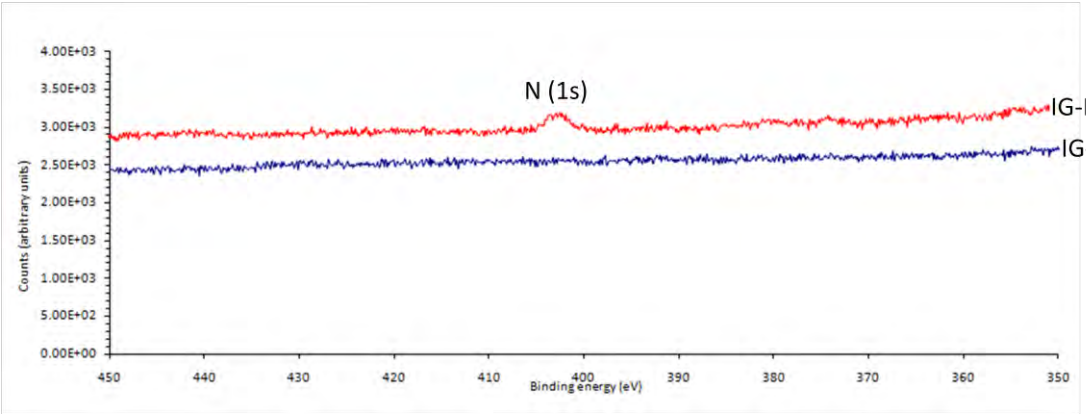

Figure 3.8: XPS spectra for untreated and plasma treated ionomer glass for BE 350 -450 eV.

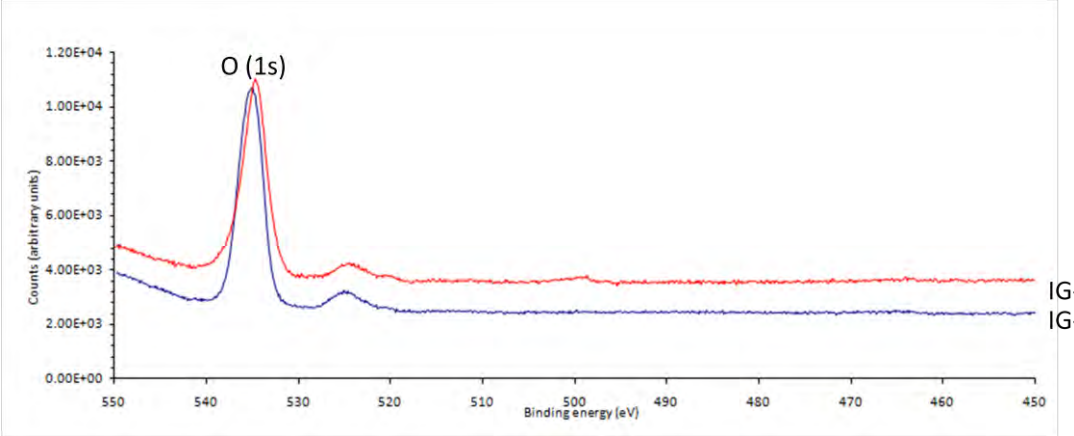

Figure 3.9: XPS spectra for untreated and plasma treated ionomer glass for BE 450 -550 eV.

Table 3.3: XPS peak assignment of IG-0 and IG-PT25.

BE (eV)	IG-0	IG-PT25
60		Fe (3p)
75		Al (2p)
105	Si (2p)	Si (2p)
120		Al (2s)
135		P (2p)
155	Si (2s)	Si (2s)
287	C (1s)	C (1s)
403		N (1s)
535	O (1s)	O (1s)

3.1.1.5 Focused Ion Beam SEM

FIB results are presented in Figures 3.10. Figure 3.10a shows the cross-section of the plasma treated ionomer glass in 3D and Figure 3.10b in 2D, after the material removal from the upper part of the surface. Four different areas can be distinguished, and for each one a separate analysis was carried out. The depth that the beam cut the surface is approximately 8 μm and three distinct layers were observed. However, no differences can be found between them since they seem to have very similar composition as it can be observed from the EDS analysis shown in Figure 3.11.

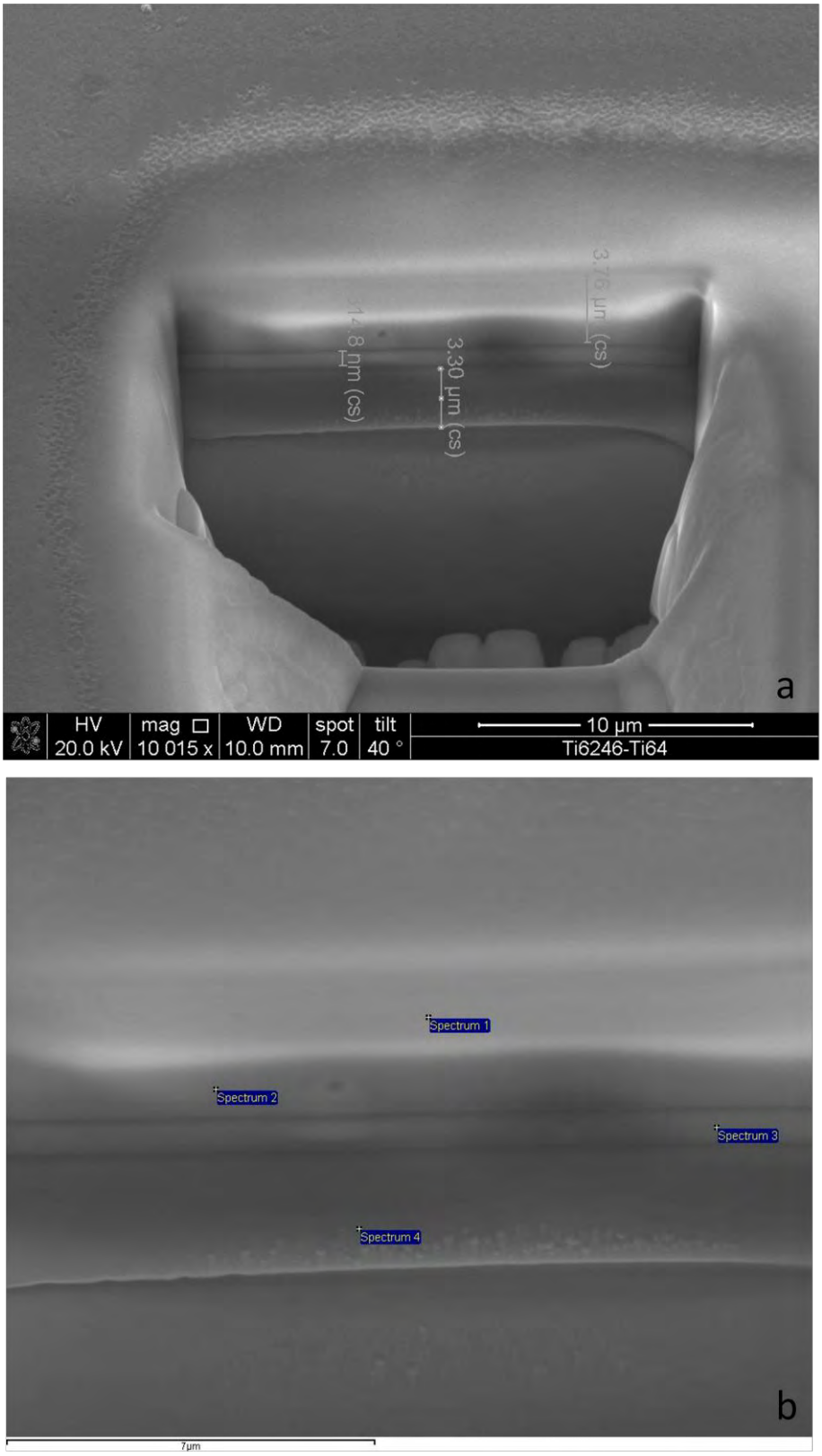

Figure 3.10: Cross-section of the plasma treated ionomer glass: a) 3D and b) 2D.

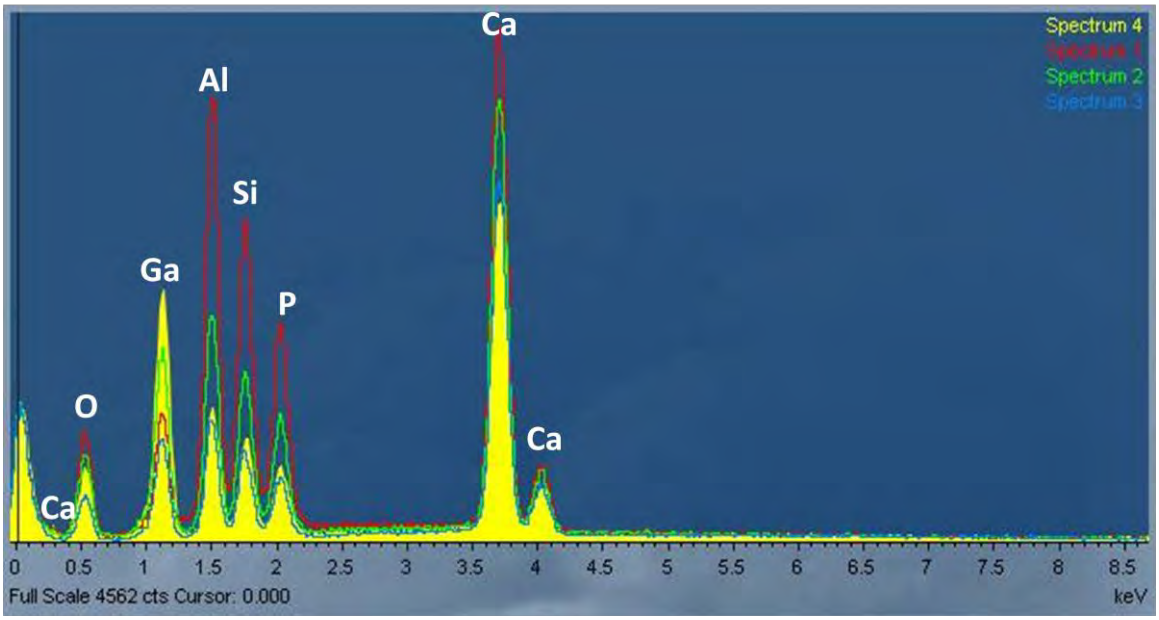

Figure 3.11: EDS spectra of all different areas on the treated ionomer glass surface.

3.1.1.6 SEM of fibroblasts seeded on the ionomer glass surfaces

Figure 3.12 shows 3T3 fibroblasts seeded on the surface of IG-0, whereas Figure 3.13 shows fibroblasts seeded on the surface of IG-PT25. From these images it is clear that there is no cell growth or attachment observed on the IG-0 surface. However, on the surface of the plasma treated ionomer glass the fibroblasts attach and proliferate. Fibroblast attachment, through the presence of cytoplasmic projections is evident.

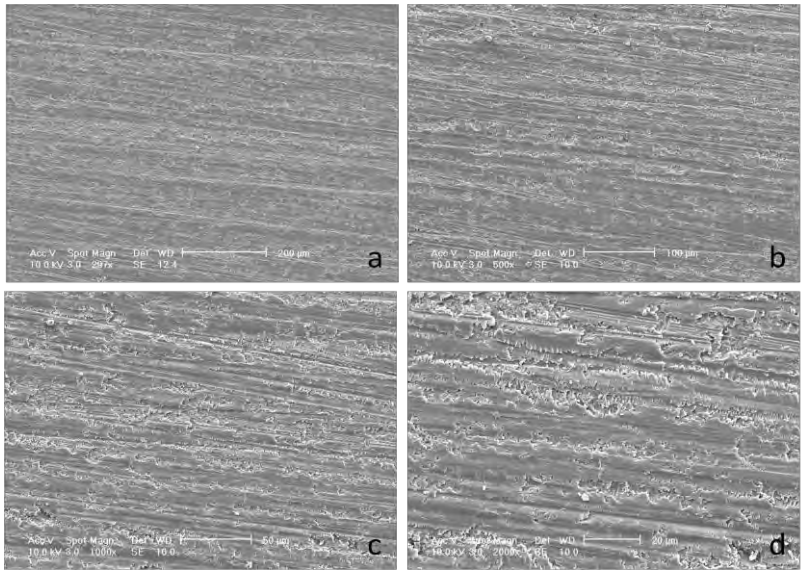

Figure 3.12: SEM micrographs of IG-0 seeded with fibroblasts with different magnifications: a) x297, b) x500, c) x 1000 and d) 2000.

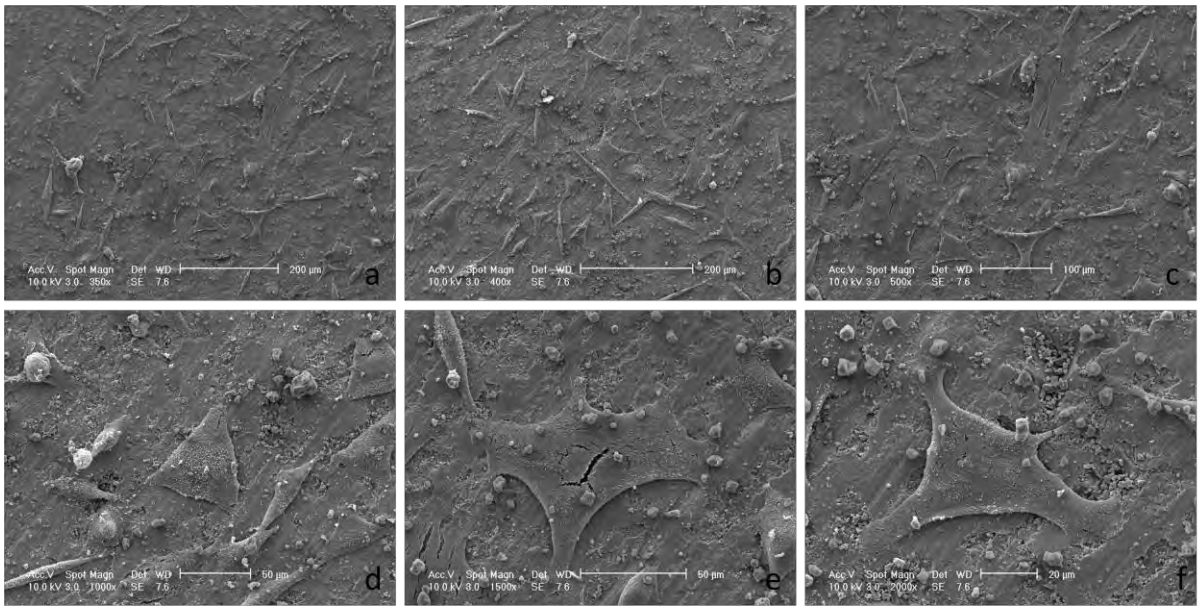

Figure 3.13: SEM micrographs of IG-PT25 seeded with fibroblasts with different magnifications: a) x350, b) x400, c) x500, d) 1000, e) x1500 and f) 2000.

3.1.2 Discussion

IG was treated by plasma nitriding for 1h at 400^{o}C in a gas mixture of 25%N_2 and 75%H_2. This treatment was generally proved to alter the materials properties such as surface hardness and elastic modulus, surface roughness and surface chemistry. Also cellular compatibility was induced to the glass surface after the treatment.

Nanoindentation measurements showed that IG-PT25 revealed improved hardness and elastic modulus compared to the untreated material. Figures 3.1a and b and Table 3.1 show clearly that the ASPN treated IG exhibits higher hardness and elastic modulus by ca 50% compared to IG-0. There is no literature available concerning plasma nitriding hardening effect on glasses; however, various other techniques have been used to achieve such results. Schrimph *et al.* have studied the incorporation of nitrogen into silicate melts and they showed that the incorporation of nitrogen onto the surface of glasses resulted in improvement of the surface physical properties, such as hardness, refractive index, chemical durability and T_g and the improvement is proportional to increase of nitrogen content [153]. Also, Grande *et al*. incorporated nitrogen on glass using quenching fused mixtures of nitrides and oxides on the glass surface or by reacting NH_3 with molten oxides. During these procedures, silicate and phosphate glasses showed increase of the surface hardness. It is believed that only one of the four oxygen atoms that surround the glass formers can be replaced by nitrogen. Thus, the suggested model is that divalent oxygen is substituted by trivalent nitrogen and consequently the produced glass network is more tightly linked [154].

In our case the improvement in hardness and elastic modulus is believed to happen through the process of the plasma nitriding treatment, which means that long treatment period and embedding of nitrogen on the surface improved the properties of the ionomer glass. It is important to mention that the treatment temperature does not have any effect on the

mechanical properties of the glass. This is because thermal analysis of the glass shows that the T_g is ~ 670^oC, a temperature that the glass network becomes mobile [155]. Thus we do not expect any annealing of the glass since the treatment was conducted below that temperature (400^oC). It is therefore expected, that the change in hardness and stiffness is due solely to the treatment with active screen plasma nitriding.

In addition to the hardness and elastic modulus, the surface roughness of IG changed after the treatment. Figure 3.2 shows the surface topography of both a) untreated and b) ASPN treated glass and Table 3.2 shows the numerical values of the surface roughness. As it can be observed, the surface roughness of the glass decreases after the treatment. The S_a difference between IG-0 and IG-PT25 is 44.48 nm and the S_q difference 48.02 nm, respectively. In general, the plasma surface modification results in an increase in surface roughness due to etching caused by bombardment of the surface with ions, absorption of light quanta from plasma and relaxation or recombination of free radicals[156]. In polymers for example it has been reported. that chitosan membranes after plasma surface modification when nitrogen was used as a working gas, exhibited an increase in the surface roughness. It was thought that the increase in surface roughness was due to plasma etching effects [140]. In our case the results are not in agreement with the literature since the materials surface become smother after the plasma treatment.

XRD was performed for the treated glasses and the diffractogram produced is presented in Figure 3.3. Figure 3.3 shows clearly that the treatment did not induce any change in the amorphous structure of the glass. As it can be observed, the diffraction pattern is very broad with a low signal to noise ratio. This is typical of an amorphous glass structure as it was expected, since the treatment temperature was much lower than the crystallisation temperature of the glass which is 793^oC [155].

One of the most important surface characteristic that must be tested when a surface is modified is the surface chemistry. Here various methods were used in order to be able to identify the surface chemical composition of the plasma treated ionomer glass. The first attempt was carried out using FT-IR spectroscopy. Unfortunately, the spectra could not give the appropriate information. The reason was that the diamond tip of the ATR FT-IR device did not have a good contact point with the glass, as the glass surface was quite brittle. As an alternative solution Raman spectroscopy was used. Figure 3.4a and b shows the Raman spectra for IG-0 and IG-PT25 respectively. From the untreated glass spectrum it can be observed that only one band has been detected at 1304 cm^{-1}. This band is associated with Si-O-Si bonds. A similar band at 1314 cm^{-1} is present in the spectrum of the treated glass surface. The band was slightly shifted but could be assigned to Si-O-Si stretching vibrations. One more band at 799 cm^{-1} is present in the plasma treated glass spectrum and can be attributed to the presence of Si-N groups. According to McMillan [157] the Raman spectra of silicate glasses can be described by four polarised bands: 1100-1050 cm^{-1}, 1000-950 cm^{-1}, near 900 cm^{-1} and near 850 cm^{-1}. Each band is assigned to symmetric Si-O stretching motions of the SiO_4 tetrahedra with 1, 2, 3 and 4 non-bridging oxygens, respectively [157]. The band at around 1300 cm^{-1} observed in our spectra was quite broad and it is very likely that in this area an overlapping of bands occurs. It was not expected that the silicon tetrahedra in the glass will have one or two non-bridging oxygens and therefore at least two peaks can be overlapping in this area. It cannot be explained why there is a shift but it is possible that this has to do with the network connectivity and the density of the glass network. In the spectrum of the IG-PT25, apart from the band at 799 cm^{-1}, more bands assigned to nitrogen containing groups were expected to be found. According to Bandet *et al*. who studied hydrogenated amorphous silicon nitride films using Raman spectroscopy, these bands should be found at: 3360 cm^{-1} (N-H stretching vibration), 3500 cm^{-1} (NH_2 stretching vibration), 2190 cm^{-1} (Si-H

stretching vibration) and 1140 cm^{-1} (N-H bending vibration). Also, the Si-N vibration should appear in the range of 700-1100 cm^{-1} [158]. Consequently, apart from the evidence of the nitrogen presence on the surface of the plasma treated glass no specific information about the layer formed after the plasma treatment can be retrieved. Thus in order to obtain more information about the surface chemistry further examination using XPS was conducted.

XPS spectra of the glass are shown in Figures 3.5-3.9 and the assignment of the peaks is presented in Table 3.3. More analytically, the spectrum of BE 50-150 eV is presented in Figure 3.5. Only one peak can be observed for the untreated glass surface at 105 eV representing the Si (2p) photoelectrons. In the same spectrum more peaks are observed at 60 eV associated with Fe (3p) photoelectrons due to contamination from the active screen and the steel specimen stub and at 75 eV and 120 eV associated with Al (2p) and Al (2s) photoelectrons, respectively. A very weak peak at 135 eV is associated with P (2p) photoelectrons. In Figure 3.6, Si (2s) peaks are present for both treated and untreated glass at 155 eV. However, for the plasma treated glass the peak is sharper. Unfortunately, there is no reasonable explanation of why this is happening. In Figure 3.7, a peak at 287 eV is present associated with C (1s) photoelectrons which is attributed to contamination due to the active screen. An unidentified peak is present at 278 eV. The XPS spectrum in Figure 3.8 shows clearly the presence of N (1s) at 403 eV for the treated glass surface and the spectrum in Figure 3.9 shows the presence of O (1s) at 535 eV on both untreated and plasma treated glass. The XPS analysis also revealed that the percentage of nitrogen that was found only on the plasma treated surface is 1.5% of the total elemental composition. To summarize, the XPS measurements showed only the presence of Si, C and O on the IG-0 surface, the reason that the XPS did not detect the rest of the elements is not clear. The spectrum of the IG-PT-25 however, showed the presence of Fe, Al, Si, P, C, O and N. A possible explanation could be that SiOH covered the outer part of the glass surface and after the plasma treatment a

rearrangement of the surface chemistry was caused, thus the rest elements were detected only after the treatment. Calcium, which is one of the main elements of the glass composition, was not detected in either treated or untreated glass, again it is not clear why. Fe and C are attributed to contaminations. Finally, as it was expected, nitrogen incorporation on the glass surface was achieved, possibly in the form of Si-N bonds, even though the amount of nitrogen (only 1.5%) is very small.

Figures 3.10-3.11 represent the FIB results of the plasma treated glass. From Figure 3.10 the cross section of the treated glass surface can be observed. The depth that the beam cut the glass was approximately 8 μm and three layers were found, the first is 3.76 μm, the second 0.814 μm and the third 3.30μm. Thus four different areas were found and analysed with EDS. In all EDS spectrum of all different areas the same elements were detected: Ca, O, Ga, Al, Si and P. The elements that EDS did not detect are Fluorine and Nitrogen. Ga is believed that it is a contamination. Also the intensity of the peaks that represent each element is higher at the outer part of the tested area, as the beam goes deeper the peaks are less sharp.

The ionomer glasses were subjected to biocompatibility tests. The method used to visualise the cell seeded untreated and plasma treated IG was SEM, employed for the observation of the cellular compatibility on the material surface. 3T3 fibroblasts were seeded with the same cell density on the ionomer glass surfaces for four days and then the samples were visualised with SEM after the appropriate fixation. Figure 3.12 (a-d) show fibroblasts seeded on the surface of IG-0 whereas Figure 3.13 (a-f) shows fibroblasts seeded on the surface of IG-PT25. From Figure 3.12 it is evident that there is no cell growth observed on the untreated glass surface. This is in good agreement with a previous work by Freeman *et al*. [86] where in an animal study the ionomer glass could not integrate well with bone and scar tissue formation was observed instead in the interface of the glass with the native tissue. On the

other hand, the implanted glass ceramic showed excellent integration with bone [77]. In our case, the ASPN treated amorphous glass IG-PT25 (Figure 3.13) showed very good cellular compatibility as well as cell prolifetarion, with the cells to be interconnected and exhibiting the appropriate stellate shape. Also the cytoplasmic extensions and the filopodia of the adjacent cells seem to be conjoined. It can be observed, that the fibroblast population is higher in the plasma treated surface in comparison to the untreated surfaces and the cells appear to be well attached to the surface.

Generally, plasma surface modification on a glass surface in order to study the attachment of cells has not been conducted before and there is no literature available in this area. However, plasma modification on glass has been studied extensively especially in the case of glass fibres in order to improve interfacial interaction in polymer composites when these fibres were used as reinforcing agents [88]. Cell culture studies have been conducted on glasses and glass-ceramics due to the fact that these materials enhance bone formation [159]. Garcia *et al*. examined the cellular compatibility of bioactive glass, synthetic hydroxyapatite and borosilicate glass using rat osteosarcoma cells. They covered all surfaces with fibronectin (Fn) in order to reinforce the cellular activity, their findings showed that only the bioactive glass had improvement of cell attachment after being covered with Fn, on the contrary borosilicate glass and hydroxyapatite did not show any improvement [134]. In our case, the inert ionomer glass, after the plasma treatment showed clearly the induction of cell compatibility and it is believed that this is due to the nitrogen incorporation on the glass surface. Unfortunately, it was not possible to examine further the glass samples and thus more detailed explanation concerning the changes in the materials composition due to the plasma treatment could not be conducted. So far, similar work has not been conducted to ionomer glasses, however the nitride effect on cell behaviour has been reported on polymeric materials which is discussed in the following chapters.

3.1.3 Summary

The surface of an ionomer glass composition (IG) was subjected to ASPN treatment for 1h at 400^{o}C in a gas mixture of 25%N_2 and 75%H_2. The treatment was proved to affect both surface characteristics and cellular compatibility of the glass. ASPN resulted in an improvement of mechanical properties of the IG which is attributed to the Nitrogen embedded on to the glass surface. The hardness and elastic modulus were increased by ca 50% whereas the materials surface morphology and roughness were also changed after the treatment with a decrease in S_a and S_q values. However, the surface structure remained the same as shown in the XRD diffractogram, since the glass maintained its amorphous structure after the treatment. The incorporation of 1.5 % nitrogen of the total elemental composition on to the surface resulted in the formation of Si-N bonds (as described in Raman spectra), showing that the treatment also affected the surface chemistry. Finally, the cell seeding tests showed that on the surface of the otherwise inert glass, after the treatment, fibroblasts attached and proliferated, showing that the treatment induced cellular compatibility. Thus, the plasma treated glass appeared to be a very good substrate for the fibroblast culture by enhancing cell adhesion. It is believed, that the above result is due to the introduction of nitrogen containing functional groups on the materials surface.

3.2 ASPN treatment of UHMWPE (25% N_2-75% H_2)

Prior to results and discussion for UHMWPE it is important to mention a few structural characteristics of the polymer in order to understand the possible changes in the materials properties because of the plasma treatment. First of all, the molecular weight of the UHMWPE that was used in this study is very high and in the order of 9×10^6 g/mol. The polymer chains are linear and mostly aligned in the same direction and each chain interacts with the others by Van der Waals secondary bonds resulting in a strong polymer structure, despite the relatively weak bonds between the molecules. It is clear, that UHMWPE derives ample strength and durability from the length of each individual molecule and the preferred orientation of the chains. Due to the linear chains, UHMWE does not have side chemical groups like esters, amides or hydroxyl groups and therefore the polymer exhibits strong resistance in chemical degradation and radiation [160].

3.2.1 Results: Materials characterization and cellular compatibility of UHMWPE first treatment (ASPN-1)

UHMWPE was subjected to ASPN in the presence of 25% N_2 and 75% H_2. The untreated material thermal analysis and the surface mechanical properties, surface roughness and chemical structure of untreated and plasma treated UHMWPE are presented and discussed below. The cell compatibility testing using SEM imaging is also presented.

3.2.1.1 Differential scanning calorimetry (DSC)

The T_m and T_c of UHMWPE were measured by DSC. As it is shown in Figure 3.14 the T_m is 132°C with an onset softening temperature of about 88°C and crystallization on cooling occurs at T_c =118°C. The degree of crystallinity was found 47.7% and was calculated from the equation:

$$\text{Crystallinity\%} = (\Delta H_{\text{sample}}/\Delta H_{\text{UHMWPE}}) \times 100$$

For the degree of crystallinity calculation it was taken into consideration that the fusion enthalpy of the fully crystalline UHMWPE is ΔH_{UHMWPE} = 290 J g^{-1} as reported by Reggianni *et al* [161].

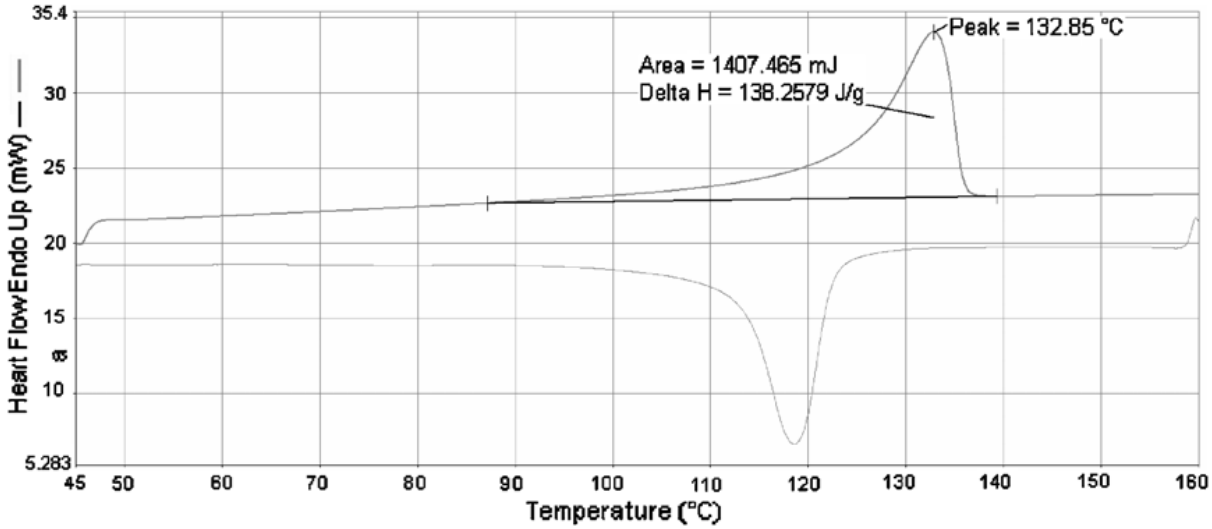

Figure 3.14: DSC trace of untreated UHMWPE.

3.2.1.2 Mechanical properties of untreated and ASPN-1 treated UHMWPE

The mean values of hardness and elastic modulus of PE-0, PE-PT25-1, PE-PT25-2 and PE-PT25-3 are shown in Table 3.4, whereas the change in hardness and elastic modulus of all UHMWPE samples with treatment time are shown in Figure 3.15. As it can be observed, the

untreated sample (PE-0) exhibits lower hardness and modulus compared to the treated samples. The duration of treatment does not seem to affect significantly the hardness and modulus of treated samples although a slight increase in modulus was observed for PE-PT3 which was treated for 60 min.

Table 3.4: Hardness (a) and Elastic modulus (b) results 25% N_2 ASPN treated and untreated UHMWPE samples.

Material	Hardness (GPa)	Elastic modulus (GPa)
PE-0	0.08 (±0.01)	1.54 (±0.27)
PE-PT25-1	0.14 (±0.07)	2.26 (±0.89)
PE-PT25-2	0.14 (±0.03)	2.22 (±0.33)
PE-PT25-3	0.13 (±0.02)	2.45 (±0.37)

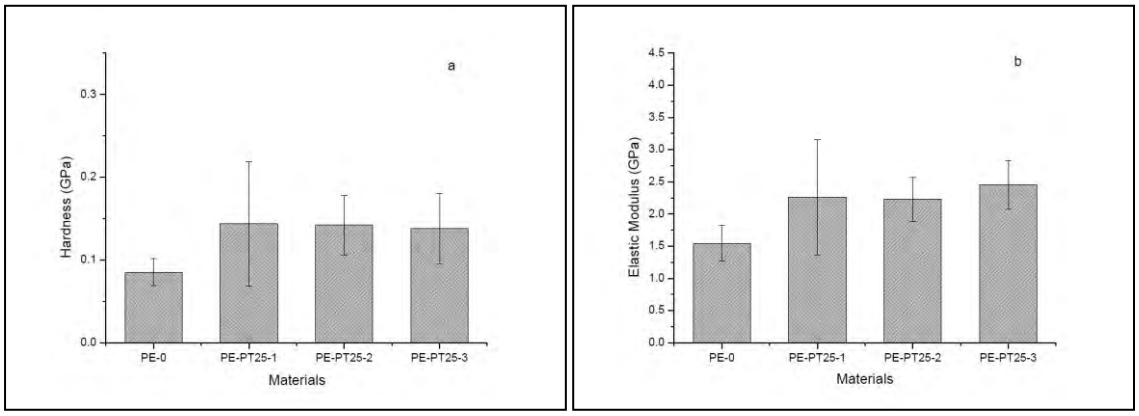

Figure 3.15: a) Hardness and b) Elastic modulus of 25% N_2 ASPN treated and untreated UHMWPE samples.

3.2.1.3 Surface roughness untreated and ASPN-1 treated UHMWPE

Figure 3.16 shows the white light interferometry results, surface topography and the 3D image of both treated and untreated samples. Figure 3.17 shows the numerical values of both S_a and S_q. The surface roughness of UHMWPE does not seem to change significantly after the ASPN treatment.

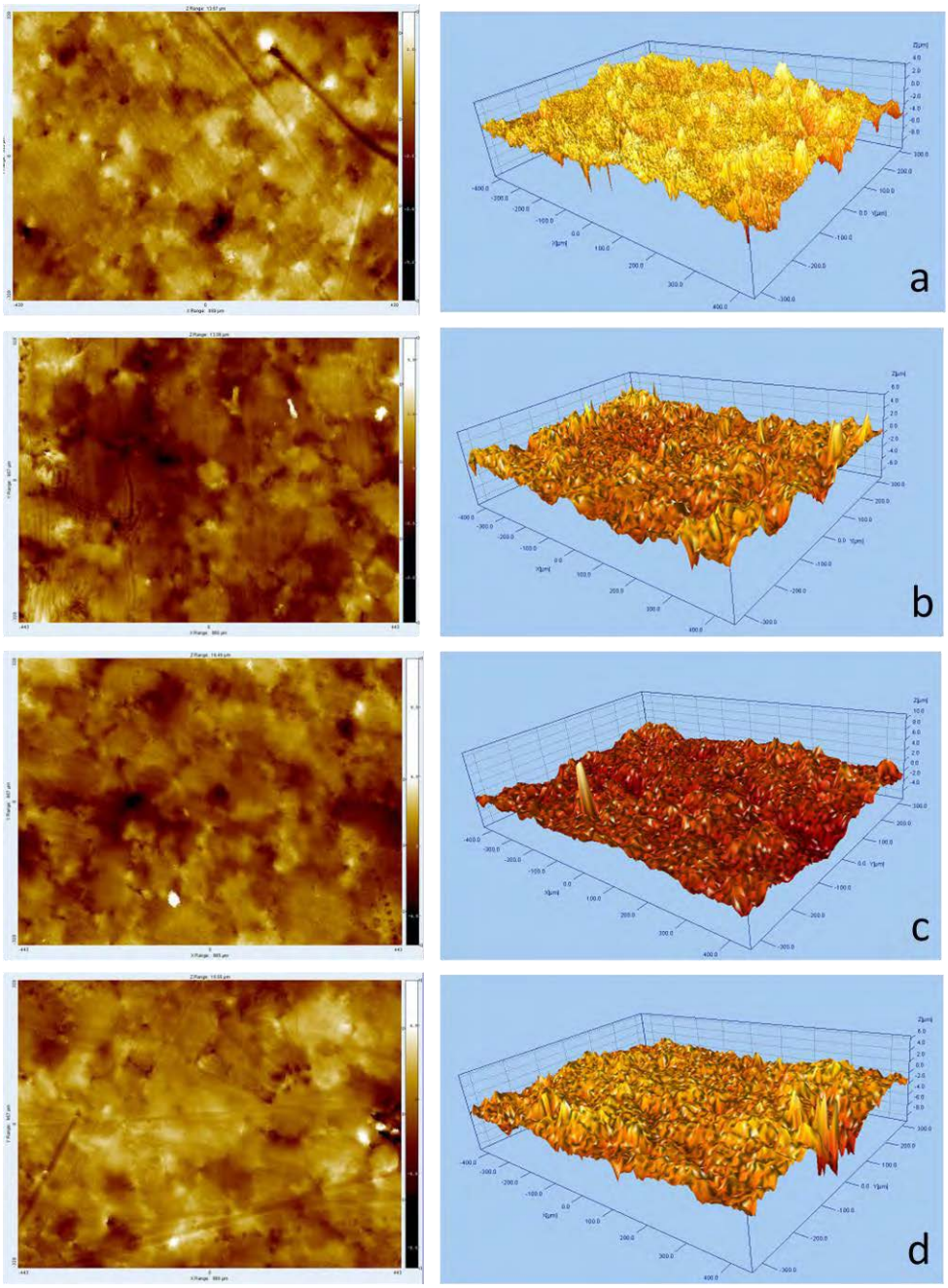

Figure 3.16: Surface topography of all 25% N_2-75% H_2 ASPN treated and untreated samples and the 3D images of sample surfaces a) untreated, b) 10 min c) 30 min and d) 60 min treated.

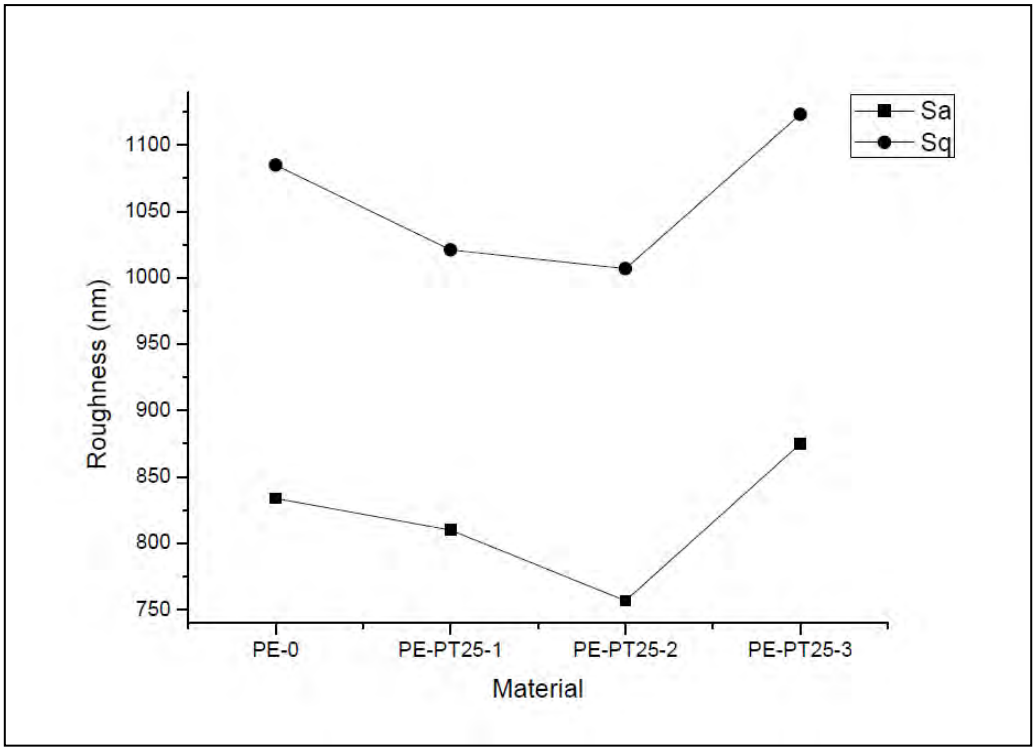

Figure 3.17: Numerical values of S_a and S_q for untreated and 25% N_2 ASPN treated UHMWPE obtained with white light interferometry.

Apart from white light interferometry measurements, AFM was also contacted to measure the surface roughness of plasma treated and untreated UHMWPE. Figure 3.18 shows the topography of a) untreated, b) 10min c) 30 min and d) 60min treated samples. Figure 3.19 shows the numerical values of both S_a and S_q. As it can be observed the results are similar to those obtained by white light interferometry, meaning that the roughness does not change significantly after the treatment.

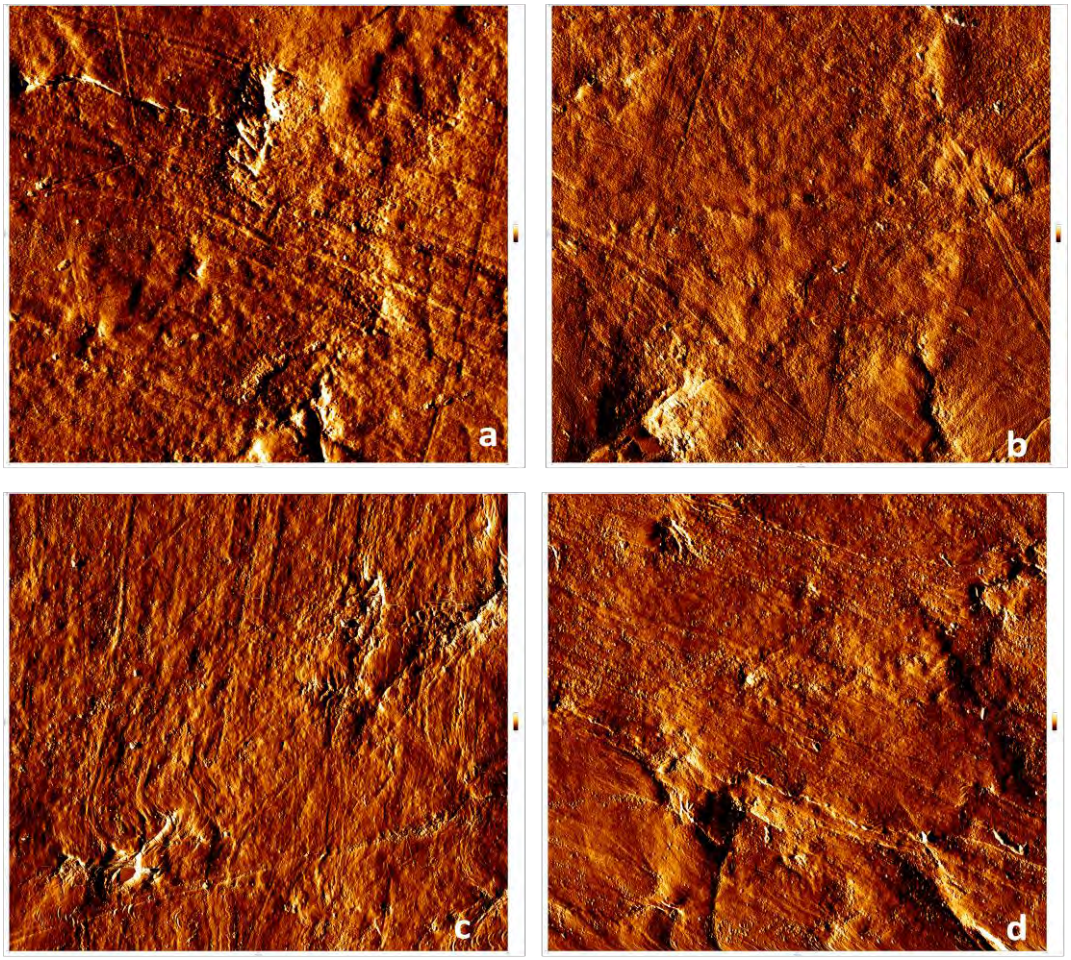

Figure 3.18: AFM imaging of the topography of a) untreated, b) 10 min, c) 30 min and d)60 min UHMWPE samples.

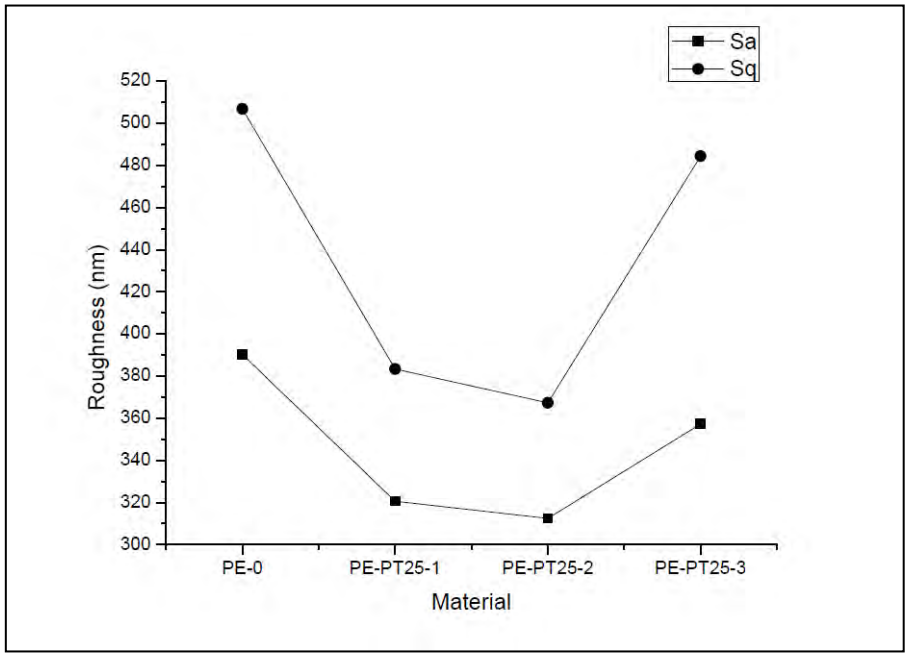

Figure 3.19: Numerical values of S_a and S_q for untreated and 25% N_2 ASPN treated UHMWPE obtained by AFM.

3.2.1.4 Chemical composition of untreated and ASPN-1 treated UHMWPE

Figure 3.20 presents the FT-IR spectra of plasma treated and untreated samples separately and Figure 3.21 is summarizing all spectra together. The description of the main FT-IR peaks is given in Table 3.5. Generally, only some small differences were observed in the FT-IR spectra between the treated and untreated samples. In all samples, the bands that represent the CH_2 bonds, that are characteristic for UHMWPE are present (717, 719, 1462, 2846 and 2914 cm^{-1}). However new bonds can be only observed for the 30 min and 60 min treated samples. For the PE-PT25-2, nitrogen containing groups such as NO_3^- and C-N and new bonds containing carbon such as C-O and C=C have been formed on the materials surface after the treatment. Finally, for the PE-PT25-3 sample apart from the CH_2 groups C-N bonds are present on the surface.

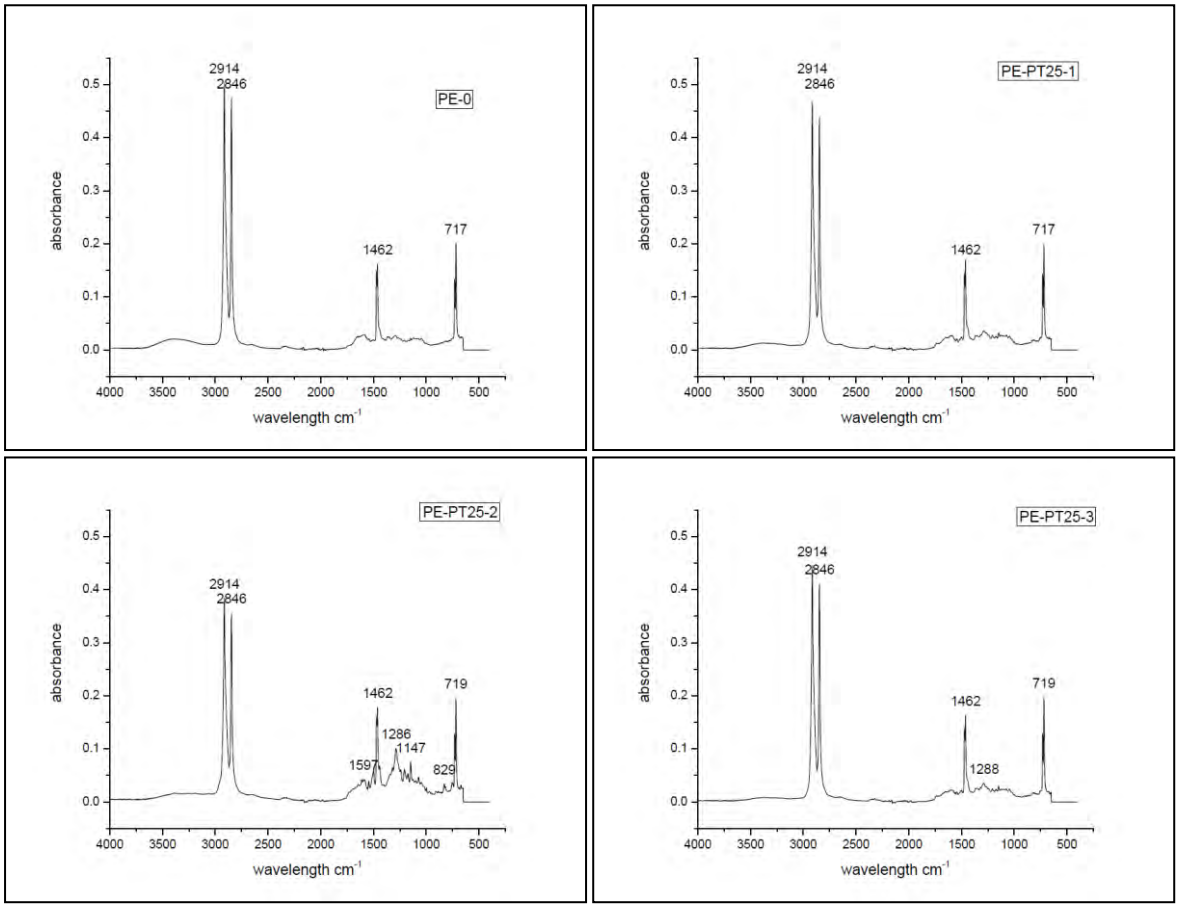

Figure 3.20: FT-IR spectra of untreated (PE-0) 10 min (PE-PT25-1). 30 min (PE-PT25-2) and 60min (PE-PT25-3) 25% N_2 plasma treated UHMWPE samples.

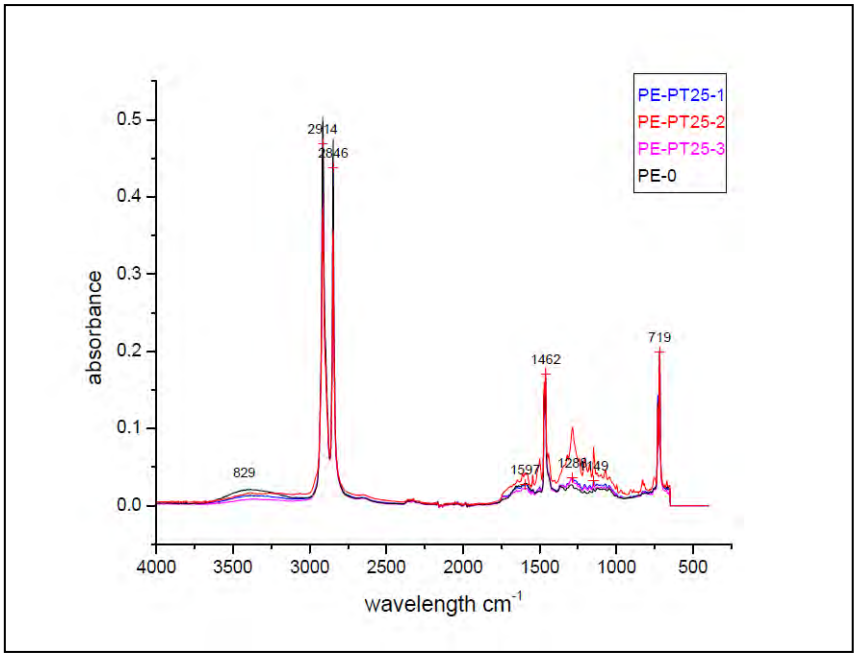

Figure 3.21: FTIR summary spectrum of the untreated and plasma treated UHMWPE samples.

Table 3.5: Description of the main FT-IR peaks.

Characteristic preaks cm^{-1}	**Description**
717	$-CH_2-$ In plane streching vibration
719	$-CH_2-$ In plane streching vibration
829	$-NO_3-$
1147	-C-O- Stretching vibration
1286	-C-N- Stretching vibration
1288	-C-N- Stretching vibration
1462	$-CH_2-$ Non-symmetric stretching vibration
1596	-C=C- Stretching vibration
2846	$-CH_2-$ Symmetric stretching vibration
2914	$-CH_2-$ Non-symmetric stretching vibration

For more detailed analysis of the surface chemistry of the ASPN UHMWPE, XPS was also employed. Figures 3.22-3.36 show the XPS survey spectra and the deconvoluted C1s, O1s and N1s high resolution spectra of the untreated and the 25% N_2-75% H_2 plasma treated samples. Table 3.6 shows the assignment of the deconvoluted peaks of all the three elements. All materials showed the presence of carbon and oxygen whereas only the treated surfaces contained also presence of nitrogen. C1s peak is found at ~285 eV, O1s at ~532 eV and N1s at ~400 eV. The N/C and O/C ratios are given in Figure 3.37 and the numerical values of the elemental composition are presented in Table 3.7.

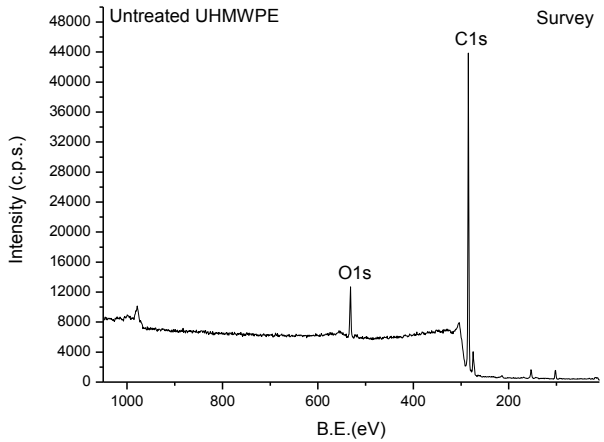

Figure 3.22: Survey spectrum of untreated UHMWPE.

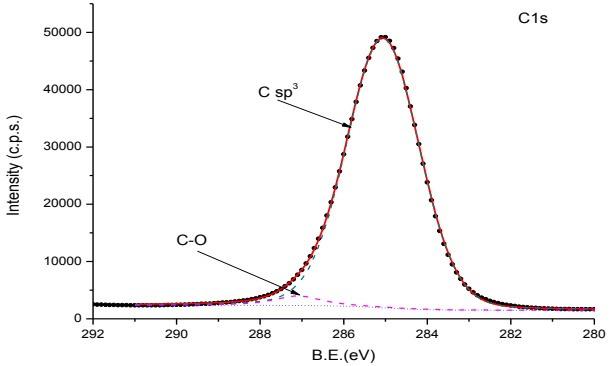

Figure 3.23: C1s peak deconvolution of untreated UHMPWE.

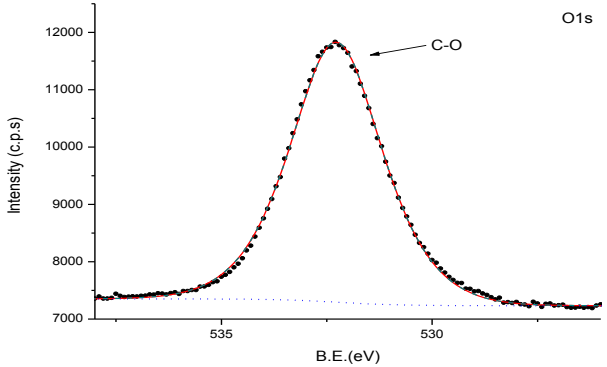

Figure 3.24: O1s deconvolution of untreated UHMWPE.

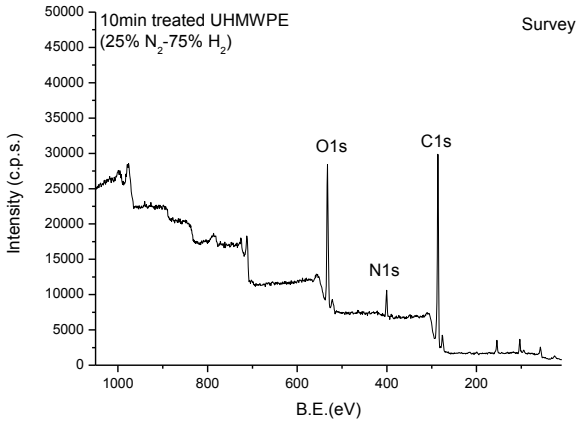

Figure 3.25: Survey spectrum of 10 min 25% N_2-75% H_2 plasma treated UHMWPE.

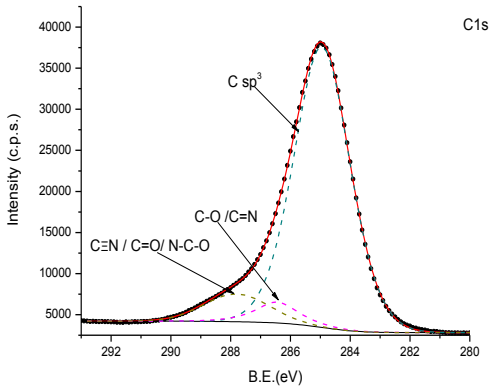

Figure 3.26: C1s peak deconvolution of 10 min 25% N_2-75% H_2 plasma treated UHMWPE.

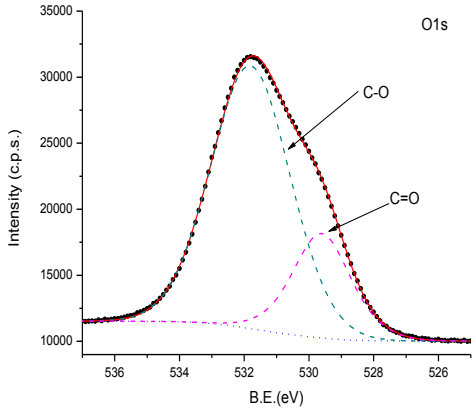

Figure 3.27: O1s peak deconvolution of 10 min 25% N_2-75% H_2 plasma treated UHMWPE.

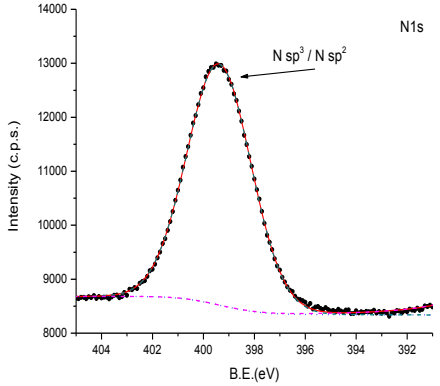

Figure 3.28: N1s peak deconvolution of 10 min 25% N_2-75% H_2 plasma treated UHMWPE.

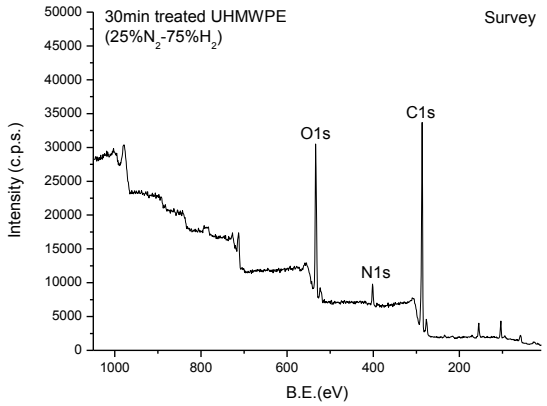

Figure 3.29: Survey spectrum of 30 min 25% N_2-75% H_2 plasma treated UHMWPE.

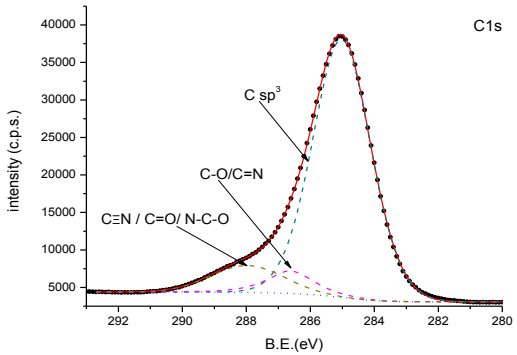

Figure 3.30: C1s peak deconvolution of 30 min 25% N_2-75% H_2 plasma treated UHMWPE.

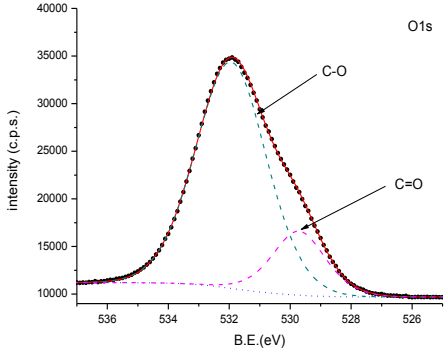

Figure 3.31: O1s peak deconvolution of 30 min 25% N_2-75% H_2 plasma treated UHMWPE.

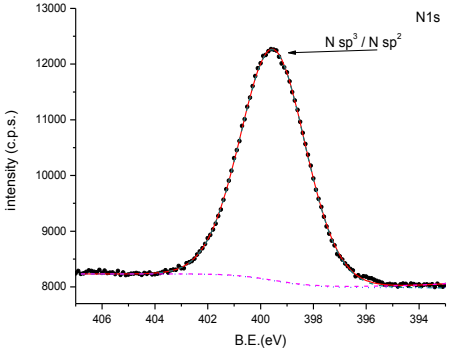

Figure 3.32: N1s peak deconvolution of 10 min 25% N_2-75% H_2 plasma treated UHMWPE.

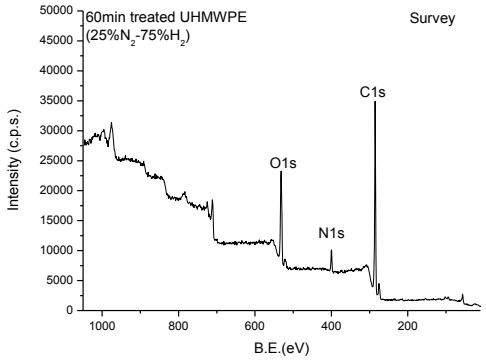

Figure 3.33: Survey spectrum of 60 min 25% N_2-75% H_2 plasma treated UHMWPE.

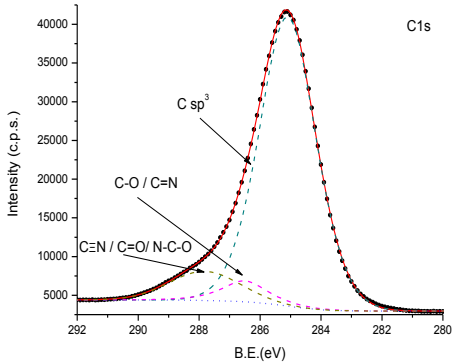

Figure 3.34: C1s peak deconvolution of 60 min 25% N_2-75% H_2 plasma treated UHMWPE.

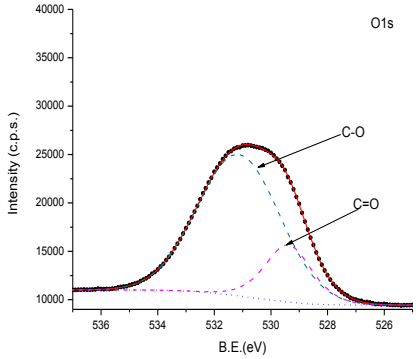

Figure 3.35: O1s peak deconvolution of 60 min 25% N_2-75% H_2 plasma treated UHMWPE.

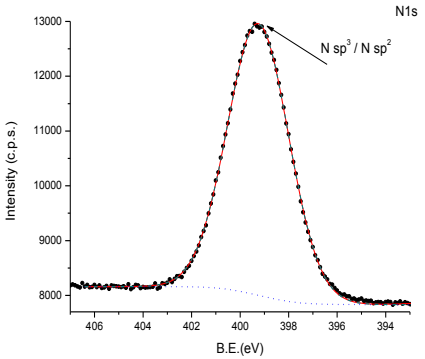

Figure 3.36: N1s peak deconvolution of 10 min 25% N_2-75% H_2 plasma treated UHMWPE.

Table 3.6: Assignment of deconvoluted peaks C1s, O1s, N1s.

Material	C1s	Assignment	O1s	Assignment	N1s	Assignment
Untreated UHMWPE	285.05 287.1	C-C C=O	532.3	C-O		
10min (25%N_2-75%H_2)	284.94 286.50 287.83	C-C C-O / C=N C=O/ C≡N/ N-C-O	529.64 531.87	C=O C-O	399.46	C-N / C=N
30min (25%N_2-75%H_2)	285.05 286.65 288.00	C-C C-O /C=N C=O/ C≡N/ N-C-O	529.73 531.96	C=O C-O	399.56	C-N / C=N
60min (25%N_2-75%H_2)	285.11 286.51 287.9	C-C C-O / C=N C=O/ C≡N/ N-C-O	529.37 531.22	C=O C-O	399.30	C-N / C=N

Table 3.7: Elemental composition of untreated and ASPN 25% treated UHMWPE.

Material	Carbon %	Oxygen %	Nitrogen %
PE-0	91.572	8.427	0
PE-PT25-1	57.984	35.392	6.622
PE-PT25-2	58.471	35.154	6.373
PE-PT25-3	62.075	30.870	7.053

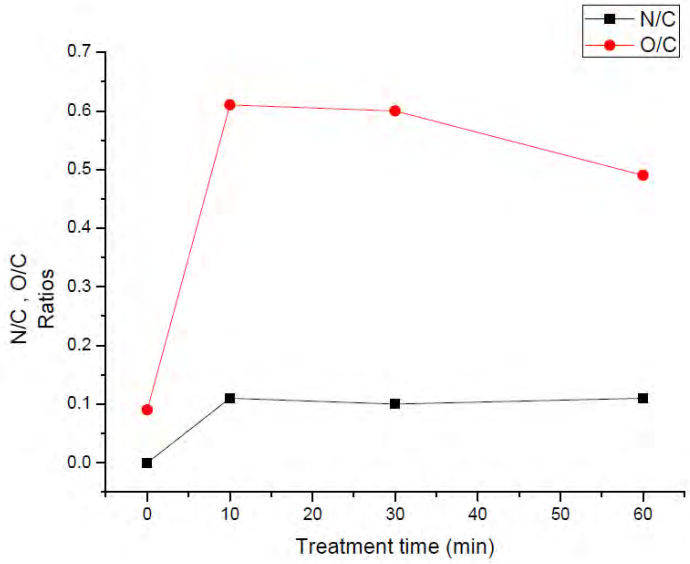

Figure 3.37: N/C and O/C ratios of the UHMWPE ASPN 25% treated and untreated samples.

3.2.1.5 Cell Compatibility Tests

Figure 3.38 shows fibroblasts seeded on PE-0, PE-PT25-1, PE-PT25-2 and PE-PT25-3 surfaces. The magnification range varies from x150 to x1800. A slight cell attachment was observed in the case of untreated samples (PE-0). Moreover, the cells were dispersed across the polymer surface, they did not seem to be connected with each other and they look unhealthy (Figure 3.38a and b). Better attachment and proliferation across the polymer surface was observed in the case of PE-PT25-1. Despite the fact, that fibroblasts had their edges connected, there were still big gaps among the cells (Figure 3.38c and d). On the other hand, in the case of PE-PT2 (Figure 3.38e and f) the fibroblasts were better connected with each other compared to PE-0 and PE-PT1 and were attached to the surface. However, the cells did not look healthy as body cracks could be observed caused probably by the treatment required to process SEM samples. The fibroblasts on the surface of PE-PT25-3 looked healthier, the cell attachment was improved and the cells exhibited a larger degree of

proliferation. The cells were well connected with each other forming layers of cells on the treated polymer surface. However, isolated cells appeared to be damaged due to the fixation treatment as was mentioned above. The fibroblasts preference to adhere on the treated surfaces rather than the untreated one was clear in Figures 3.38.g and h.

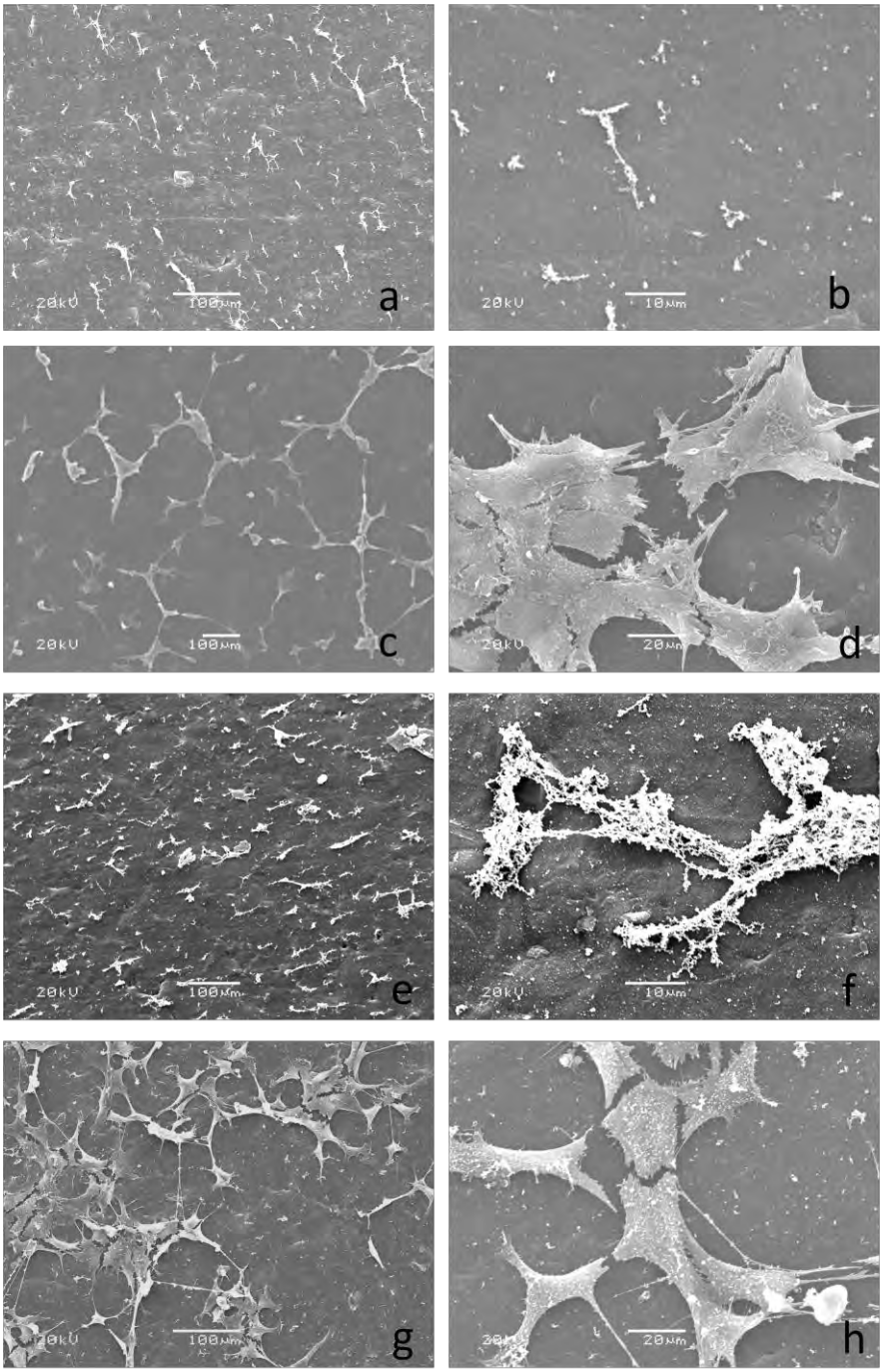

Figure 3.38: SEM micrographs of UHMWPE seeded with fibroblasts; (a and b) PE-0, (c and d) PE-PT25-1, (e and f) PE-PT25-2, (g and h) PE-PT25-3.

3.2.2 Discussion

The first plasma treatment that UHMWPE was subjected was at 120^{o}C, in a gas mixture of 25% N_2 and 75% H_2 and for three different durations, 10, 30 and 60 min. All treated samples together with the control were subjected to surface characterization first, in order to examine the plasma nitride effect on the materials surface.

Initially, nanoindentation measurements were conducted. Figure 3.15 a and b show the hardness and elastic modulus results, respectively and Table 3.4 presents the numerical values of the measurements. It is clear, that after the treatment all treated materials exhibit higher hardness and elastic modulus compared to the untreated UHMWPE. Also, it can be observed that all treated samples show almost the same increase of their mechanical properties independently of the duration of the treatment, although a slight increase in modulus was observed for the 60 min treated sample.

It is well known, that the degree of crystallinity can significantly affect the mechanical properties of UHMPWE. More specifically, in the case of recrystallization on heating both tensile strength and modulus of elasticity could increase [162-163]. In our case, the plasma treatment was conducted at 120 ^{o}C and at 90 ^{o}C. At 120 ^{o}C is possible that softening of the polymer chains occur. However, crystallization on heating was not observed in the DSC curve (Figure 3.14.) and therefore crystallisation is not expected at the temperatures at which the treatment took place (120 ^{o}C and 90 ^{o}C). Therefore it is clear that the increase in mechanical properties of the treated UHMWPE surface was caused only due to the plasma treatment.

Plasma techniques in general have been proven to enhance the mechanical properties of a polymer surfaces [164-166]. Hardening and stiffening are the most proven effects on plasma treated polymers. The most common explanation of this effect is that when a polymer is

plasma treated or ion implanted, cross linking is caused on the polymers chains, thus a three dimensional connected network is encouraged to form. The cross linking on the polymer surfaces results in a very strong chemically bonded network and in increasing rigidity of the backbone structure and restraining of the movement of the polymer chains. Consequently, improvement of the dimensional stability, hardness and elastic modulus is achieved [167].

Dong *et al*. have been investigated the effect of plasma on medical grade UHMWPE using the technique of plasma immersion ion implantation (PIII). It was reported, that the surface hardness and elastic modulus of the treated UHMWPE were both significantly increased. This improvement was attributed to the ion introduction on the polymers surface which creates a crossed-linked and therefore rigid 3D network that involves covalent bonds [74]. Similar results have been obtained by Toth *et al.* who treated UHMWPE using hydrogen plasma immersion ion implantation. The treatment was found to be beneficial for the materials mechanical properties increasing the surface hardness and elastic modulus [168].

Another surface characteristic has been shown to change after plasma treatment, the surface roughness. Here, the surface roughness of untreated and plasma treated UHMWPE was tested using white light interferometry and AFM. The topography of the materials is shown in Figures 3.16 and 3.18 and the numerical values of the measurements are presented in Figures 3.17 and 3.19, respectively. As mentioned previously, plasma methods have been proved to increase the surface roughness [63, 140]. Sanchis *et al*. treated low density polyethylene with RF oxygen plasma and observed that the surface roughness of LDPE was increased after the treatment. It is thought that one of the plasma effects on the polymers surface is etching, as a result of the introduction of plasma species on the materials surface; consequently this causes increase of surface roughness and improves surface wettability. AFM analysis showed that the surface roughness increases with an increase of the plasma treatment time [169]. In our case, however the surface roughness did not change significantly due to the treatment. A

possible explanation could be that the surface of UHMWPE already exhibited a degree of roughness (Sa = 834 nm) as shown in Figure 3.17.

Following to the surface mechanical properties and morphology, the chemical composition was also studied using FT-IR spectroscopy and XPS. This is because the main effect of nitrogen plasma surface modification method is the surface functionalization by inserting polar groups in to the materials surface. The active species present in the plasma gas interacts with the polymer surface resulting in the formation of free radicals, which functionalize the surface. According to Shanchis *et al.* nitrogen plasma can functionalise a surface after chain scission during the treatment that results in the formation of free radicals [170]. Thus it is very important to analyse in details the changes on the surface chemistry caused by ASPN.

Figure 3.20 represents the FT-IR spectra of plasma-treated and untreated samples. The description of the main FTIR bands is given in Table 3.5. Generally, only some small differences were observed in the FTIR spectra between the treated and untreated samples and the description of peaks is in good agreement with the literature [171-172]. The FTIR spectra for the plasma-treated and untreated samples (Figure 3.20) showed that untreated and 10 min treated samples had very similar bands indicating that the surface chemistry did not change significantly due to the ASPN treatment. The situation however is different in the case of PE-PT25-2. Clearly, nitrogen containing groups are present shown by the presence of bands at 829 cm^{-1} associated with N−H stretching vibrations and at 1288 cm^{-1} associated with C−N stretching vibrations leading to the conclusion that new bonds were formed on the surface after the treatment. The surface of PE-PT25-3 appeared to be also affected by the plasma treatment. However, only the band at 1288 cm^{-1} shows the presence of nitrogen since it is assigned to C-N stretching vibration since it was not possible to resolve all the bands observed in the case of PE-PT25-2. This could not be explained as it was expected that the

effect of treatment on the surface chemistry would be stronger after 60 min. Teodoru *et al.* [63] reported that N_2 plasma treatments of polymer surfaces can induce the formation of olefinic hydrocarbons and the surface becomes more dense due to the increase in C=C bonding. A similar observation was made in the case of PE-PT25-2 where a peak at 1596 cm^{-1} associated with C=C stretching vibration is present. In addition, due to sample exposure in air during sample transfer, possible oxidation could occur that would result in surface cross-linking due to the presence of C=C bonds resulting in an increase in hardness and modulus of the surface [63].

The main effect of nitrogen containing plasma treatments is the functionalisation of the polymer surface by inserting new polar groups onto the materials surface (such as oxygen containing species) . It is believed that the functionalisation with nitrogen plasma occurs due to chain scission which promotes the formation of free radicals during the treatment [170]. From the low resolution spectra (Figures 3.22, 3.25, 3.29, 3.33) carbon (C 1s at 285 eV), oxygen (O 1s at 532 eV), and nitrogen (N 1s at 400 eV) contributions can be clearly distinguished. These chemical assignments are in accordance with Beamson and Briggs [173]. In our case, the plasma treatment in a gas mixture of 25% N_2 + 75% H_2 shows the insertion of new oxygen and nitrogen containing groups (Figures 3.22-3.36).

Starting from the untreated UHMWPE analysis (Figure 3.22-3.24) two peaks are present: the expected C1s photoelectron peak and the O1s peak which is attributed to surface contamination due to air exposure (explained later). The deconvoluted C1s peak appears to have contributions from two peaks: the first at 285.05 eV is assigned to sp^3 carbon atoms and the second of much smaller intensity at 287.1 eV which is assigned to C=O bonds. The surface of the untreated material is quite pure since it contains very small amount of oxygen (8.4%) out of the total elemental composition (Table 3.7). After the treatment the C1s

photoelectron peak changes as it is shown in Figures 3.26, 3.30 and 3.34. It is clear that after 10, 30 and 60 minutes of treatment very similar bonds have been formed on the UHMWPE surface. Binding energies of 284.94 eV, 285.05 eV and 285.11 eV are attributed to C-C bonds, binding energies of 286.5 eV, 286.65 eV and 286.51 eV are attributed to C-O and C=N bonds and binding energies of 287.83, 288.00 and 287.9 are attributed to C=O, C≡N and N-C-O bonds. Similar results have been suggested in the literature. Marcondes *et al.* have modified the surface of UHMWPE by plasma immersion ion implantation. After the treatment the C1s deconvolution showed four different contributions at 284.4 eV, 285.2 eV, 286.6 eV, and 288.3 eV corresponding to C=C, C-C, C-O and C=O/O-C-O bonds[174]. Gancarz *et al*. have studied ammonia pulsed plasma treatment on polymer films. After XPS deconvolution measurements on the plasma treated films they found that the C1s peak can be attributed to five different chemical assignments: 284.5 eV to C-C bonds, 285.6 eV to C-N bonds, 286.6 eV to C-O and C=N bonds, 287.8 eV to C=O and O=C-NH bonds and 288.5 eV to C≡N bonds. They believe that the nitrogen that is present on the polymer surface after the treatment appears mainly in the form of C-N groups [175]. Arefi-Khonsari *et al.* used low frequency ammonia plasma to modify the surface of polypropylene. The deconvoluted C1s photoelectron peak showed the formation of C-N, C-O, C=O and N-C=O groups [176]. Similar observations were reported by Vesel *et al*. for PET nitrogen containing plasma treatment. Their XPS results showed that after the nitride treatment all samples exhibited a peak at a binding energy of 287.4 eV which was attributed to amide carbon atoms in O=C-N groups. More specifically they believe that C-N bonds are found in the region of 285.5-286.3 eV, C=N in the region of 285.5-286.6 eV and C≡N bonds in the region of 286.7-287.0 eV [177]. Thus, in our case the plasma treated UHMWPE shows similar behaviour of C1s photoelectron peak to previously investigated polymers.

Furthermore, the O1s photoelectron peak appears to change due to the treatment as well. For the untreated sample (Figure 3.24) the peak is symmetrical and corresponds to C-O bonds. For all the plasma treated materials (Figures 3.27, 3.31, 3.35) the O1s peaks are asymmetrical and their deconvolution showed the presence of C=O bonds around 529 eV (Table 3.7). In the literature O1s deconvoluted peaks are assigned to similar bonds [173]. Arpagaous *et al.* have treated the surface of HDPE with oxygen plasma. The fitting of the O1s photoelectron peak revealed the presence of two oxygen species. The first at 532.5 eV contained contributions of binding energies at 532.3 and 532.6 eV corresponding to C-O and C-O-C groups respectively, and the second at 533.6 eV which corresponds to the O-C-O species [178]. Wilson *et al*. treated PTFE surface with low power plasma using N_2 and NH_3 gas. Their XPS analysis showed that the spectra of O1s photoelectrons were broader compared to the untreated material and could be resolved into three different groups: C=O at 532 eV, C-O at 533 eV and O-C=O at 534.5 eV [179]. From Table 3.7 a considerable increase in the oxygen contribution from 8% on the untreated materials surface is approaching 30-35% even if oxygen was not a part of the gas mixture. The presence of oxygen after the plasma treatment can be explained as 1) oxygen impurities in the plasma chamber and 2) post plasma reactions due to the sample exposure to air during the transfer (post plasma functionalisation) given that the species that are generated during the treatment are unstable and thus readily react [170, 180]. In our case it is believed that the bonds that contain oxygen can be attributed to chemisorption of oxygen as a result of exposure to air during sample transfer and this is the reason of the increased amount of oxygen that was found in the elemental composition. According to Kurtz [181] UHMWPE might contain peroxides used for cross-linking during the processing of the polymer to rods or sheets. These peroxides during plasma treatment may form free radicals along the polymer chains that could lead to oxidation of the surface resulting in the formation of ketones, alcohols, esters and carboxylic acids. Although there is

no direct evidence of surface oxidation nor any optical change in the morphology of the surface after treatment, oxidation of the surface cannot be ruled out completely. Also Arefi *et al.* attribute the presence of oxygen on the surface to either the surface oxidation in the plasma chamber due to residual air or to post oxidation after the exposure of the sample to ambient air, interfered with the incorporation of nitrogen species into the surface, because of the competition of the active sites by oxygen species [176]. It has been reported by Junkar *et al*. who treated polymers with nitrogen plasma, they found out that the concentrations of nitrogen and oxygen increased during only 3s of treatment, thus surface saturation with these elements was completed within this duration and further treatment did not affect chemically the materials surface [182]. Thus we believe that the peaks around 532 eV are associated with carbon-oxygen groups created during or after the plasma treatment due to possible oxidation and post reactions on the UHMWPE surface. However, from the elemental analysis it can be observed that the % of oxygen is almost the same for all treated samples (~35%), thus the duration of the treatment did not affect the formation of carbon-oxygen bonds on the surface.

N1s photoelectron peaks are found at 399.46 eV for 10min treated UHMWPE, at 399.56 for the 30 min and at 399.30 for the 60 min. The high resolution spectra (Figures 3.28, 3.32 and 3.36) show that the N1s peaks are symmetrical and the deconvolution did not reveal more peaks. According to the literature the peaks at ~399 eV are contributions of N sp^2 and N sp^3 bonds [173, 175, 179]. Toth et al. have treated with nitrogen ion implantation UHMWPE surfaces. The XPS measurements that they conducted detected the N1s peak at around ~402 eV and 398.5 eV. They attributed the presence of these peaks to C=N and C-N bonds, respectively [183]. Another study on the characterization of CN_x layers that were grown on Si and NaCl slides using DC plasma nitride showed peaks at 398.3 eV assigned to N=C bonds and 400.2 eV assigned to N-C bonds [184]. A review on the characterization of nitride coatings with XPS, was conducted by Bertoti [185]. The assignment of the N(1s) peak that he

suggests is based on N-implanted polyethylene, thus the binding energy of 398.3 eV is attributed to C=N bonds, at 400.7 at N-C bonds and to nitrogen incorporated ring structure [185]. N1s photoelectron peak deconvolution was examined by Arefi *et al.* who treated polypropylene with low frequency NH_3 plasma. The peak was deconvoluted into two peaks at 399.2 eV assigned to C-N bonds and at 400.6 eV attributed to amide moieties [176]. Similar results were obtained for PTFE that was treated with low power plasma in gases containing N_2 and NH_3. The deconvolution of the N1s peak showed that the main peak was resolved into three chemical components at 399 eV, 400 eV and 401.5 eV assigned to C-N, C=N and C≡N or N-C-O bonds, respectively [178]. Wagner *et al.* treated the surface of polyethylene using neutral nitrogen species and nitrogen ion bombardment. The analysis of the N1s region of both methods showed three types of carbon-containing nitrogen functionalities. Amine (C-N) bonds at 398.8 eV, imine (C=N) bonds at 400.2 eV and a third type at 401.6 eV which was not specified and could be a number of chemical groups such as –C=N moiety with a delocalized non-bonding electron pair or quaternary nitrogen ions or amide groups O=C-NH or nitrogen present in a graphite like structure or C≡N groups [186]. Based on the literature as mentioned above, in our case the peak observed at 399 eV can be associated with C=N and C-N groups, suggesting that during the plasma treatment new covalent bonds between carbon and nitrogen were formed in all treated surfaces. The amount of nitrogen present in all plasma treated samples did not change significantly with the treatment time suggesting that the surface was saturated with nitrogen during the first 10 min of treatment.

After the surface characterization, which showed clearly that the ASPN treatment affected the surface characteristics of UHMWPE, cellular compatibility tests were carried out. 3T3 fibroblasts were seeded for four days on both treated and untreated surfaces. The specific cell line (NIH 3T3 fibroblasts) was used due to the fact that these cells are the most common to use in cellular compatibility experiments and easy to grow as described in the introduction.

All seeding conditions were the same for all samples. The purpose of this study was to observe the type of surfaces that cells prefer to grow upon, to investigate the plasma treatment effects on the cell behaviour compared to untreated surfaces and the effect of the treatment duration on cell spreading and proliferation. Figure 3.38 shows fibroblasts seeded on PE-0, PE-PT25-1, PE-PT25-2 and PE-PT25-3 surfaces. It can be observed, the untreated surface did not significantly attract fibroblasts. The situation is different however for the ASPN treated surfaces where the number of cells attached on the surface is higher, and as the duration of the treatment increases, an increase of the number of cells on the plasma treated surfaces, better proliferation and attachment are observed. It is clear though, from Figure 3.38 the preference of fibroblasts to adhere on the plasma treated surfaces rather than on the untreated.

As mentioned in the Chapter 2, the cell behaviour is generally affected by the surface properties of the material they come in contact. The surface characteristics may favour cells proliferation, differentiation and growth or discourage them. All surface characteristics (e.g: surface energy, chemistry, roughness) of a material determine the cell-material interaction and therefore the formation of a new tissue [187]. In our case, UHMWPE appears to be inactive when cells are seeded on its surface. However, the ASPN treatment shows that cell attachment and proliferation were favoured. It is believed that the main reason is the presence of nitrogen containing groups on the surface of plasma treated samples as well as the increase of the oxygen percentage as discussed in the FT-IR and XPS sections previously. For the purpose of this study it was not possible to examine oxygen plasma treatment and thus we cannot be sure if it is the presence of oxygen, nitrogen or both due to which the cell behavior was favored. It is suggested that the amine groups are good promoters for cell attachment in nitrogen-containing plasma surfaces. This is due to the fact that glycoproteins such as fibronectin (Fn) and vitronectin (Vn), which mediate cell attachment on a substrate are highly

influenced by the substrate properties and mainly by N-containing surfaces which have Fn and Vn adsorptive characteristics [188].

In general, contact, attachment and proliferation of cells onto a substrate are time dependent procedures [189]. Additionally, cell adhesion and spreading are phenomena that occur by a series of events and are mediated by ECM proteins, the integrins. The integrins are highly involved in the binding of ECM proteins and in the signaling events towards cell proliferation [190]. It has been reported, that plasma treatments enhance cell attachment and proliferation due to the fact that carboxyl functional groups are present on the substrate's surface and Fn and Vn activity is favored. Ramsey *et al.* reported the O_2 plasma treatment of a polystyrene surface. The treatment increased the polymers surface energy and the incorporation of oxygen containing groups enhanced kidney cells growth [191]. More specifically, it has been found that surface modification with ammonia plasma, improves Fn adsorption, e.g. PEEK surface has been treated with pure ammonia microwave plasma resulting in human osteoblasts attachment. The improved cellular behavior was solely attributed to the presence of amino groups that were induced during to the plasma treatment and it was independent of the treatment duration [192]. Plasma discharge modification with the introduction of Ar gas has been applied to different kinds of polymers (polyethylene, polytetrafluoroethylene, poly(ethylene terephtalate), polystyrene and polypropylene) in order to study the effect of the treatment on cell adhesion. Seeding of L murine fibroblasts on treated and untreated surfaces resulted in a general improvement of the cell attachment on the modified surfaces due to the increase of the surface roughness or the generation of functional groups (e.g. carboxyl) after the treatment [193]. PET (polyethyleneterephthalate) surfaces have been treated with NH_3, NH_3/H_2, O_2/H_2 and O_2/H_2O plasmas. On the plasma treated surfaces endothelial cells isolated from the human umbilical cord vein were seeded for different incubation periods (2-9 days). Generally on the plasma treated samples, the cell proliferation was shown to be improved in

comparison to the untreated surfaces. Moreover, the nitrogen containing plasma treated surfaces proved to be the best substrates for endothelial cell proliferation compared to surfaces that were treated with oxygen or hydrogen plasma [194]. Tseng *et al*. reported that expanded polytetrafluoroethylene (e-PTFE) vascular grafts treated with radio frequency glow discharge in amide and amine plasma exhibited higher hydrophilicity and incorporated nitrogen groups. Endothelial cell seeding on to the plasma treated surfaces showed that they were better substrates for the endothelial cell attachment compared to the untreated. The number of cells was higher after 5 days of incubation and the cells formed a monolayer on the plasma treated surfaces [195]. Another study on PS surface where oxygen-containing films were plasma deposited with the addition of oxygen to the plasma gas, showed an increase of bovine cells growth with the increase of oxygen content. This was due to new oxygen containing functionalities introduced on the materials surface such as the presence of ketones. The presence of hydroxyl and carboxyl groups however, did not have any influence on the cells behaviour [196]. Finally, Ho *et al.* investigated the effect of nitrogen plasma on UHMWPE surface and the results showed clearly that the treatment enhanced protein retention compared to the untreated materials [197]. To conclude, UHMWPE plasma treated surfaces can be very good substrates for 3T3 fibroblasts showing enhanced adhesion and proliferation. The main reason is believed that is the incorporation of nitrogen containing groups on to the surface of UHMWPE.

3.2.3 Summary

UHMWPE was treated with ASPN for three different durations, 10, 30 and 60 min treatment at 120^{o}C, in a gas mixture of 25% N_2 and 75% H_2. The treatment was proved to affect both surface characteristics and cellular compatibility of the polymer. Starting with the surface

mechanical properties, both hardness and elastic modulus increased after the treatment. The duration of treatment did not seem to affect this increase since it was similar of all treated samples. Continuing, the surface roughness did not show significant differences before and after the treatment. Thus ASPN did not induce any changes to the surface morphology of UHMWPE. Changes due to the treatment were also observed in the surface chemistry such as the introduction of new chemical bonds containing nitrogen (C-N bonds) and the incorporation of ~6-7 % of nitrogen on to the surface. However, the distribution of nitrogen on to the polymer surface after the treatment was almost the same for all treated samples showing that the increase of treatment duration did not affect the % of nitrogen incorporated on to the surface. Finally, cell seeding tests showed that the ASPN treatment affected the fibroblasts behaviour. More specifically, cells did not seem to attach on the untreated polymer surface, however they attached on the surface of all plasma treated samples. The duration of the treatment seemed to affect the cellular behaviour since it was observed that the higher the duration the more the cells attached and proliferated on to the surface.

3.3 ASPN treatment of UHMWPE (80%N_2-20%H_2)

3.3.1 Results: Materials characterization and cellular compatibility of UHMWPE second treatment (ASPN-2)

In this section the results obtained for UHMWPE subjected to ASPN treatment in a mixture of 80% N_2 and 20% H_2 are presented. Straight after the treatment all samples were tested in order to understand the chemical and physical changes occurring on the surface as well as the cellular compatibility. Untreated and ASPN treated samples were also subjected to an ageing study in order to understand the effect of different environments on the surface chemistry especially after the treatment. During a period of time of 28 days the surface mechanical properties, roughness, chemistry and adhesion forces were measured. Finally, only the 60 min ASPN treated samples were seeded with fibroblasts and for a period of 28 days and the cell compatibility, morphology and proliferation were examined.

3.3.1.1 Chemical composition of untreated and ASPN-2 treated UHMWPE

Figures 3.39-.3.50 show the XPS survey spectra and the deconvoluted C1s, O1s and N1s high resolution spectra of the untreated and the 80% N_2-20% H_2 plasma treated samples and Table 3.8 shows the assignment of the deconvoluted peaks of all the three elements. In all survey spectra it can be observed the presence of carbon and oxygen and nitrogen. C1s peak is found at ~285 eV, O1s at ~532 eV and N1s at ~400 eV. The N/C and O/C ratios are given in Figure 3.51 and the numerical values of the elemental composition are presented in Table 3.9.

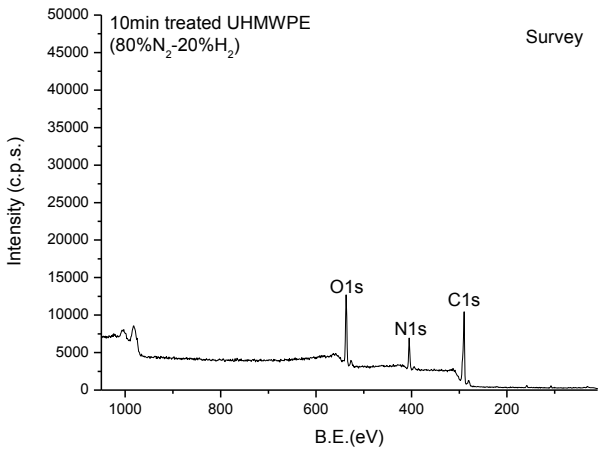

Figure 3.39: Survey spectrum of 10 min 80% N_2-20% H_2 plasma treated UHMWPE.

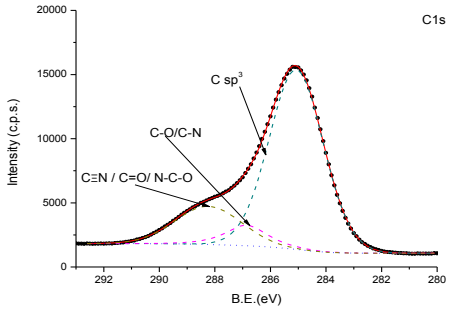

Figure 3.40: C1s peak deconvolution of 10 min 80% N_2-20% H_2 plasma treated UHMWPE.

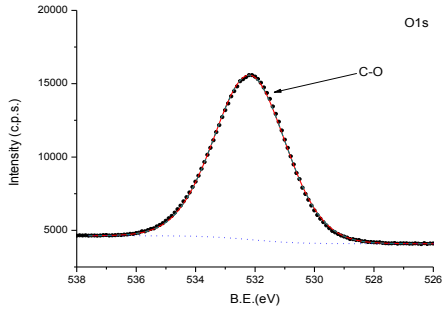

Figure 3.41: O1s peak deconvolution of 10 min 80% N_2-20% H_2 plasma treated UHMWPE.

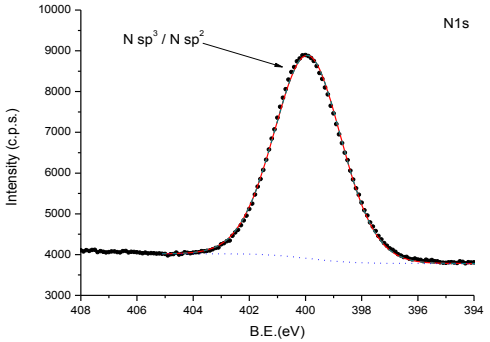

Figure 3.42: N1s peak deconvolution of 10 min 80% N_2-20% H_2 plasma treated UHMWPE.

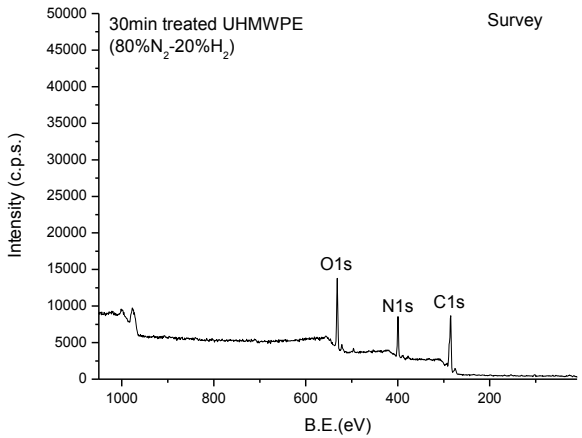

Figure 3.43: Survey spectrum of 30 min 80% N_2-20% H_2 plasma treated UHMWPE

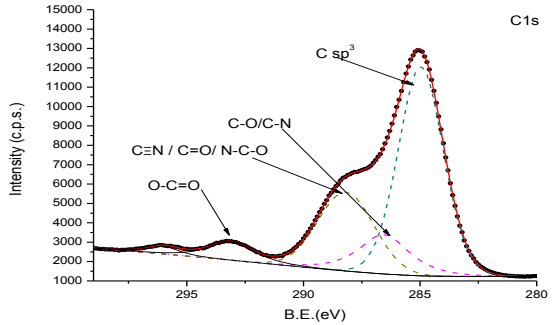

Figure 3.44: C1s peak deconvolution of 30 min 80% N_2-20% H_2 plasma treated UHMWPE.

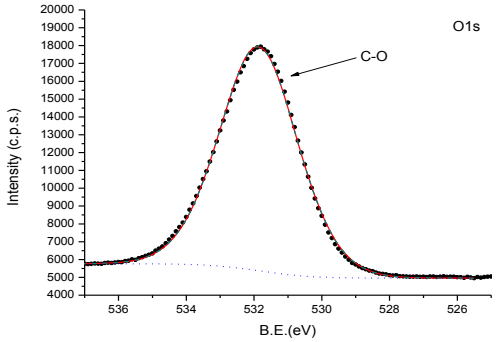

Figure 3.45: O1s peak deconvolution of 30 min 80% N_2-20% H_2 plasma treated UHMWPE

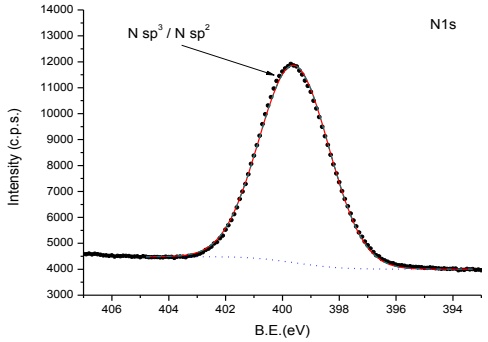

Figure 3.46: N1s peak deconvolution of 30 min 80% N_2-20% H_2 plasma treated UHMWPE.

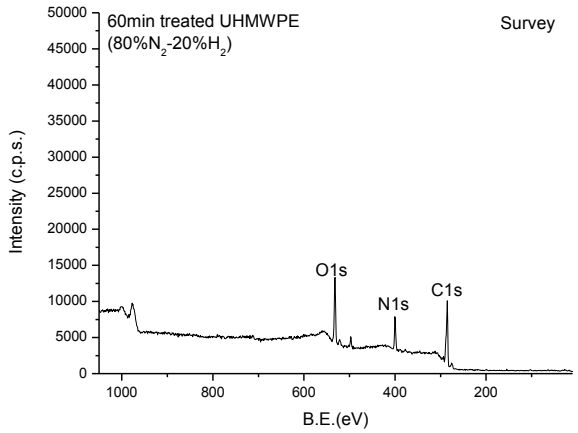

Figure 3.47: Survey spectrum of 60 min 80% N_2-20% H_2 plasma treated UHMWPE.

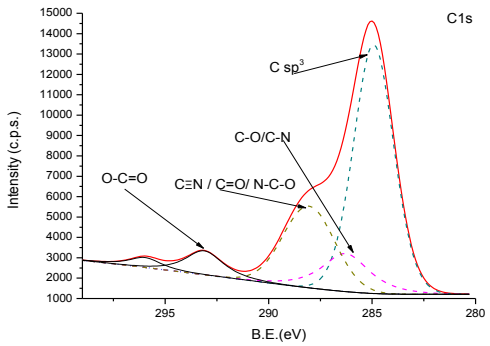

Figure 3.48: C1s peak deconvolution of 60 min 80% N_2-20% H_2 plasma treated UHMWPE.

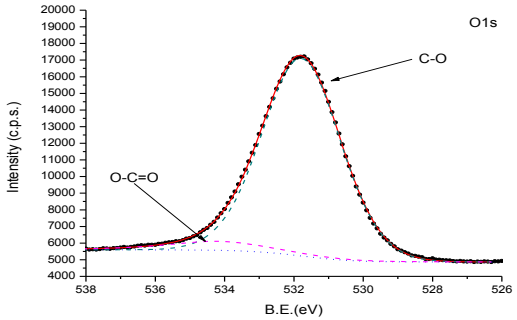

Figure 3.49: O1s peak deconvolution of 60 min 80% N_2-20% H_2 plasma treated UHMWPE.

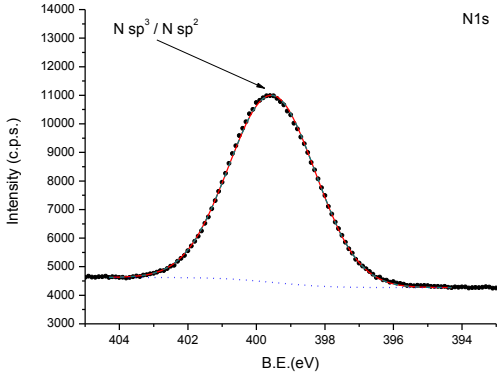

Figure 3.50: N1s peak deconvolution of 60 min 80% N_2-20% H_2 plasma treated UHMWPE.

Table 3.8: Assignment of deconvoluted peaks C1s, O1s, N1s.

Material	C1s	Assignment	O1s	Assignment	N1s	Assignment
10min ($80\%N_2$-$20\%H_2$)	285.1 286.89 288.31	C-C C-O / C=N C=O/ C≡N/ N-C-O	532.14	C-O	399.99	C-N / C=N
30min ($80\%N_2$-$20\%H_2$)	284.95 286.61 288.2 293.11	C-C C-O / C=N C=O/ C≡N/ N-C-O O-C=O	531.82	C-O	399.66	C-N / C=N
60min ($80\%N_2$-$20\%H_2$)	284.95 286.29 288.09 293.12	C-C C-O / C=N C=O/ C≡N/ N-C-O O-C=O	531.80 534.34	C-O O=C-O	399.63	C-N / C=N

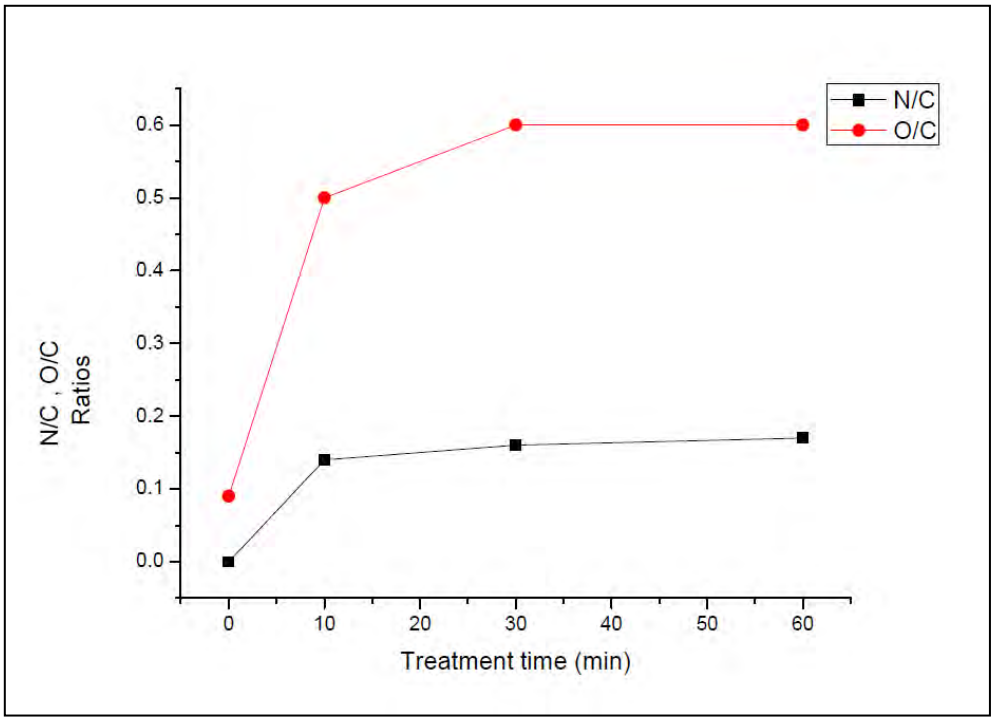

Figure 3.51: N/C and O/C ratios of the UHMWPE ASPN 80% treated and untreated samples.

Table 3.9: Elemental composition of untreated and ASPN 80% treated UHMWPE.

Material	Carbon %	Oxygen %	Nitrogen %
PE-0	91.572	8.427	0
PE-PT80-1	61.385	30.18	8.430
PE-PT80-2	55.076	35.811	9.112
PE-PT80-3	56.240	34.220	9.523

3.3.1.2 Surface roughness

Figure 3.52 shows the white light interferometry results, surface topography and the 3D image of both treated and untreated samples are presented. Figure 3.53 shows the numerical values of both S_a and S_q. The surface roughness of UHMWPE seems to have a slight increase after the ASPN treatment. However, the change is not significant. Thus treatment does not seem to induce any changes on the UHMWPE surface roughness.

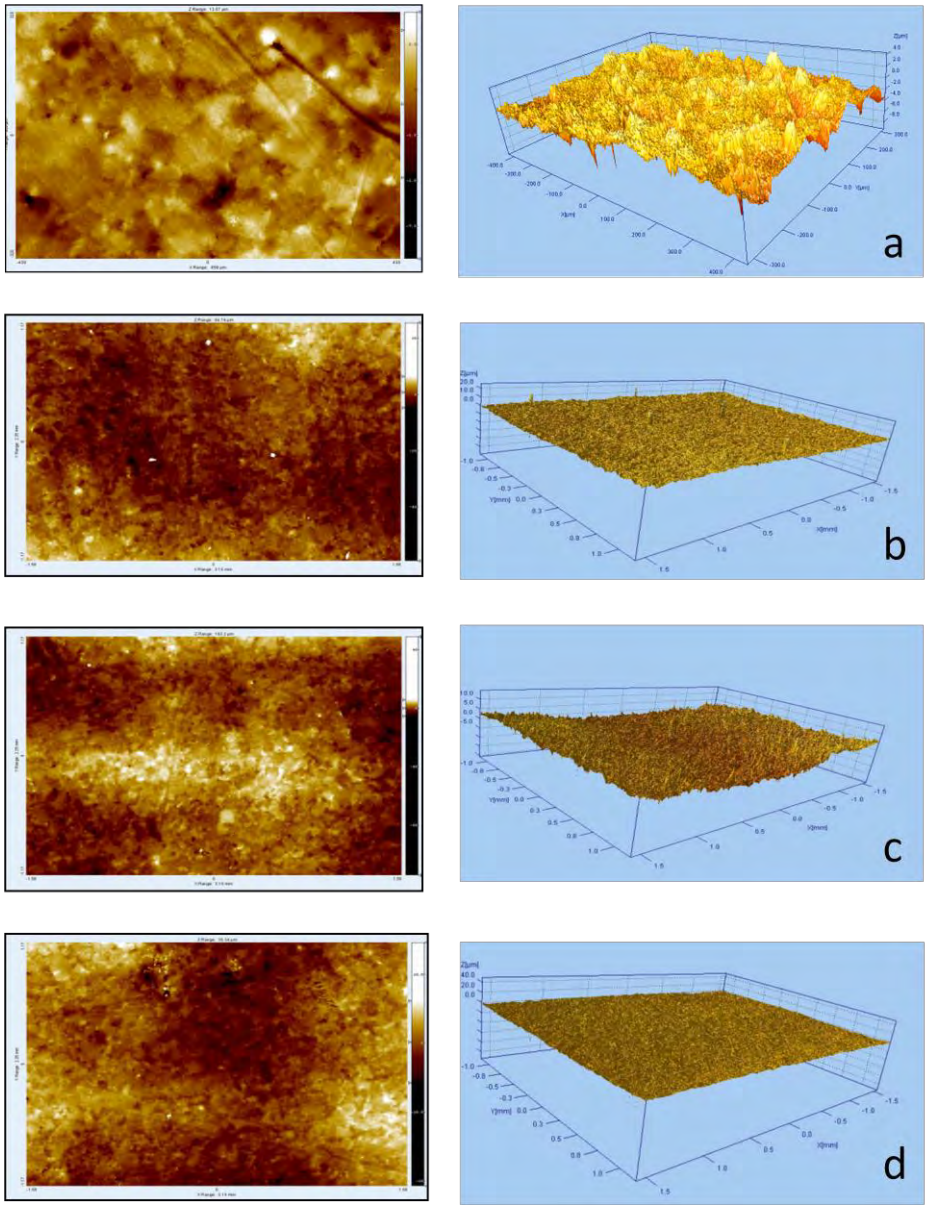

Figure 3.52: Surface topography of all 80% N_2-25% H_2 ASPN treated and untreated samples and the 3D images of sample surfaces a) untreated, b) 10 min c) 30 min and d) 60 min treated.

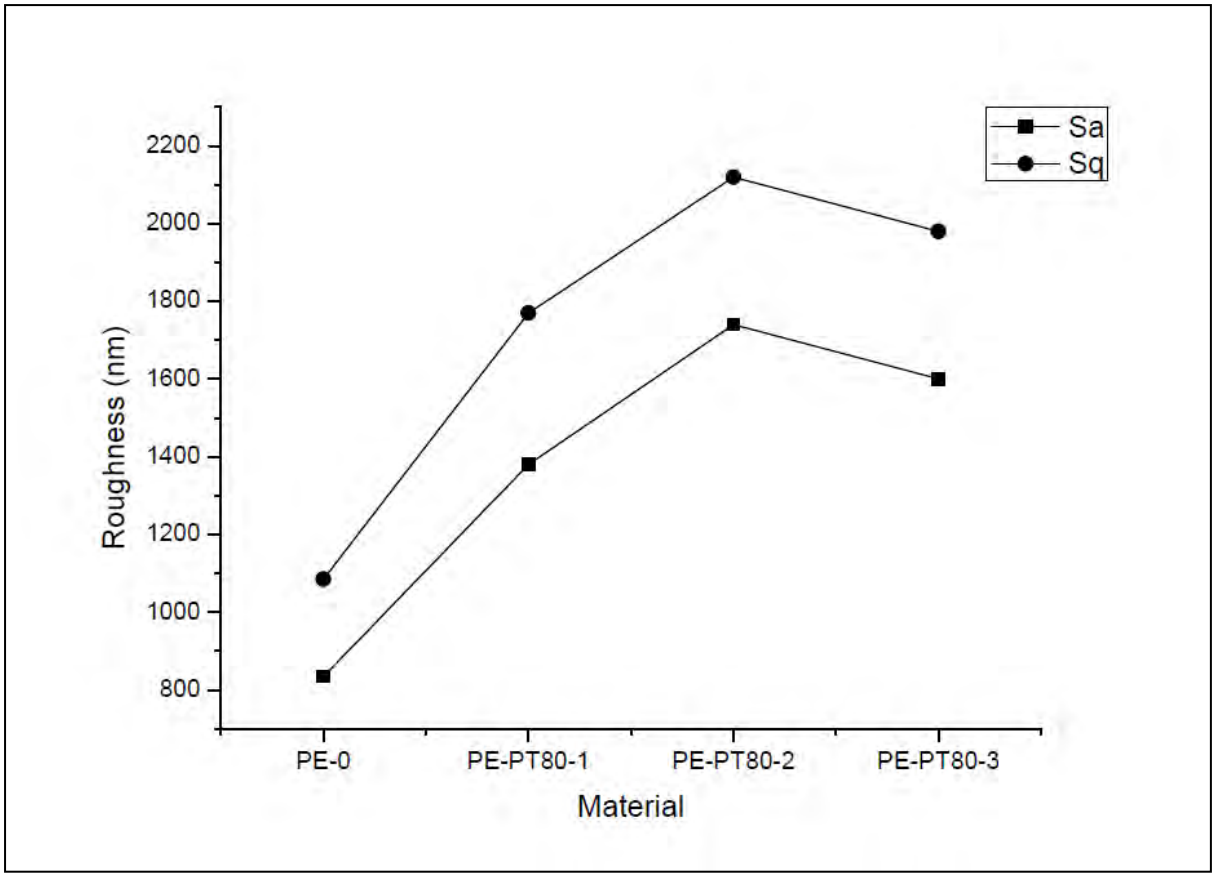

Figure 3.53: Numerical values of S_a and S_q for untreated and 80% N_2 ASPN treated UHMWPE obtained with white light Interferometry.

3.3.1.3 Cell compatibility tests

Figures 3.54-3.57 show the SEM results of the untreated (PE-0) and plasma treated UHMWPE surfaces (PE-PT80-1, PE-PT80-2 and PE-PT80-3) seeded with fibroblasts for 24 hr. The magnification varies from x100 to x 2000. More analytically, as it was expected when cells were seeded onto the polymers surface, in the absence of surface treatment, there was no evidence of cell attachment as shown in Figure 3.35 a and b. In this case, no cell attachment was observed. Following the treatment of the surface using ASPN, however, there was significant attachment within 24 hr of seeding as shown in Figures 3.55-3.57. The treatment time appeared to have little influence on the extent of cell attachment, with samples treated

for 10, 30 and 60 min each covered with several layers of cells. The fibroblasts preference to adhere on the treated surfaces rather than the untreated one is clear.

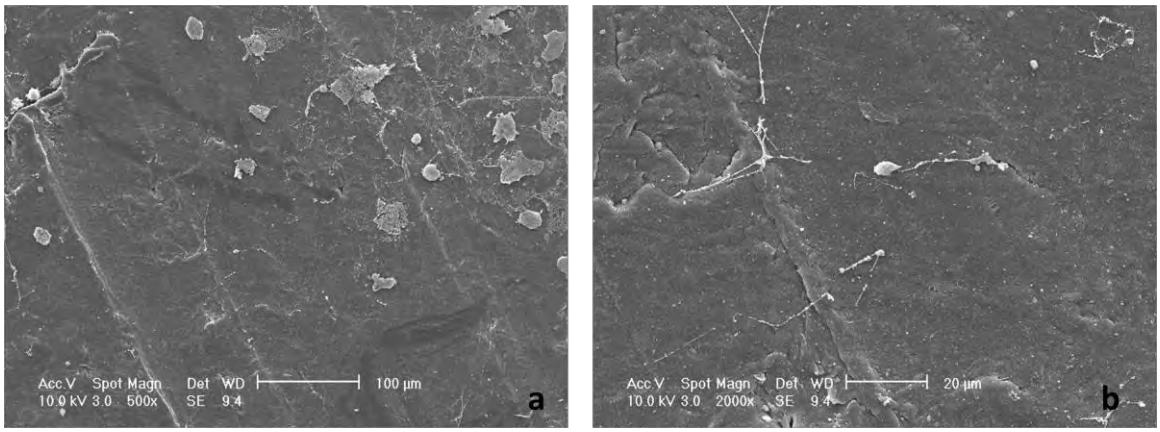

Figure 3.54: SEM micrographs of untreated UHMWPE after 24 hr of fibroblasts seeding with magnifications a) x 500 and b) x 2000.

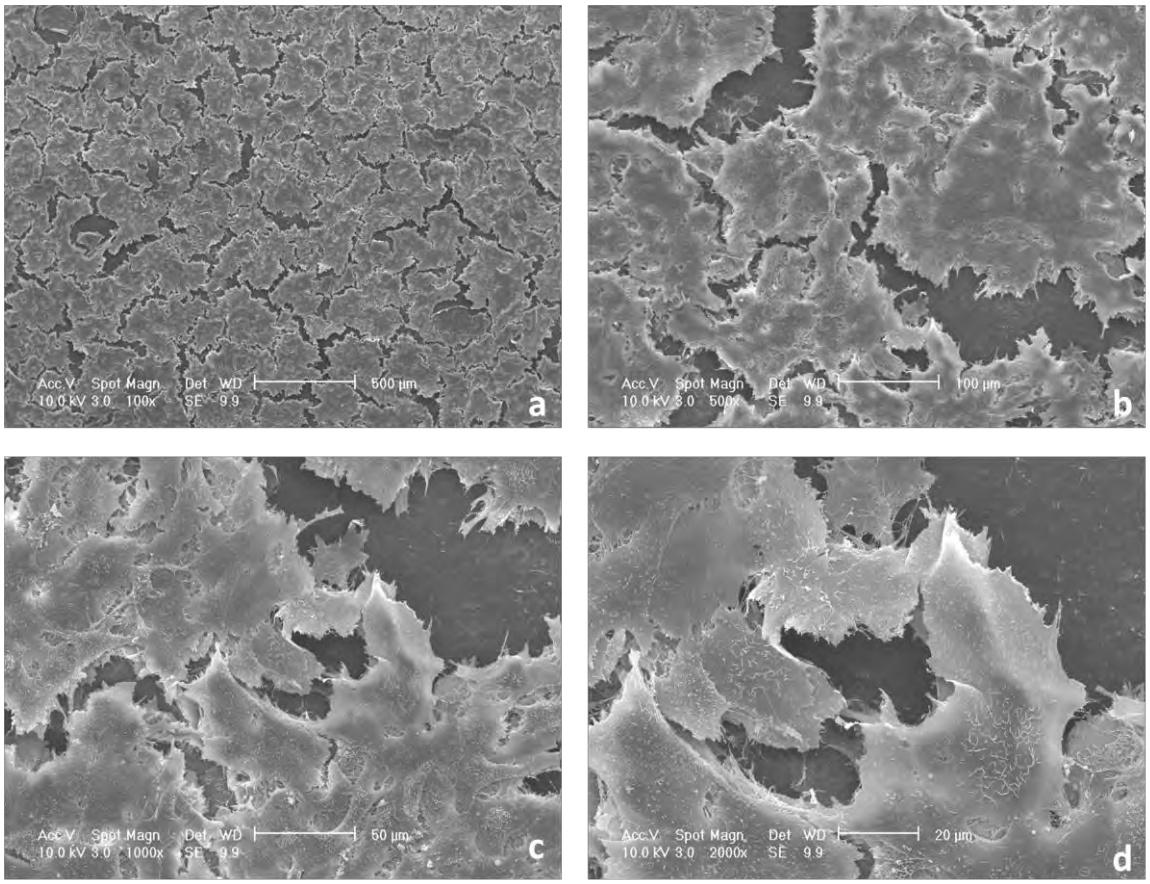

Figure 3.55 SEM micrographs of 10 min ASPN treated UHMWPE after 24 hr of fibroblasts seeding with magnifications: a) x 100, b) 500, c) 1000 and d) 2000.

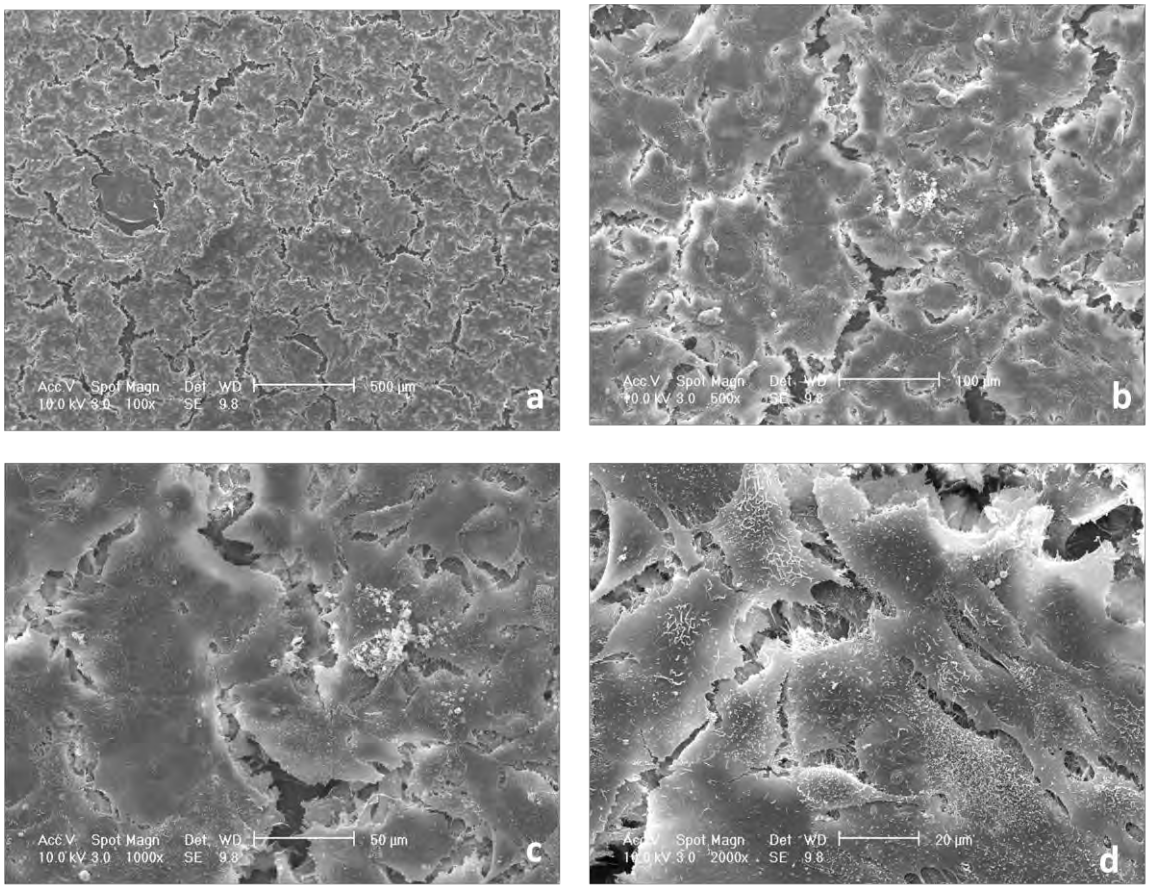

Figure 3.56: SEM micrographs of 30 min ASPN treated UHMWPE after 24 hr of fibroblasts seeding with magnifications: a) x 100, b) 500, c) 1000 and d) 2000.

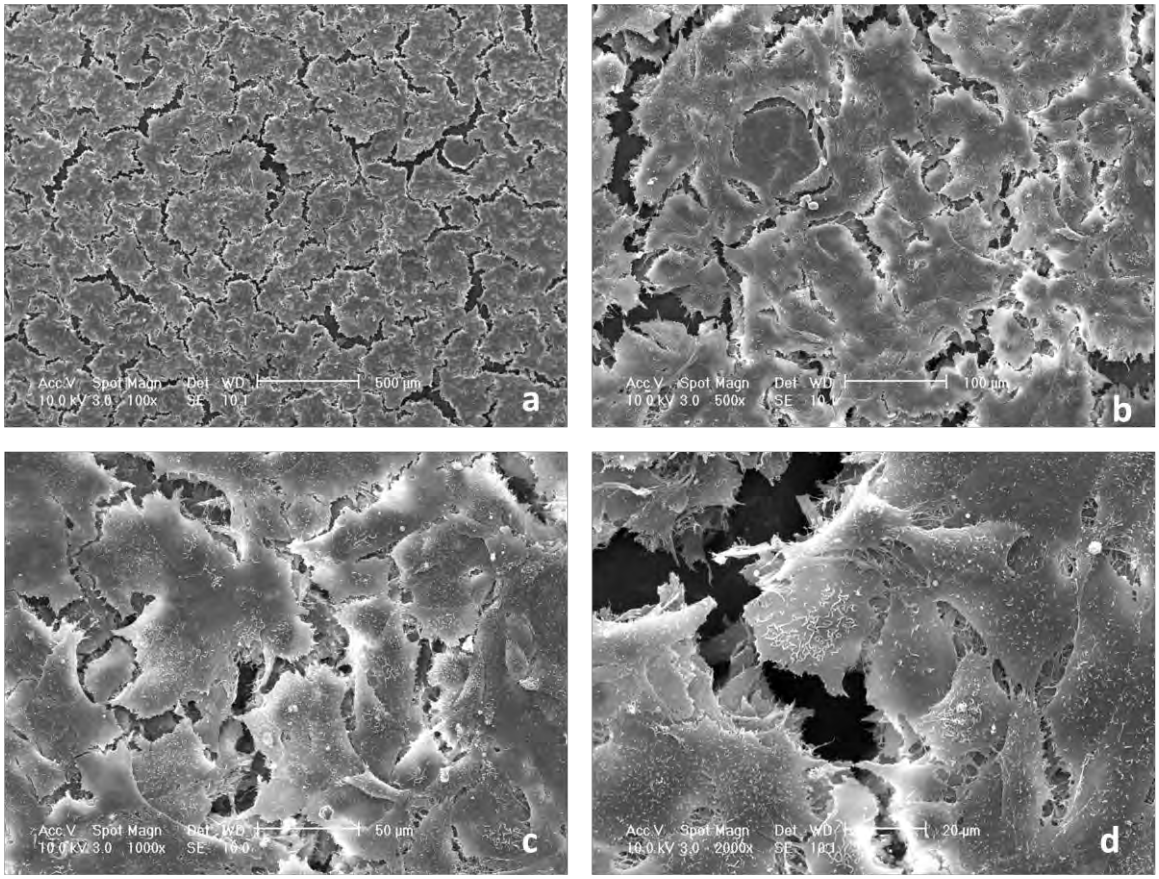

Figure 3.57: SEM micrographs of 60 min ASPN treated UHMWPE after 24 hr of fibroblasts seeding with magnifications: a) 100, b) 500, c) 1000 and d) 2000.

3.3.1.4 Ageing study of ASPN-2 UHMWPE: Mechanical properties

For the ageing study all 80% N_2 - 20% H_2 plasma treated samples were placed in three different environments: air, PBS and S-DMEM. The mechanical testing results are presented in Tables 3.10 (air), 3.11 (PBS) and 3.12 (S-DMEM) with the graph representing each table in Figures 3.58-3.60 respectively. As it can be observed, the modification of the surface with nitrogen did not have any notable effect on either the hardness or reduced modulus of the samples after treatment or following ageing in air, PBS or S-DMEM. The hardness and reduced modulus of the treated samples did not change significantly with ageing time in

aqueous media but there was a small but significant ($p<0.05$) deterioration in mechanical properties following storage in air.

Table 3.10: Hardness and Reduced modulus for all samples in Air.

AIR					
Time (days)	**Sample***	**H (MPa)**	**St. Err.**	**E(MPa)**	**St. Err.**
	PE-0	62	5.0	1277	92.8
1	PE-PT80-1	91	12.1	1453	123.3
	PE-PT80-2	67	9.2	1382	164.9
	PE-PT80-3	65	6.8	1277	105.6
7	PE-PT80-1	77	6.3	1708	108.2
	PE-PT80-2	81	6.7	1588	111.1
	PE-PT80-3	86	9.3	1811	142.5
14	PE-PT80-1	78	7.8	1552	99.2
	PE-PT80-2	60	6.2	1258	129.8
	PE-PT80-3	82	9.9	1885	217.7
21	PE-PT80-1	54	4.6	1159	111.0
	PE-PT80-2	88	21.2	1520	188.2
	PE-PT80-3	66	18.0	1127	74.3
28	PE-PT80-1	76	18.3	1400	140.6
	PE-PT80-2	63	9.1	1423	178.2
	PE-PT80-3	49	11.8	998	246.3

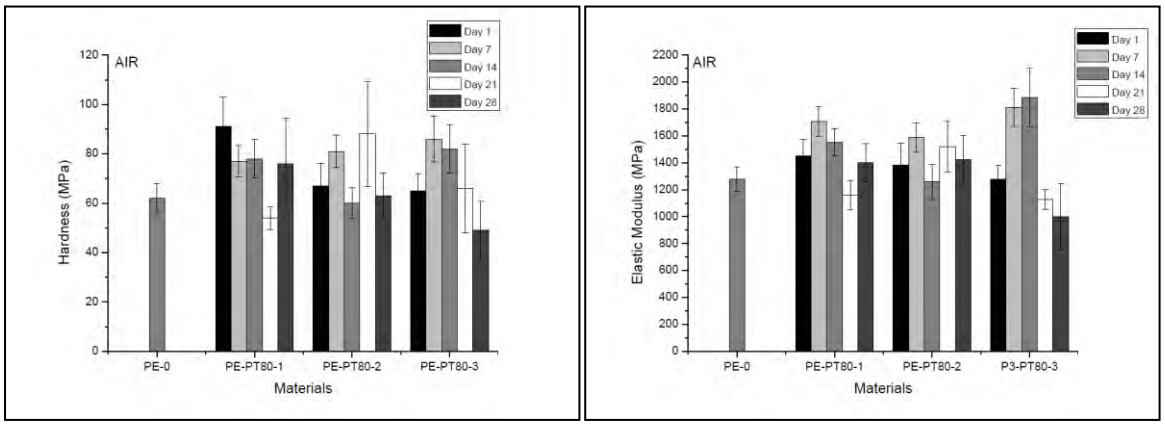

Figure 3.58: Hardness and Elastic modulus of 80% ASPN treated and untreated samples under air conditions.

Table 3.11: Hardness and Reduced modulus for all samples in PBS.

PBS					
Time (days)	**Sample**	**H (MPa)**	**St. Err.**	**E(MPa)**	**St. Err.**
	PE-0	62	5.0	1277	92.8
1	PE-PT80-1	77	10.1	1371	116.7
	PE-PT80-2	57	8.4	1107	86.5
	PE-PT80-3	59	5.3	1292	113.2
7	PE-PT80-1	59	9.7	1147	77.0
	PE-PT80-2	59	9.2	1325	174.6
	PE-PT80-3	64	7.1	1434	155.0
14	PE-PT80-1	58	5.6	1249	123.2
	PE-PT80-2	63	8.9	1384	169.0
	PE-PT80-3	75	9.8	1461	165.9
21	PE-PT80-1	73	8.7	1539	147.7
	PE-PT80-2	68	7.1	1327	120.5
	PE-PT80-3	69	10.8	1446	171.9
28	PE-PT80-1	46	6.2	799	93.1
	PE-PT80-2	44	4.5	645	44.3
	PE-PT80-3	72	7.1	1476	198.1

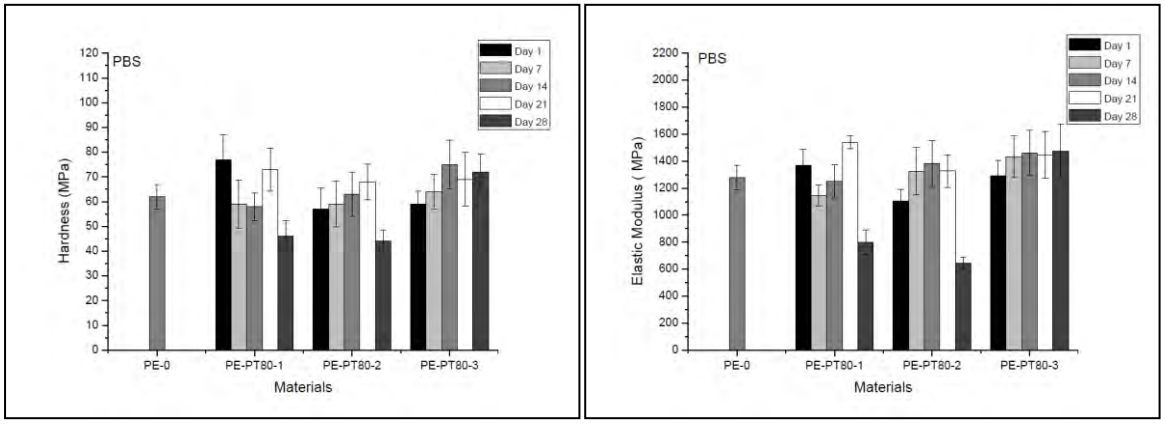

Figure 3.59: Hardness and Elastic modulus of 80% ASPN treated and untreated samples under PBS conditions.

Table 3.12: Hardness and Reduced modulus for all samples in S-DMEM

S-DMEM					
Time (days)	**Sample**	**H (MPa)**	**St. Err.**	**E(MPa)**	**St. Err.**
	PE-0	62	5.0	1277	92.8
1	PE-PT80-1	53	7.8	1014	68.0
	PE-PT80-2	53	3.8	1091	66.1
	PE-PT80-3	67	9.5	1494	126.8
7	PE-PT80-1	86	14.1	1885	182.6
	PE-PT80-2	81	11.9	1569	185.7
	PE-PT80-3	60	12.2	1461	233.7
14	PE-PT80-1	68	10.9	1472	226.6
	PE-PT80-2	58	8.8	1210	174.6
	PE-PT80-3	68	11.1	1370	145.7
21	PE-PT80-1	65	11.0	1418	239.5
	PE-PT80-2	55	6.3	1233	170.1
	PE-PT80-3	72	8.9	1524	180.3
28	PE-PT80-1	58	6.7	1490	152.4
	PE-PT80-2	60	6.9	1189	111.2
	PE-PT80-3	54	7.2	1232	143.2

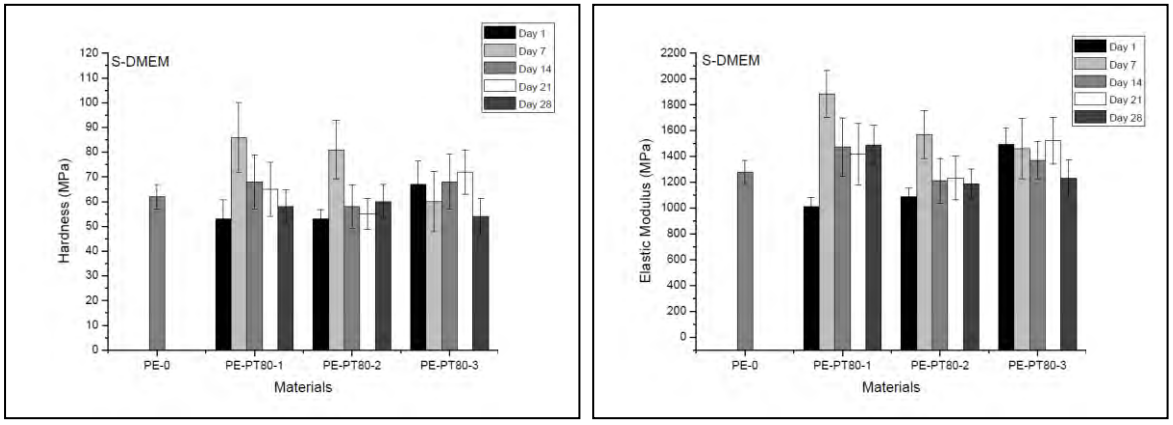

Figure 3.60: Hardness and Elastic modulus of 80% ASPN treated and untreated samples under S-DMEM conditions.

3.3.1.5 Ageing study of ASPN-2 UHMWPE: Surface roughness

Roughness tests are presented in Table 3.13 and Figures 3.61-3.63 present the graphs for each environment (Air, PBS, S-DMED) separately. The treatment of the surfaces with ASPN did not have a notable effect on the roughness of the surface (S_a). The surface roughness (S_a) does not change significantly according to treatment time or exposure to different environmental conditions in the period of 28 days. For all samples the S_a varies between 710-1010 nm. During the ageing study where the treated surfaces were exposed to different environmental conditions, it was not expected to observe any changes in the surface roughness since changes of the surface roughness of UHMWPE (if any) should occur only due to the plasma treatment. This study was conducted only for comparison reasons.

Table 3.13: Interferometry results for all samples and environments.

		Air		**PBS**		**S-DMEM**	
Time (days)	**Sample***	**Sa (nm)**	**St. Err.**	**Sa (nm)**	**St. Err.**	**Sa (nm)**	**St. Err.**
	PE-0	720	70				
1	PE-PT80-1	720	110	720	70	790	120
	PE-PT80-2	750	110	810	70	820	160
	PE-PT80-3	700	20	780	100	700	70
7	PE-PT80-1	710	90	740	30	800	150
	PE-PT80-2	920	20	1010	34	710	80
	PE-PT80-3	770	90	720	40	770	50
14	PE-PT80-1	810	90	840	10	680	70
	PE-PT80-2	870	70	840	110	860	200
	PE-PT80-3	710	70	750	30	870	90
21	PE-PT80-1	710	60	720	180	710	60
	PE-PT80-2	780	80	680	40	770	50
	PE-PT80-3	790	170	820	280	680	70
28	PE-PT80-1	780	50	720	50	770	60
	PE-PT80-2	840	160	740	50	930	100
	PE-PT80-3	790	60	720	90	840	170

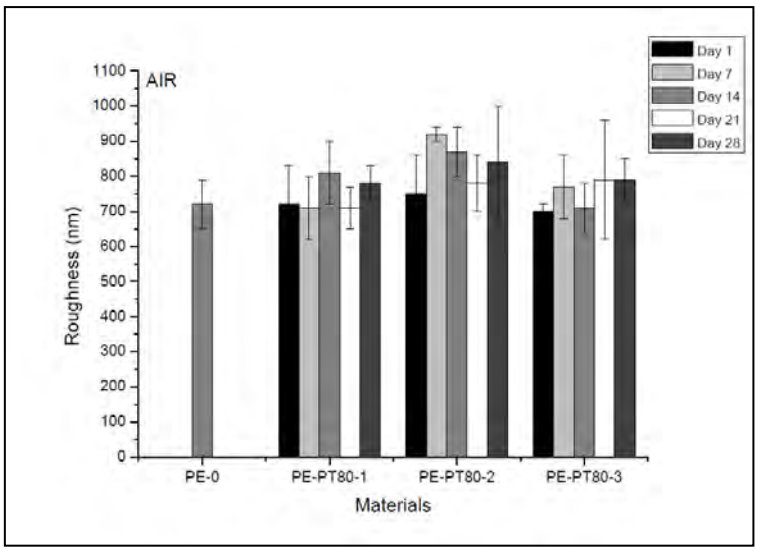

Figure 3.61: Surface roughness of 80% ASPN treated and untreated samples under AIR conditions.

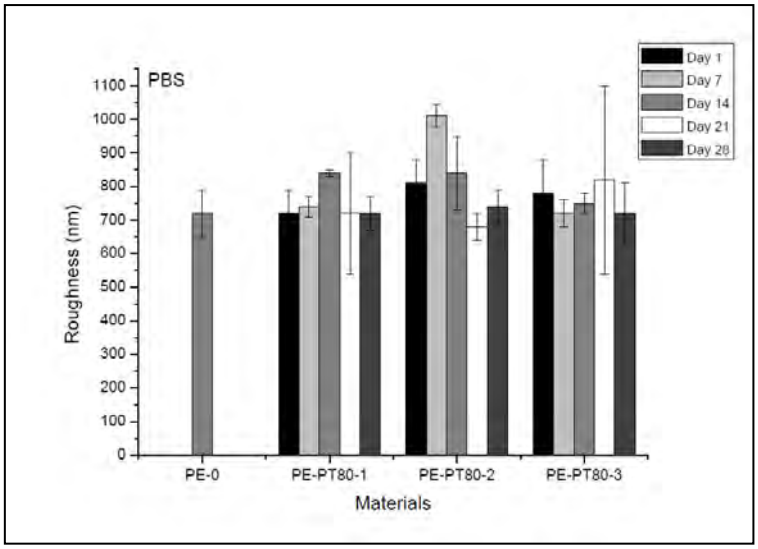

Figure 3.62: Surface roughness of 80% ASPN treated and untreated samples under PBS conditions.

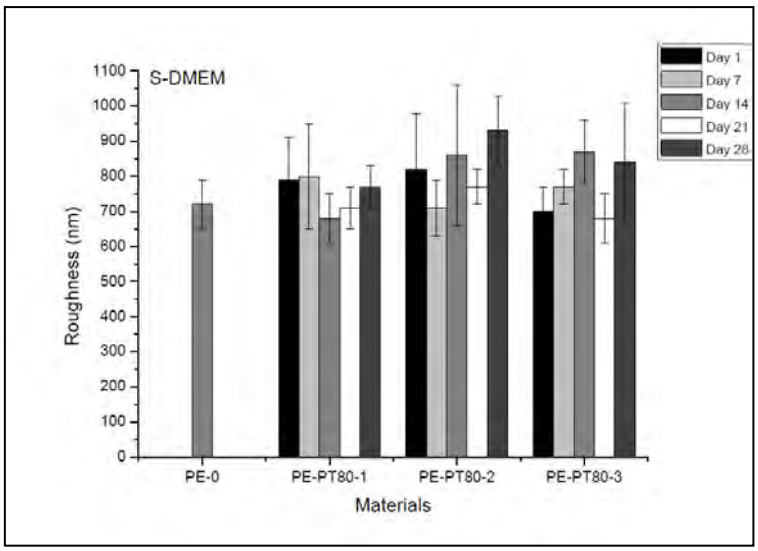

Figure 3.63: Surface roughness of 80% ASPN treated and untreated samples under S-DMEM conditions.

3.3.1.6 Ageing study of ASPN-2 UHMWPE: Chemical composition

For the surface chemistry analysis of UHMWE that was treated in a gas mixture of 20%H_2/ 80%N_2, only air conditions were used. The ageing study was conducted for 28 days. All samples after the treatment were left in ambient conditions and were tested using XPS on days 1, 7, 14, 21, and 28. For all treated samples (10 min, 30 min and 60 min) the survey spectra and the deconvoluted spectra of each element (C1s, O1s and N1s) are presented below.

Figures 3.64-3.67 present the 10 min samples spectra over 28 days with low resolution spectra and the high resolution C1s, O1s and N1s, Figures 3.68-3.71 the spectra for the 30 min treated material and Figures 3.72-3.75 the spectra for the 60 min treated samples. Also the N/C and O/C ratios for all ageing study samples and the elemental compositions are presented in Figures 3.76-3.78 and Table 3.14 respectively. The ageing of the samples did not seem to affect the nature of the bonds present on the treated surfaces and identified by the relevant peaks in the graphs.

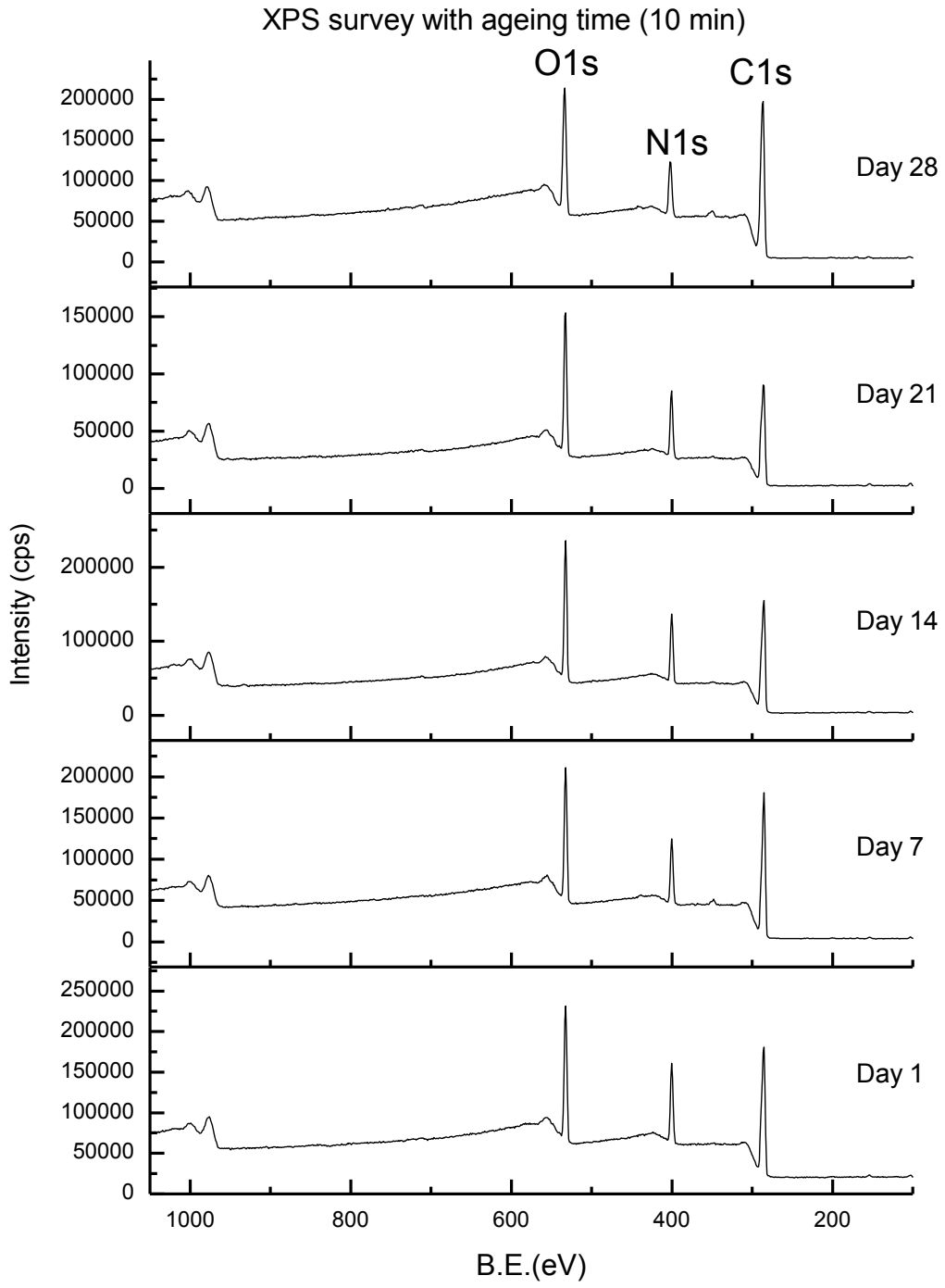

Figure 3.64: XPS survey spectra of the 10 min treated UHMWPE in 80%N_2-20%H_2 over 28 days.

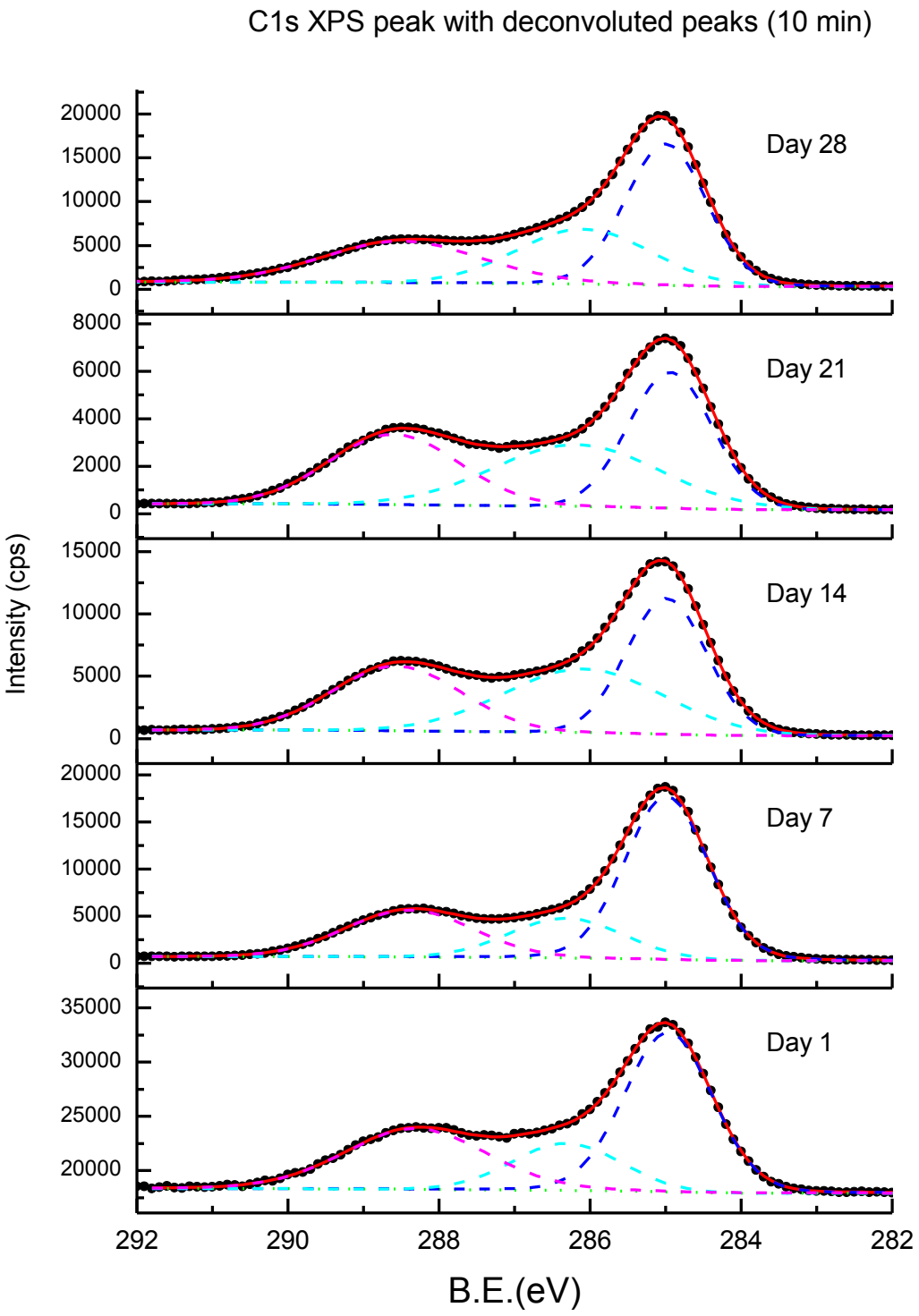

Figure 3.65: C1s XPS high resolution spectra of10 min treated UHMWPE in 80%N_2-20%H_2 over 28 days.

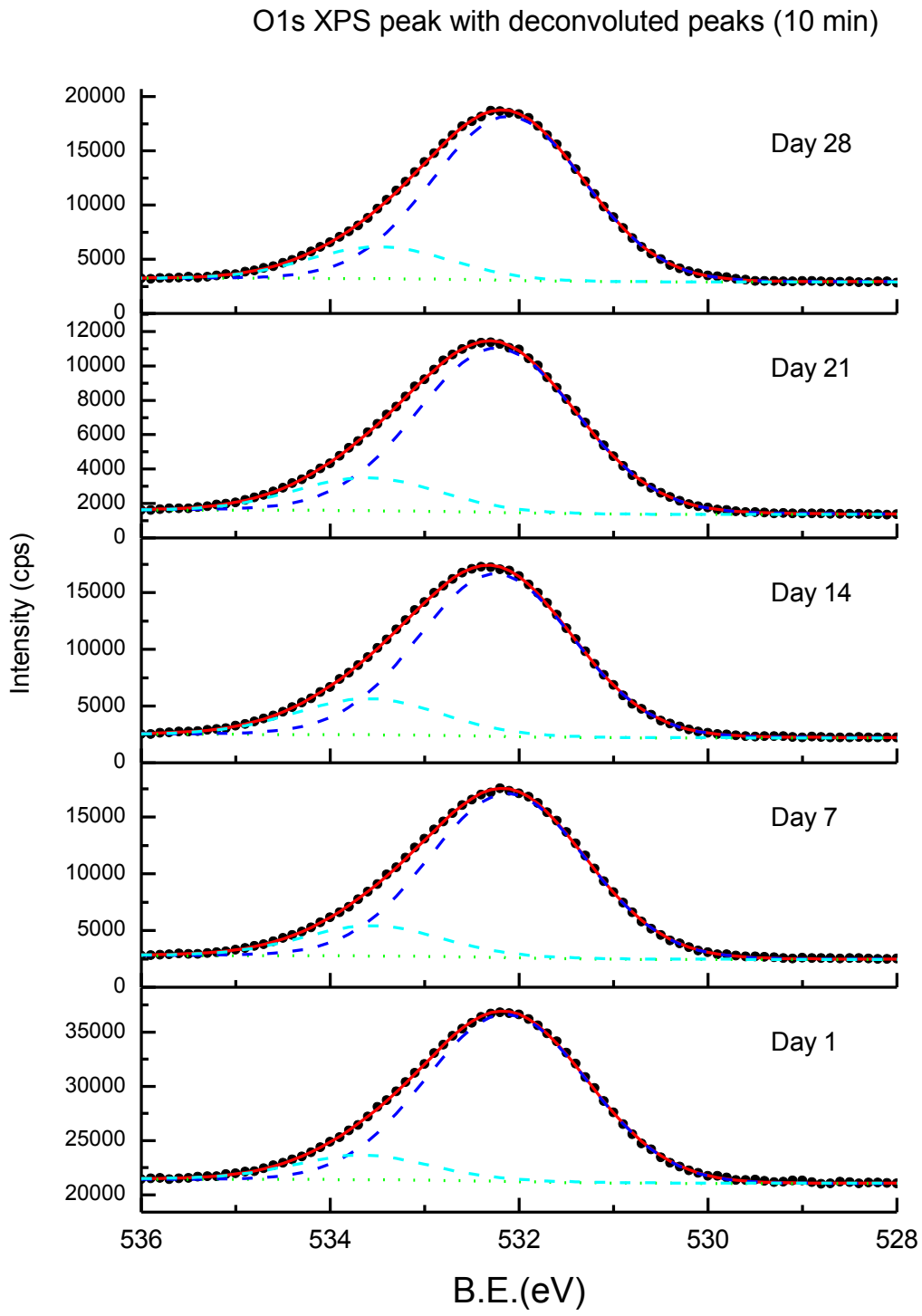

Figure 3.66: O1s XPS high resolution spectra of10 min treated UHMWPE in 80%N_2-20%H_2 over 28 days.

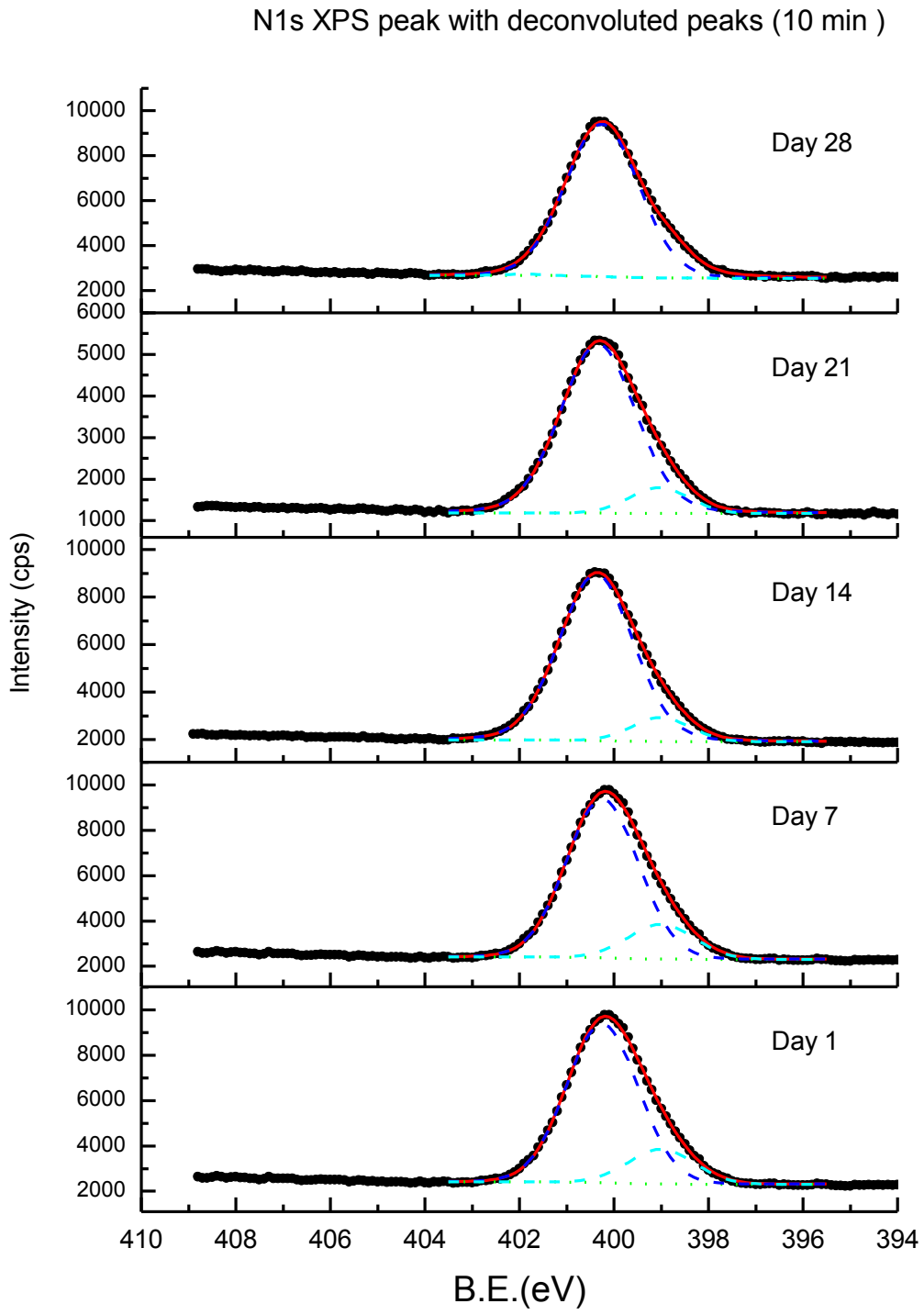

Figure 3.67: N1s XPS high resolution spectra of10 min treated UHMWPE in 80%N_2-20%H_2 over 28 days.

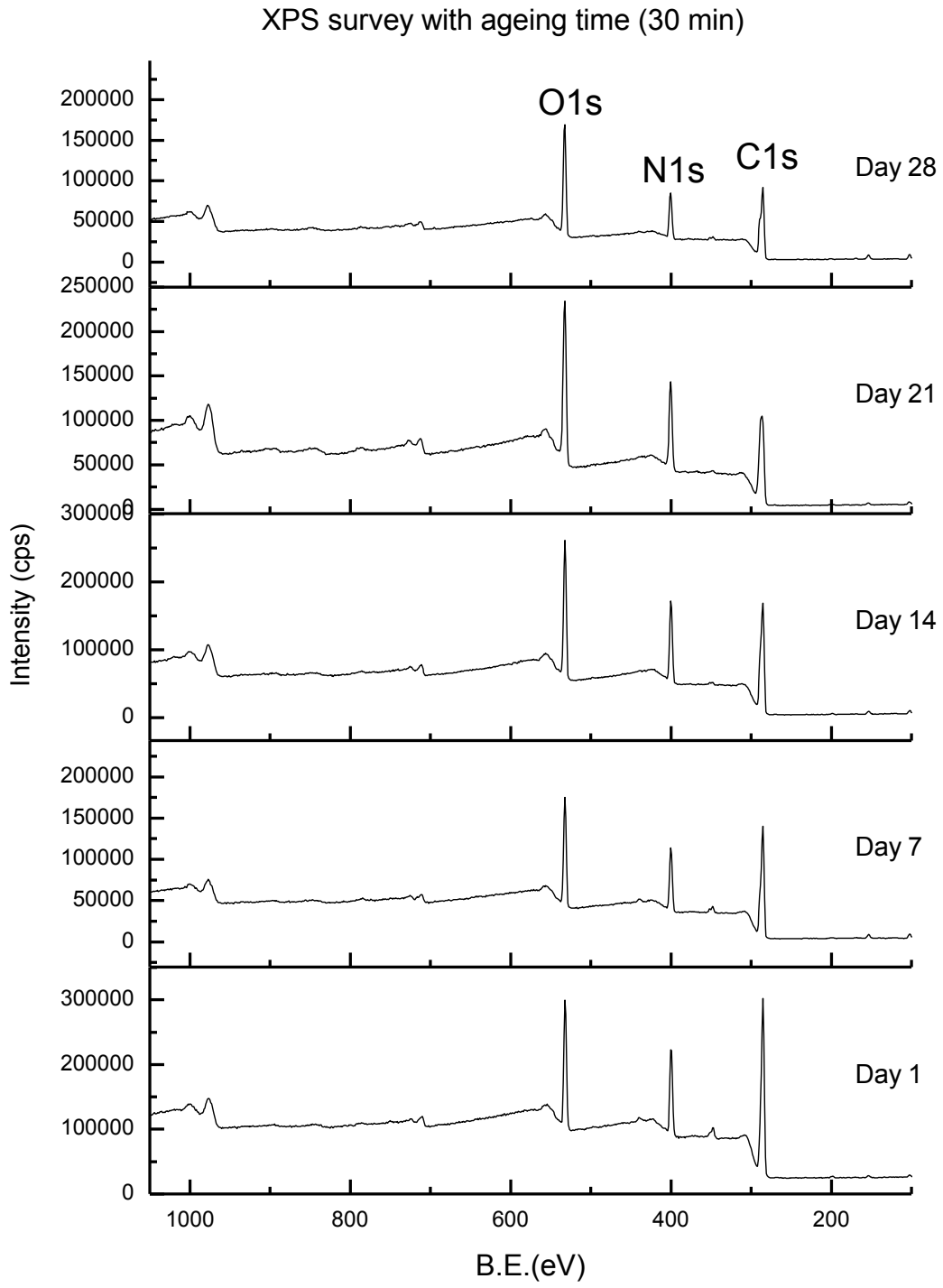

Figure 3.68: XPS survey spectra of the 30 min treated UHMWPE in 80%N_2-20%H_2 over 28 days.

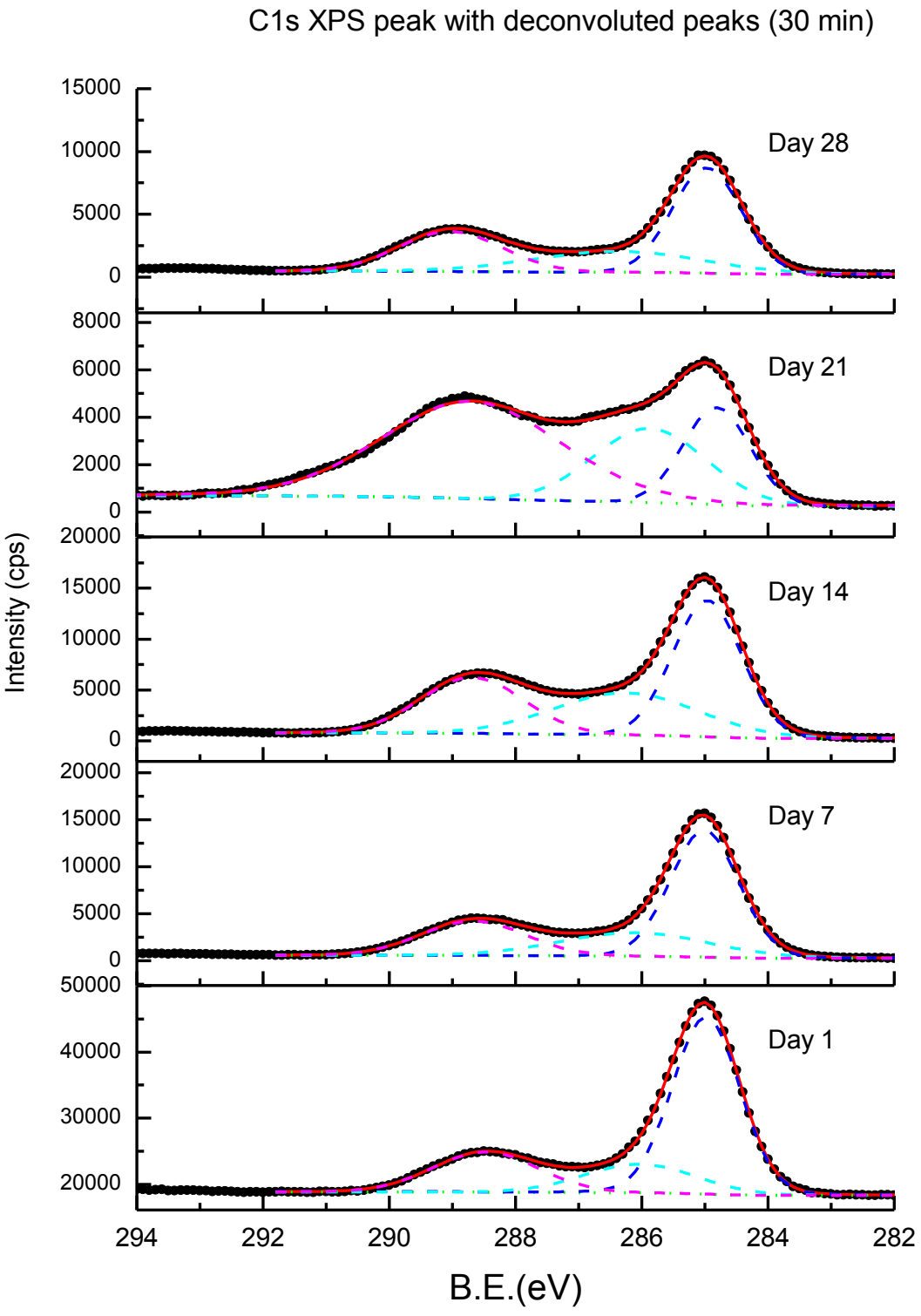

Figure 3.69: C1s XPS high resolution spectra of30 min treated UHMWPE in 80%N_2-20%H_2 over 28 days.

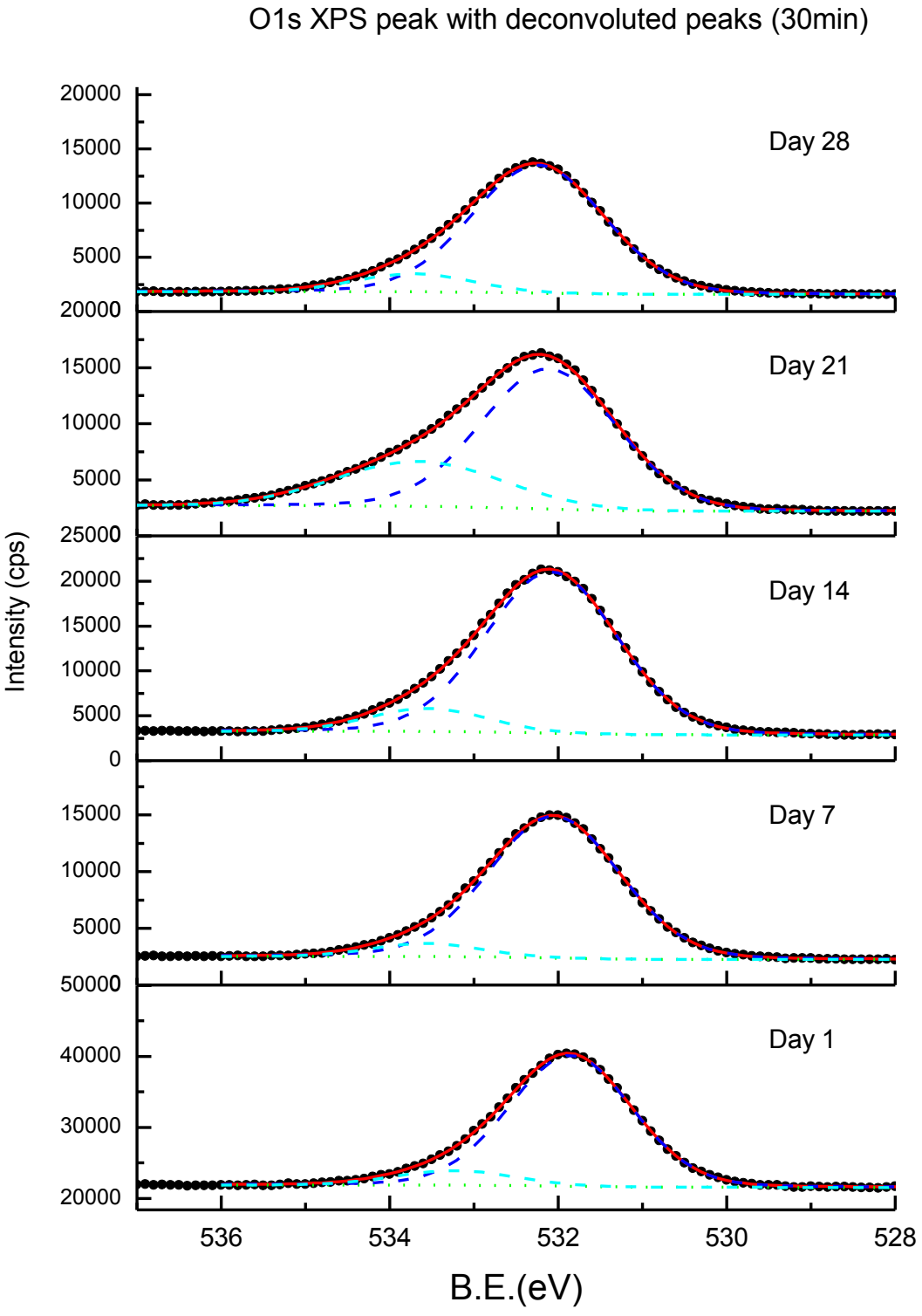

Figure 3.70: O1s XPS high resolution spectra of30 min treated UHMWPE in 80%N_2-20%H_2 over 28 days.

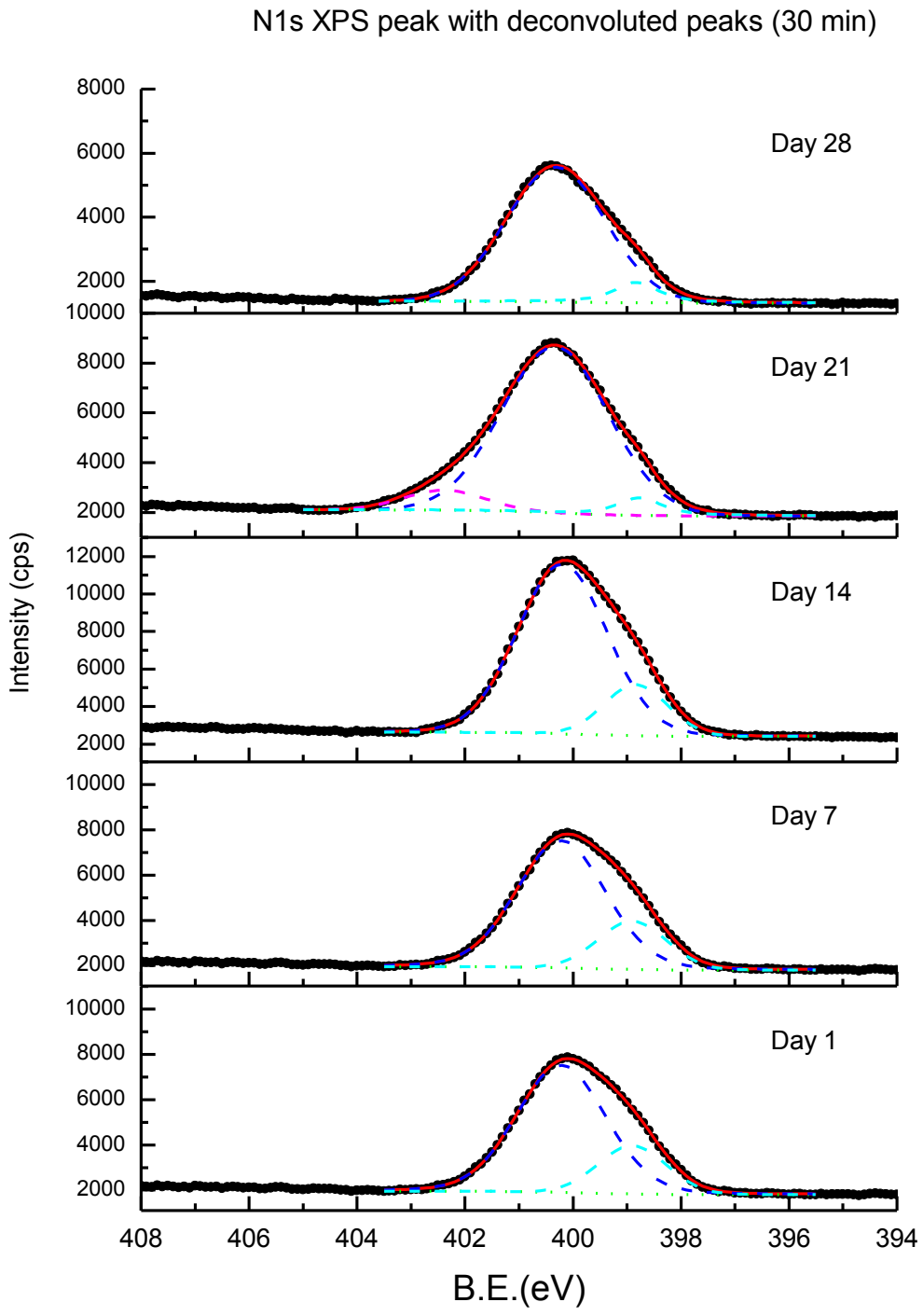

Figure 3.71: N1s XPS high resolution spectra of30 min treated UHMWPE in 80%N_2-20%H_2 over 28 days.

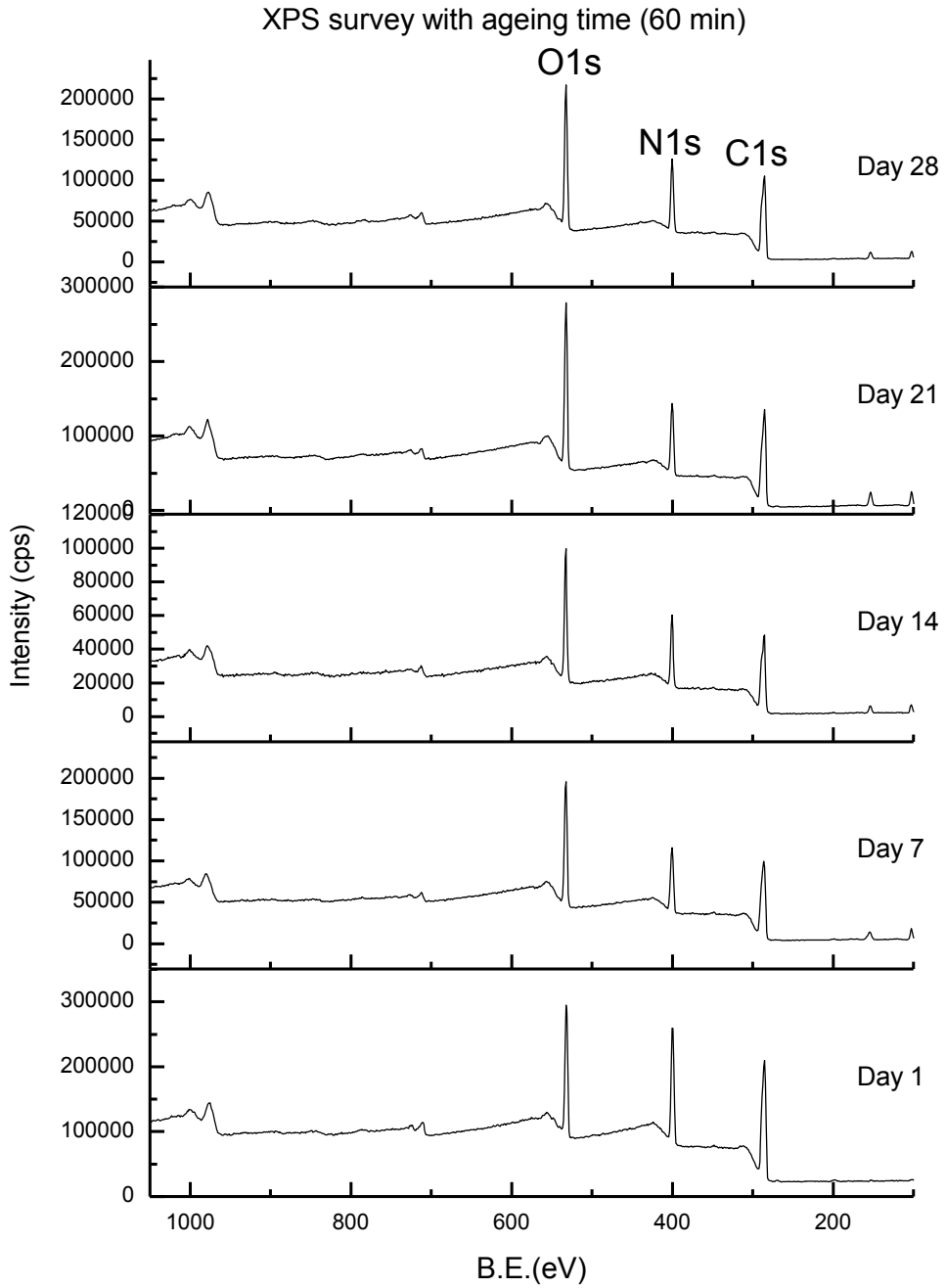

Figure 3.72: XPS survey spectra of the 60 min treated UHMWPE in 80%N_2-20%H_2 over 28 days.

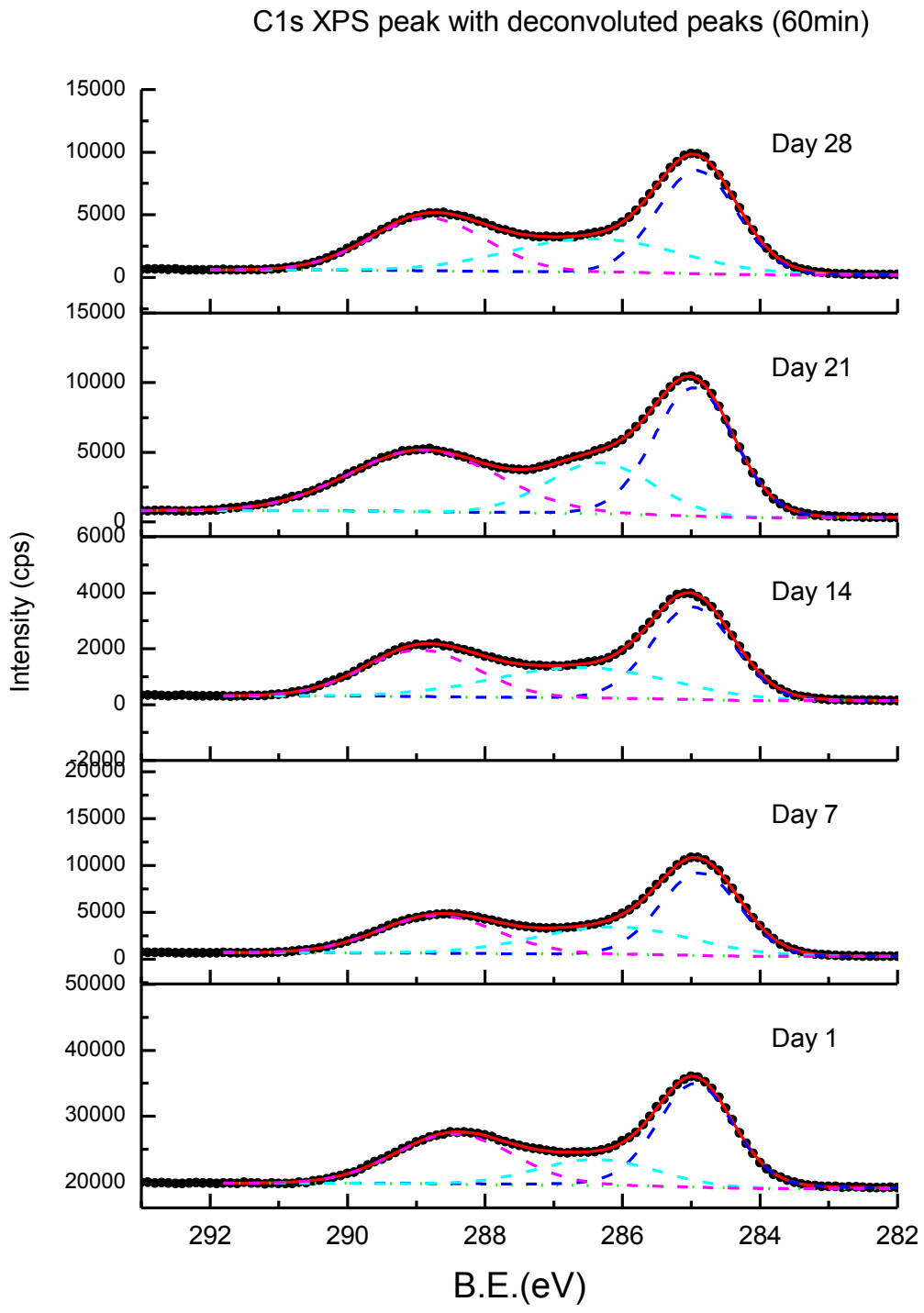

Figure 3.73: C1s XPS high resolution spectra of60 min treated UHMWPE in 80%N_2-20%H_2 over 28 days.

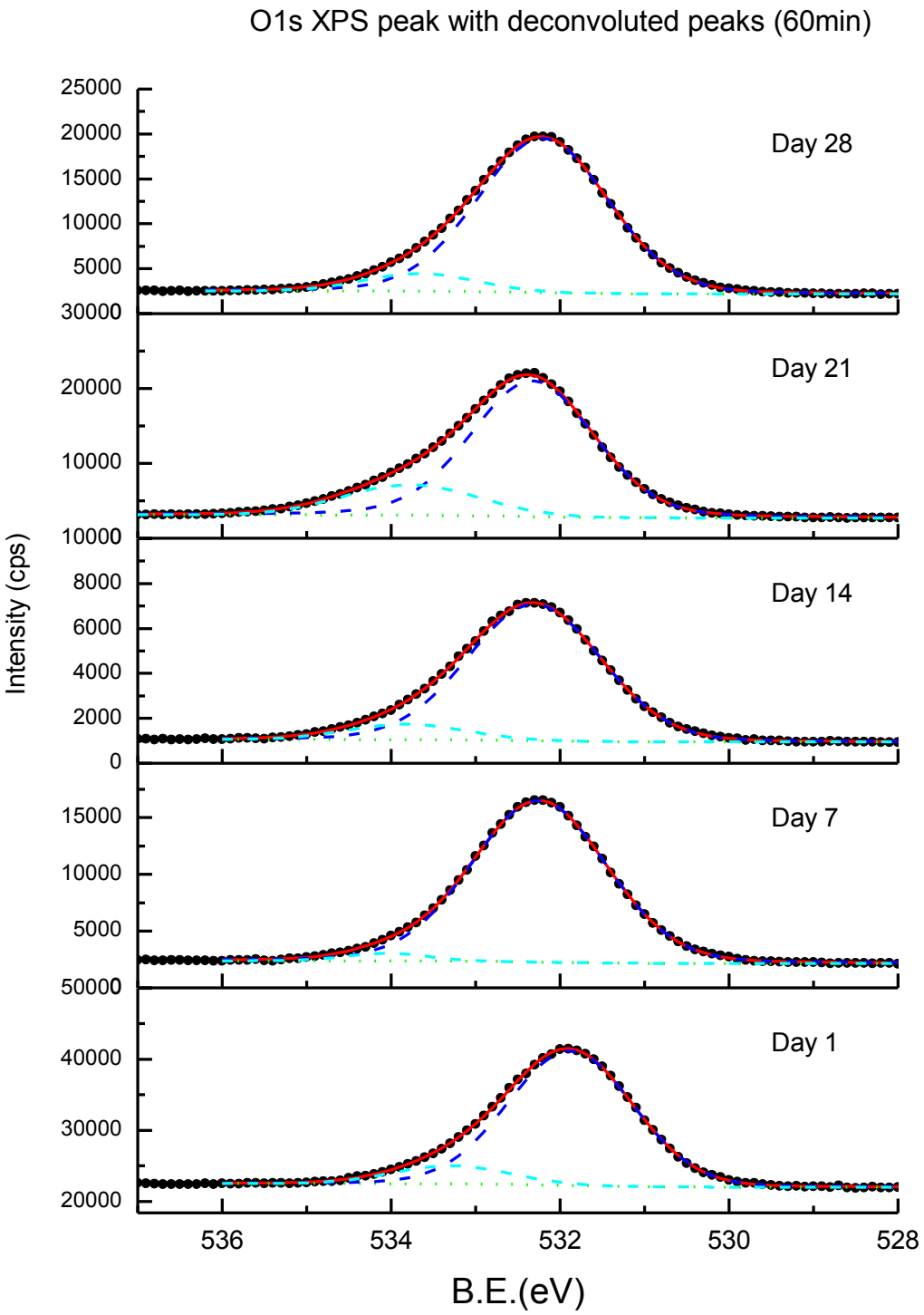

Figure 3.74: O1s XPS high resolution spectra of60 min treated UHMWPE in 80%N_2-20%H_2 over 28 days.

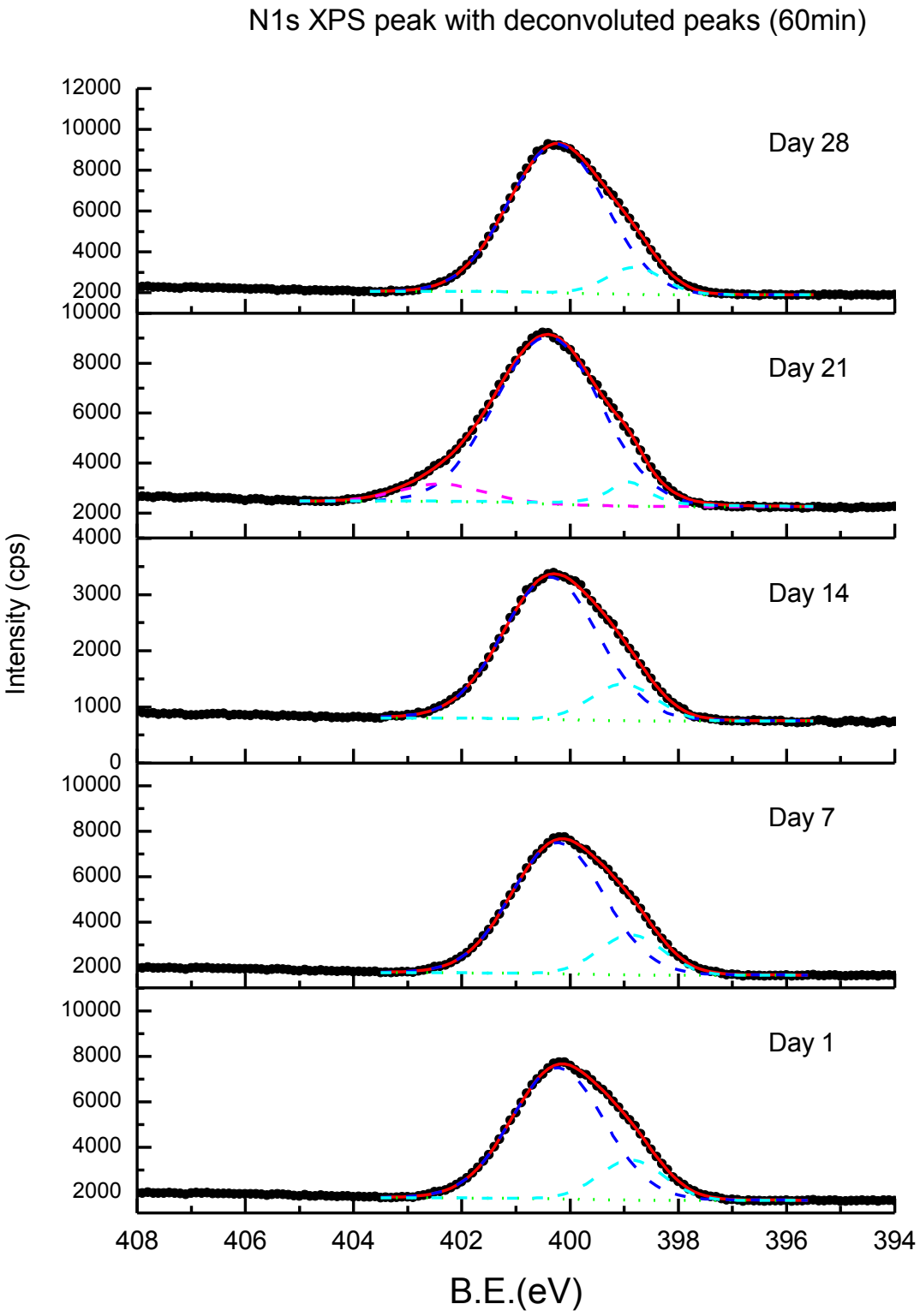

Figure 3.75: N1s XPS high resolution spectra of60 min treated UHMWPE in 80%N_2-20%H_2 over 28 days.

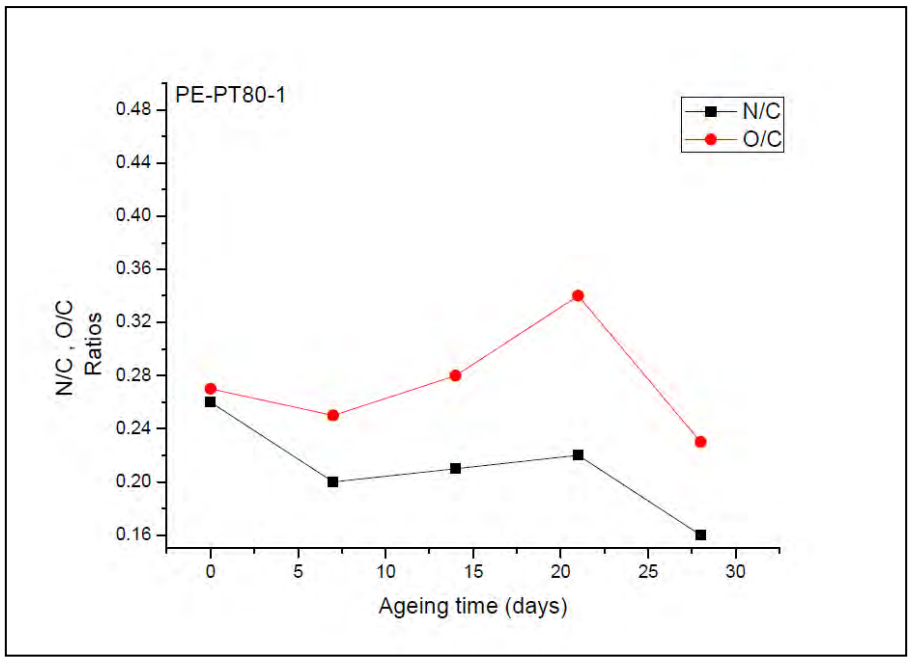

Figure 3.76: N/C and O/C ratios of the ASPN 10 min treated UHMWPE in the ageing study.

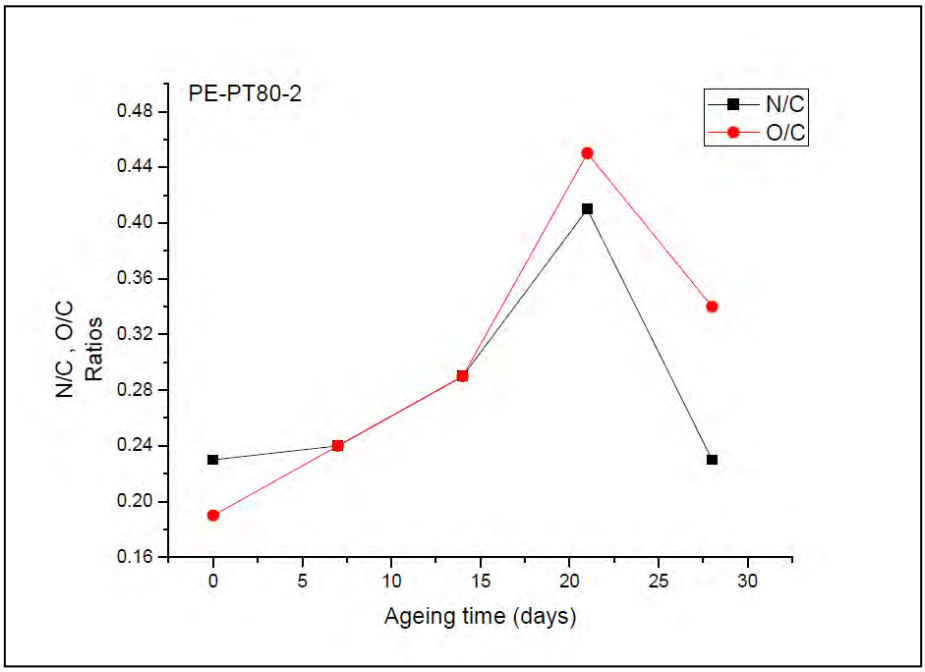

Figure 3.77: N/C and O/C ratios of the ASPN 30 min treated UHMWPE in the ageing study.

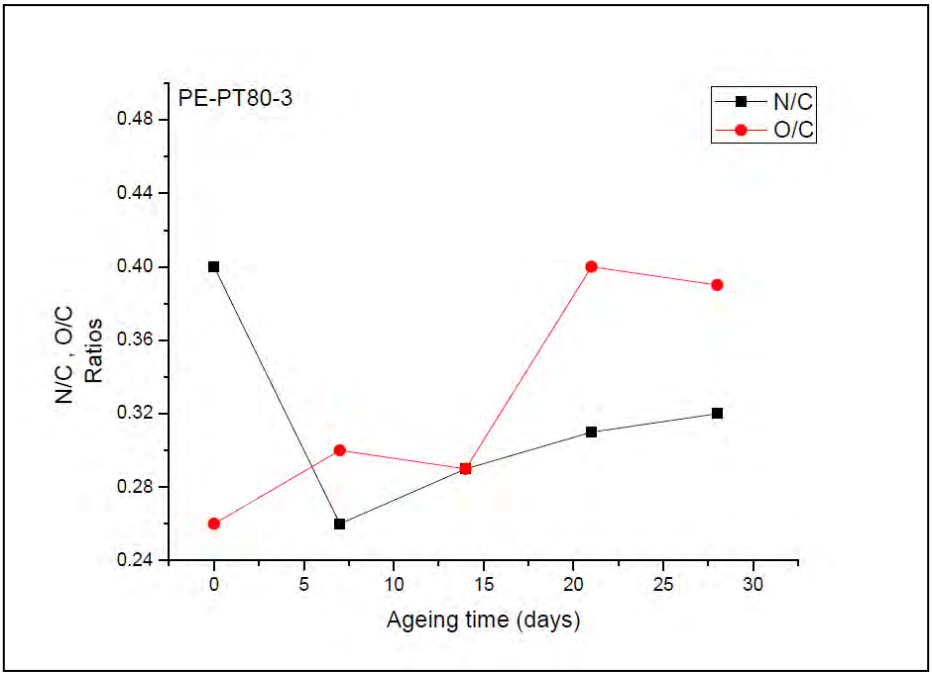

Figure 3.78: N/C and O/C ratios of the ASPN 60 min treated UHMWPE in the ageing study.

Table 3.14: Numerical values of the elemental composition of all 80% ASPN treated samples in a decay study.

Days	**Elemental Composition (%)**								
	PE-PT80-1*			**PE-PT80-2**			**PE-PT80-3**		
	Carbon	**Oxygen**	**Nitrogen**	**Carbon**	**Oxygen**	**Nitrogen**	**Carbon**	**Oxygen**	**Nitrogen**
1	65.133	17.694	17.172	70.010	13.855	16.134	60.050	15.871	24.077
7	68.943	17.263	13.792	67.259	16.498	16.242	63.459	19.546	16.994
14	67.045	18.759	14.195	63.065	18.544	18.390	60.739	21.214	18.045
21	63.609	21.948	14.442	53.522	24.480	21.996	58.103	23.813	18.083
28	71.721	16.599	11.679	63.087	21.933	14.972	58.049	22.902	19.048

3.3.1.7 Ageing study of ASPN-2 UHMWPE: Adhesion forces

Figure 3.79-3.81 show the F_{peak}/R results for 80% ASPN treated samples in air, PBS and S-DMEM respectively. From Figure 3.79, it can be observed that the adhesion forces of the polymer under ambient conditions decrease from day 1 to day 7 and remain almost constant up to day 28, also the 60 min treated sample exhibits much higher electrostatic forces on day 1 compared to the other two samples. Moreover, on day 1, treated UHMWPE stored under aqueous solution exhibited smaller adhesion forces than treated UHMWPE stored in air. Figure 3.80 represents the adhesion forces of the samples stored in PBS. Clearly there is a trend of decrease from day 1 to day 28. Similar results are presented on Figure 3.81, with the exception of the 10 min treated sample where the adhesion forces increase slightly from day 1 to day 28. In general, the adhesion forces appear to decrease towards the end of the decay study in all three environments, revealing that the treatment had an effect on the surface energy of the samples, however it was not a permanent change.

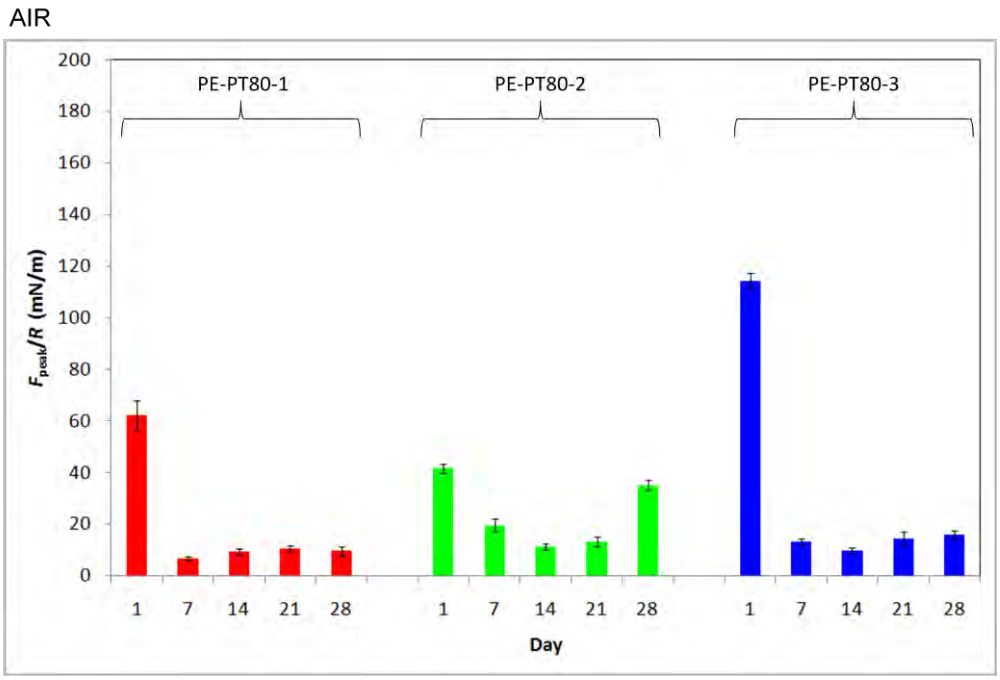

Figure 3.79: F_{peak}/R results for 80% N_2 10, 30 and 60 min treated samples in ambient conditions for the ageing study.

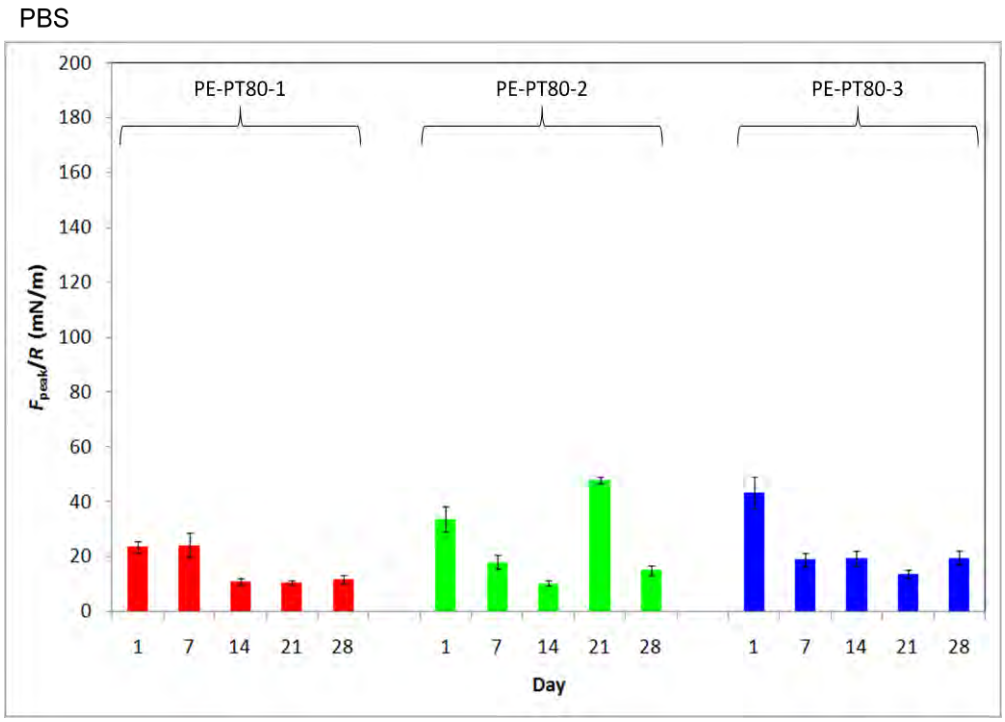

Figure 3.80: F_{peak}/R results for 80% N_2 10, 30 and 60 min treated samples in PBS conditions for the ageing study.

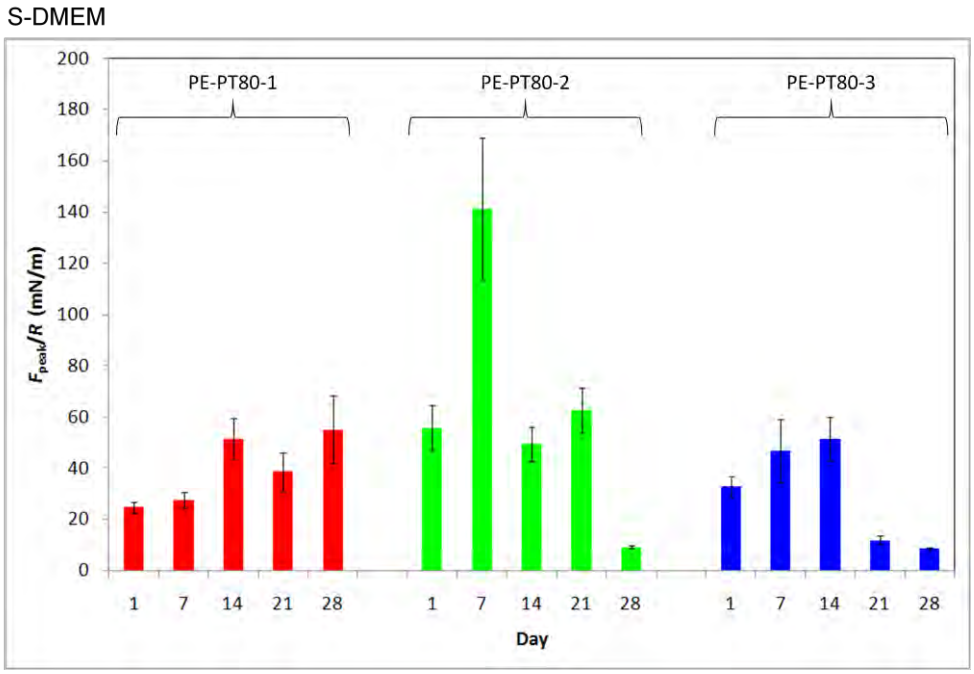

Figure 3.81: F_{peak}/R results for 80% N_2 10, 30 and 60 min treated samples in S-DMEM conditions for the ageing study.

3.3.1.8 Cell compatibility tests: A month study

For the one month cell compatibility study, fibroblasts were seeded on to the surface of 60 min treated 80% UHMWPE (PE-PT80-3). The methods used to characterize the cell seeded samples were SEM, white light interferometry, AFM and MTT assay.

The SEM micrographs for the cell seeding time of 0, 14 and 28 days are presented in Figures 3.82-3.84. The magnifications used were x100, x200 x500, x2000, x5000 and x10000. As it can be observed over a period of four weeks of culture, there were fewer gaps between the cells attached to the surface and the cell culture reached confluency. Increasing culture time, flattening of the cell layers occurred as observed in Figure 3.83. Also in Figure 3.84 there is evidence that the upper cell layer starts to peel off due to the fact that the cell population has been significantly increased in the period of 28 days.

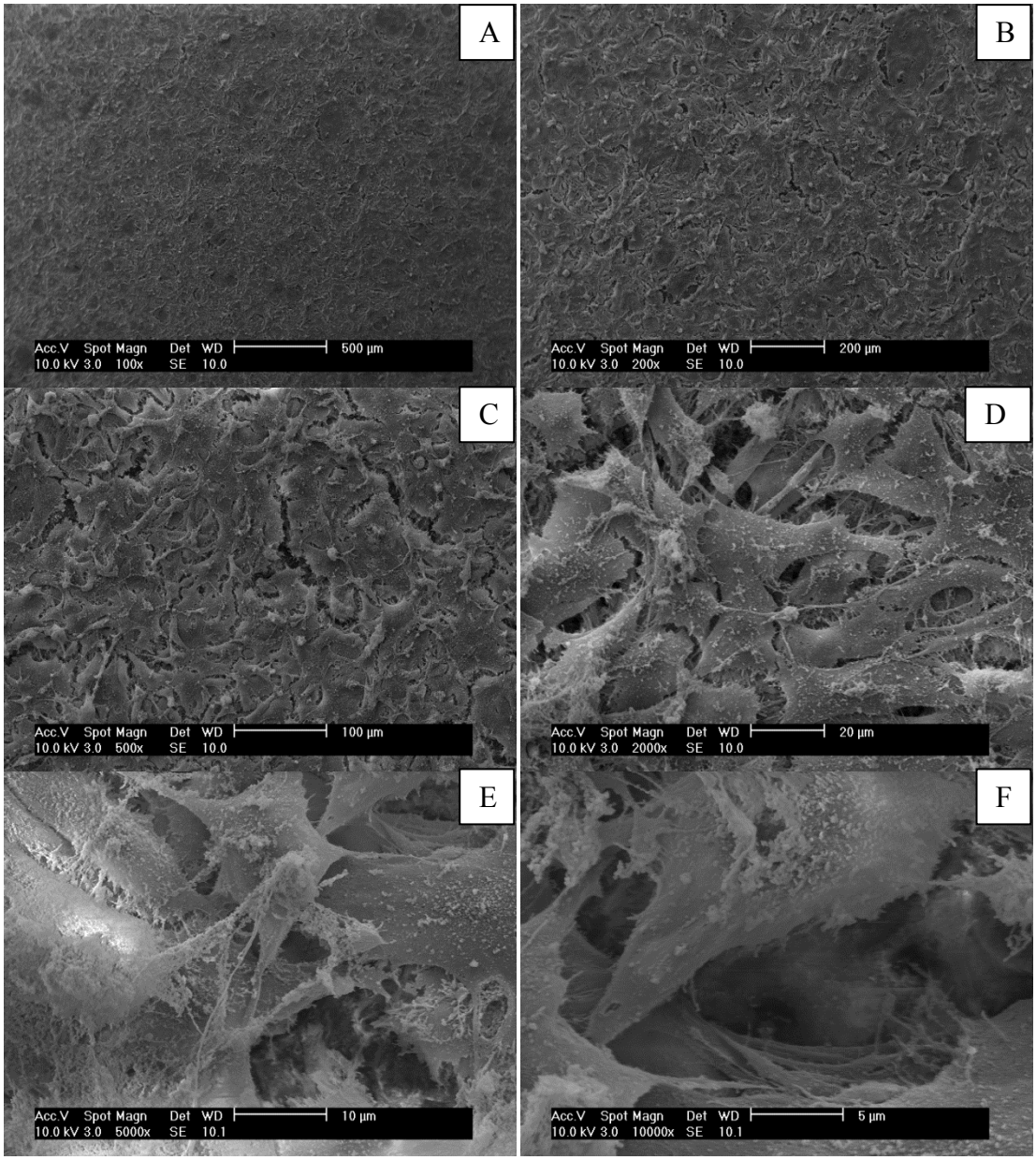

Figure 3.82: SEM imaging of PE-PT80-3 after 3 hrs of seeding with fibroblasts. Magnification varies between x100 to x10000: A) x100, B) x200, C) x500, D) x 2000, E) x 5000 and F) X10000.

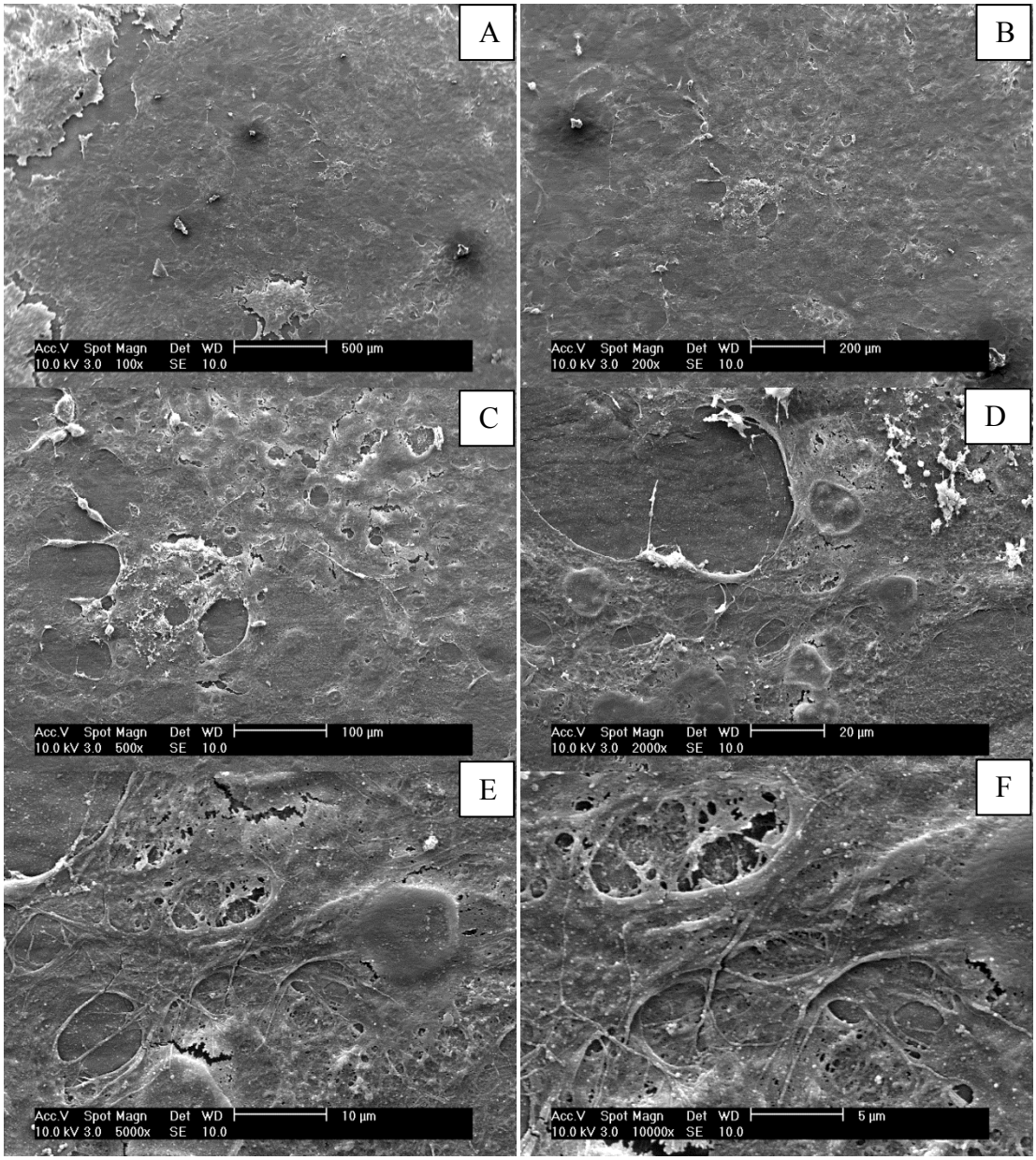

Figure 3.83: SEM imaging of PE-PT80-3 after 14 days of seeding with fibroblasts. Magnification varies between x100 to x10000: A) x100, B) x200, C) x500, D) x 2000, E) x 5000 and F) X10000.

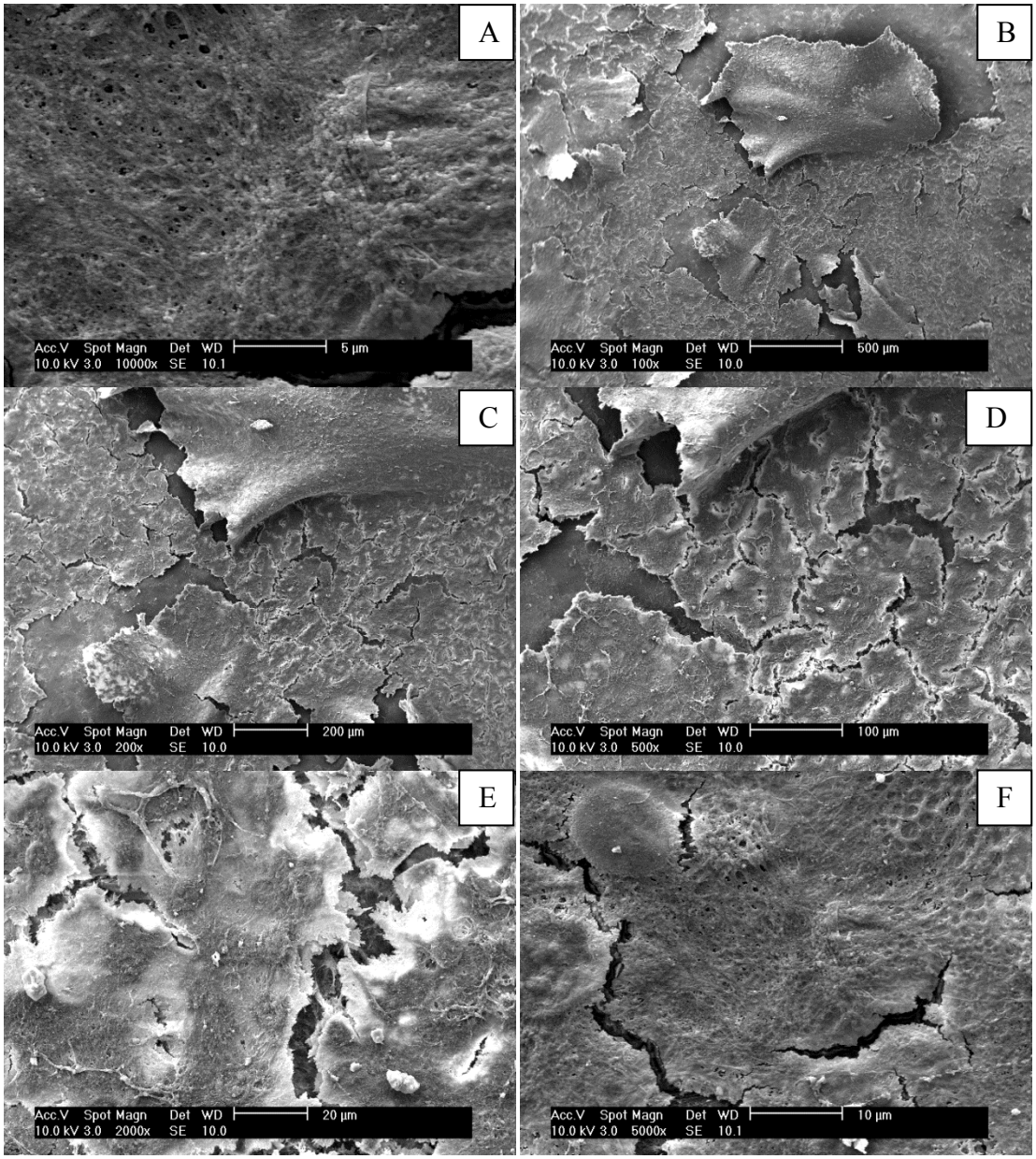

Figure 3.84: SEM imaging of PE-PT80-3 after 28 days of seeding with fibroblasts. Magnification varies between x100 to x5000: A) x100, B) x200, C) x500, D) x 2000, E) x 5000 and F) X5000.

Following to the SEM, white light interferometry was also used in order to image the cells and measure the thickness of the layer that the cells form on to the PE-PT80-3 surface. Three hours following cell seeding (Figure 3.85A); the cells were shown to form layers, which flattened out over the period of cell culture (Figure 3.85 B&C). At the early time-points,

individual cells were easily distinguishable and demonstrated a more rounded morphology than at the later time-points when the individual cells were indistinguishable due to intimate apposition between the cells and the deposition of ECM. Quantitative analysis of cell thickness showed that the cell layer decreased in thickness with time from 18 to 12 µm over a period of four weeks in cell culture (Figure 3.85 D).

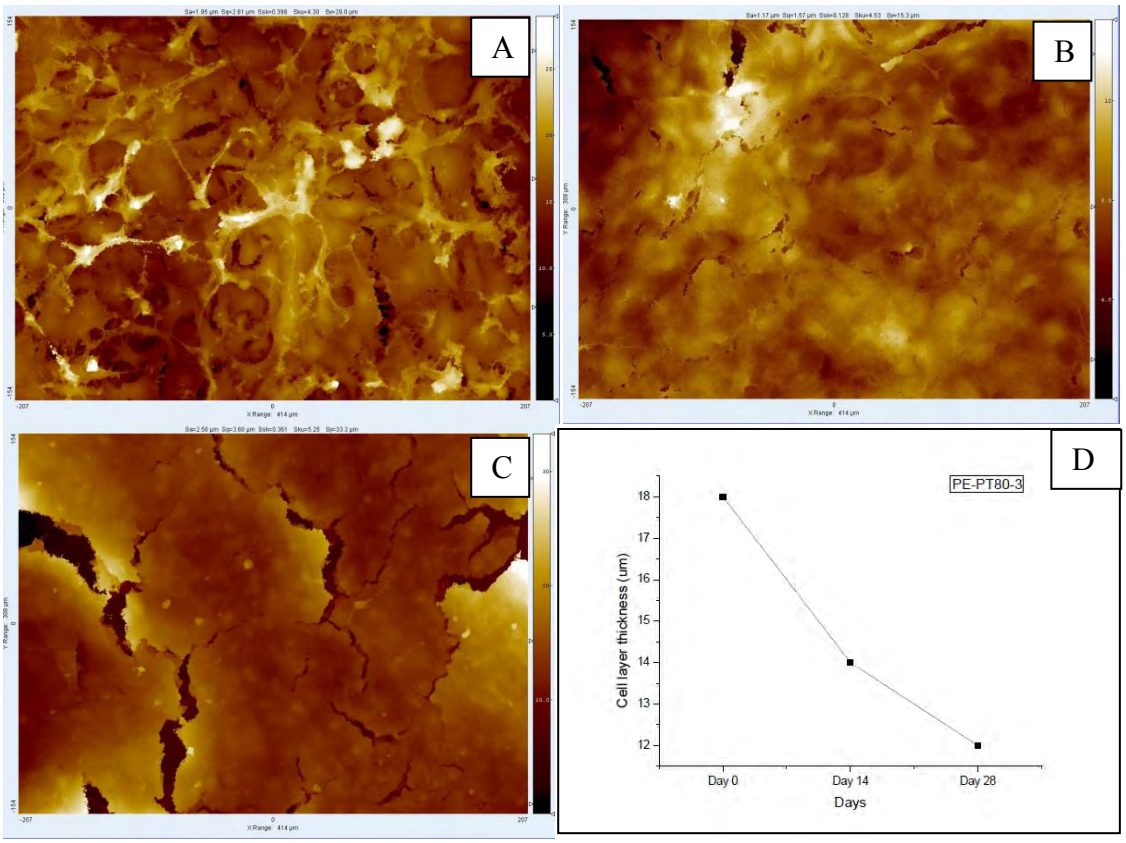

Figure 3.85: Interferometric images of fibroblasts on PE-PT80-3 surface during A) day 0, B) day 14 and C) day 28 of cell seeding. D) Shows the thickness of the cell layer.

The attached samples were also imaged and characterised using AFM. Once more the images demonstrated that the cells were well attached to the polymer surface following three hours and 7 days of cell culturing, respectively (Figure 3.86). Figure 3.87 shows the 3D image of day 7. The AFM adhesion force measurements revealed that F_{peak}/R (peak force normalised by tip radius) between the SiO_2 AFM cantilever tip and the fibroblast cell surface increased

from 6 ± 1 mN/m at day 0 to 25± 5 at day 7 and 46 ± 12 mN/m at day 14. At day 28 there was a reduction in F_{peak}/R to a value of 23 ± 5 mN/m. At day 28, a number of adhesion force curves exhibited the phenomenon of polymer chain pulling, which occurs when surface polymers adhere to the AFM cantilever tip and are stretched and unfolded, until the elastic response of the protein chain is sufficient to overcome the adhesion of the polymer to the tip, whereupon a snap-off event occurs, which is further evidence of ECM deposition. A worm-like-chain (WLC) model was employed to model the persistence length and contour length of these surface polymers (JPK Data Processing software, JPK, Germany) which were calculated as 370 pm and 54 µm, respectively. The polymers exhibited a breaking force in the order of 140 pN. For all days, the Young's Modulus of the fibroblasts was calculated to be in the order of 1-5 µPa. The Young's Modulus was calculated using a Hertzian model, employing JPK Data Processing software, with the Poisson's ratio of the fibroblasts assumed to be 0.5.

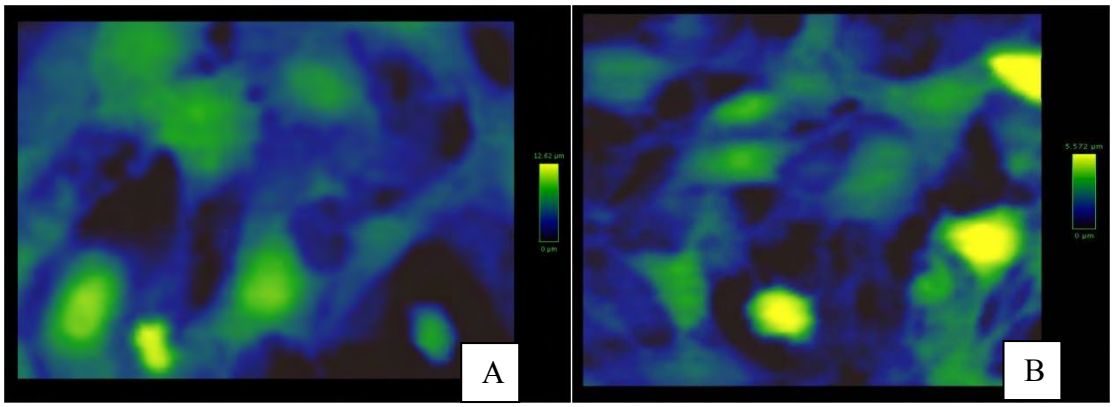

Figure 3.86: AFM image for fibroblasts seeded on the PE-PT80-3 surface for day 0 (A) and day 7 (B). The scale of the x-axis is 100 µm for both images.

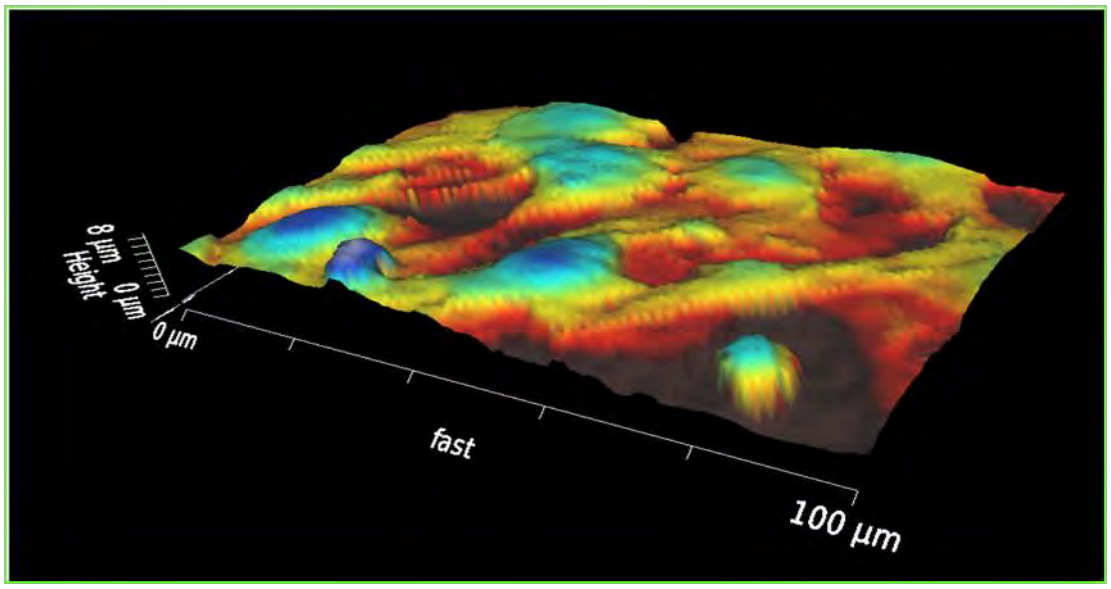

Figure 3.87: The image shows the three-dimensional arrangement of living fibroblast cells on PE-PT80-3 substrate on day 7 of cell culture. The image was acquired using an atomic force microscope operating under aqueous S-DMEM solution at room temperature.

Finally, an MTT assay was conducted for 28 days showing the mitochondrial activity of fibroblasts seeded on PE-PT80-3 surface. Figure 3.88 shows the MTT graph, obtained for the calibration curve. As it can be observed, the mitochondrial activity of fibroblasts is higher on day 7 of the cell culture showing that cell viability and proliferation is higher on day 7.

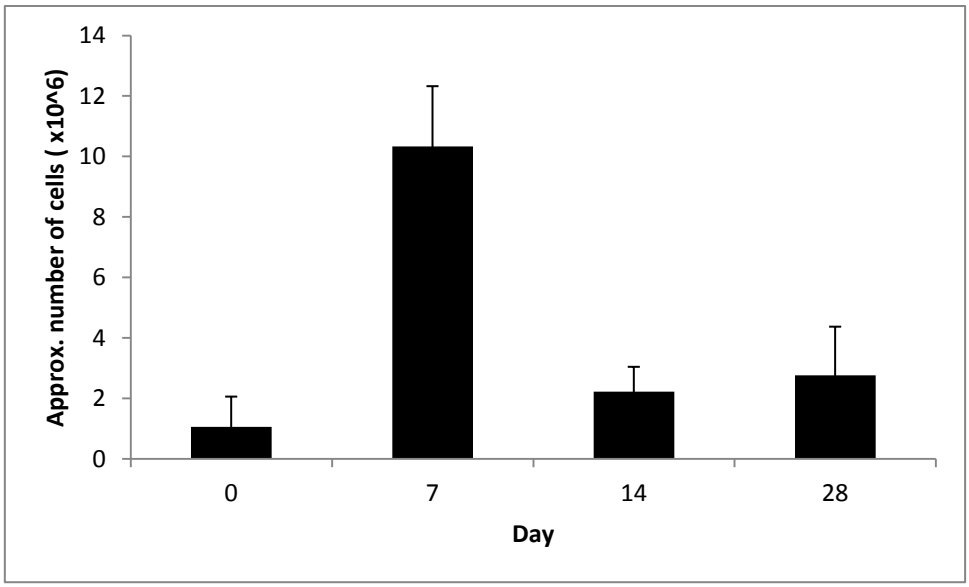

Figure 3.88: MTT graph of fibroblasts seeded on the PE-PT80-3 surface.

3.3.2 Discussion

The second plasma treatment that UHMWPE was subjected was at 90^{o}C, in a gas mixture of 80% N_2 and 20% H_2 and for three different durations, 10, 30 and 60 min. All ASPN treated samples together with the control (untreated UHMWPE) were subjected to surface chemical characterization, to roughness tests and also an initial cell compatibility study was conducted. Further examination of materials was carried out for a month study where the surface chemistry, the mechanical properties, the surface roughness and the adhesion forces were tested during this period. Following to the materials decay study, the 60 min treated sample was chosen for a one month cellular compatibility study.

Initially, the chemical analysis using XPS showed that nitrogen containing groups were present on the ASPN treated surfaces. The same peaks that are present in the UHMWPE that was treated in the gas mixture of 25% N_2 and 75% H_2 are also found here. Briefly, Figures 3.39-3.50 show the survey spectra and the high resolution spectra of UHMWPE that was treated with plasma for 10, 30 and 60 minutes in a gas mixture of 80% N_2 and 20% H_2. From the low resolution spectra (Figures 3.39, 3.43, 3.47) carbon (C 1s at 285 eV), oxygen (O 1s at 532 eV), and nitrogen (N 1s at 400 eV) contributions can be clearly distinguished. These chemical assignments are in accordance with Beamson and Briggs [173]. Here again the plasma treatment shows the insertion of new oxygen and nitrogen containing groups which are very similar to the first treatment at 25%N_2 -75%H_2.

The high resolution spectra of C1s photoelectron peak (Figures 3.40, 3.44, 3.48) shows binding energies of 284.1 eV, 284.95 eV and 284.95 eV which are attributed to C-C bonds, binding energies of 286.89 eV, 286.61 eV and 286.29 eV attributed to C-O and C=N bonds, binding energies of 288.31, 288.2 and 288.09 attributed to C=O, C≡N and N-C-O bonds and only the 30 and 60 min samples appear to have an extra peak at 293.11 eV and at 292.12 eV

respectively which attributed to O-C=O bonds. The assignment of C1s photoelectron peak was discussed in details in the XPS section of 25% N_2 and 75% H_2 plasma treated UHMWPE. Here again, it is believed that the nitrogen presence on the polymer surface after the treatment is appeared mainly in the form of C-N groups. The C1s photoelectron peak of the UHMWPE that was treated in 25% N_2/75% H_2 appears to have slight differences compared to the peak of the 80% N_2/20% H_2 treated material.

The high resolution spectra of O1s photoelectron peak (Figures 3.41, 3.45 and 3.49) show binding energies of 532.14 eV, 531.82 eV and 531.80 eV which are attributed to C-O bonds, and only the 60 min treated samples appears to have one more peak at 534.34 eV which corresponds to O=C-O bonds. These assignments are in accordance with the literature as discussed previously. From Table 3.9 it can be observed that the percentage of oxygen increases after the treatment to around 30-35% of the total elemental composition. A discussed previously the increase of the oxygen contribution has to do with possible oxidation and post reactions on the UHMWPE surface.

Finally, N1s photoelectron peak (Figures 3.42, 3.46 and 3.50) is found at around 399 eV, and is associated with the contributions of N sp^2 and N sp^3 bond according to the literature. The peaks are found at 399.99 eV for 10min treated UHMWPE, at 399.66 for the 30 min and at 399.63 for the 60 min. The percentage distribution of nitrogen on the surface of the samples (Table 3.9) was almost the same for all treated materials which suggested that the treatment time did not affect the amount of nitrogen containing groups on the surface. It may be that a 10 min treatment time results in the chemical saturation of the surface by nitrogen groups and further modification does not have any effect on the number of functional groups formed on the surface. Comparing with the first treatment in the gas mixture 25% N_2-75% H_2 the nitrogen % here is slightly increased (from 6.6-7.0% to 8.4-9.5%) suggesting that the increase

of nitrogen in the gas mixture had a very little influence on the % of nitrogen on the surface of UHMWPE

The surface roughness was tested using white light interferometry. Results are shown in Figures 3.52 and 3.53 where the surface topography and the numerical values S_a and S_q are presented. As it can be observed a very small (not significant) increase in surface roughness is introduced after the treatment. This is in contrast with the literature, where it has been reported, that generally plasma treatments result in an increase of the surface roughness of polymeric surfaces [12, 63, 140]. Similar results were obtained on the PE-PT25 treated materials. The surface roughness did not change due to the treatment as it was revealed by Interferometry and AFM measurements. Thus it could be concluded that the ASPN treatment independently of the duration and the amount of nitrogen used in the gas mixture does not affect the UHMWPE surface morphology and roughness.

An initial observation after 3 h of seeding on plasma treated and untreated materials was conducted, SEM showed that only the treated surfaces attracted cells and the surface treatment was beneficial for the cell attachment and proliferation (Figures 3.55 -3.57). 3T3s immediately attached on the plasma treated surfaces. Very little differences were observed on the cell adhesion on to the treated materials surface. Thus, the time of treatment did not affect the cells behaviour. It is important, however to mention that the cell attachment was very high within the first 3 hours of the cell seeding to all treated materials. As it was discussed in a previous chapter (3.2.2) the nitrogen presence on the surface of polymers affects the cellular behaviour by attracting the proteins responsible for the cells attachment on the surface. Comparing the cellular behaviour on the PE-PT25 treated surfaces significant differences can be observed. The cell attachment and proliferation rate is much higher on the PT-PT80

treated materials. We believe that this is due to the increase of nitrogen percentage in the gas mixture. However, there are not similar studies in the literature.

Following to the initial characterization and compatibility tests, further studies concerning the ageing effect on the plasma treated UHMWPE and the cellular behaviour on the 60 min treated sample over a month were conducted. Cell adhesion on different substrates is controlled by the substrates topography, chemistry and mechanics [94]. Also, the relationship between cells reaction and physicochemical characteristics of substrates such as free energy, functional groups and surface charges, are of great importance for cell culture experiments [97] as mentioned previously.

Surface hardness and reduced modulus (Figures 3.58-3.60) did not show any differences with increasing the time of treatment, suggesting that the modified surface layer was of a similar modulus to the untreated UHMWPE. This result contrasts with the increase in hardness and reduced modulus of the ASPN treated UHMWPE observed during the treatment with 75/25 H_2/N_2 ratio discussed in section 3.2 and reported by Kaklamani *et al*. [198]. Toth *et al.* [199] treated UHMWPE with hydrogen plasma immersion ion implantation (PIII), and their findings showed clearly, that hydrogen treatment increased the surface mechanical properties such as hardness (*H*), reduced modulus (*E*) and slope of scratch (*S*). To this end, the UHMWPE surface mechanical properties can be tailored somewhat through careful selection of the H_2/N_2 ratio. It has been reported, that cells can be strongly influenced by the mechanical properties (i.e. stiffness) of the surface they adhere [200]. Cells receive the mechanical information from the surrounding environment and proceed to their proliferation and differentiation according to the way they translate this information. However, this is not the case here, as the surface mechanical properties did not change, suggesting that fibroblasts were not influenced in such a way.

As it was observed from Figures 3.61-3.63 the surface roughness of plasma treated UHMWPE was not influenced by the different environments, the duration of the treatment or the decay. Curtis *et al.* have extensively reported, that surface topography influences cell proliferation and differentiation suggesting that the higher the roughness, the better the cell attachment [201]. In conclusion from the above, the surface treatments and the environmental conditions during the decay study did not affect the surface roughness. Consequently, the treated UHMWPE is stable under physiological conditions, allowing cellular adhesion and growth to occur without surface degradation.

The ageing of the samples did not seem to affect the nature of the bonds present on the treated surfaces and identified by the relevant peaks in the graphs. From Figures 3.64, 3.68 and 3.72 it can be observed that C1photoelectron peak is found at 285 eV, O1s at 532 eV and N1s at 400 eV, which as mentioned previously are in agreement with the literature.

The high resolution spectra of C1s (Figures 3.65. 3.69 and 3.73) when deconvoluted show the contribution of the same three peaks: at ~285 eV the peak is attributed to C-C bonds, at ~286.5 to C-O/C≡N bonds and at ~288 eV to C=O/ C≡N/ N-C-O bonds. The high resolution spectra of O1s (Figures 3.66. 3.70 and 3.74) when deconvoluted show the contribution of the same two peaks: at ~532 eV the peak is attributed to C-O bonds and at ~534 eV to O=C-O bonds. Finally, The high resolution spectra of N1s (Figures 3.67. 3.71 and 3.75) when deconvoluted show the contribution of the same two peaks: at ~400 eV the peak is attributed to C-N bonds and at ~398 eV to C=N bonds.

Table 3.14 shows that the percentage of nitrogen had a slight decrease during the 28 days however the nature of the bonds that were formed onto the treated material surface (described in previous section) did not seem to change. It is worth noticing that the percentage of nitrogen content on the treated surfaces was much higher (ca 20%) compared to the nitrogen

content measured for the treated surfaces before the decay in air (ca 9%). This is most likely because in the first case, the treated surfaces were left in air where the nitrogen content is as high as 80%, in contrast with the treated surfaces before the decay where a lot of care had been taken to protect the surfaces from exposure to air storing the samples under vacuum and performing XPS very soon after the treatments. In the literature it is suggested that nitrogen plasma treated PE changes in terms of the surface chemistry when left to age in ambient conditions. Gerenser *et al.* suggest that exposing nitrogen plasma treated surfaces to air results in hydrolysis of the imine groups that are present on the surface [202]. O'Kell *et al.* treated PE films with low-power nitrogen plasma and exposed the samples to air after the treatment. They suggest that oxygen replaces nitrogen on the surface according to the equation:

$$C\text{-}NH_2 + H_2O \longrightarrow C\text{-}OH + NH_3$$

They believe that in this process which is happening the first few days after the treatment the amount of nitrogen remains constant but the amount of oxygen increases with the ageing time. In the long term processes however they suggest gradual oxidation of the polymer itself [203].

Figures 3.79-3.81 show the AFM analysis of the treated UHMPWE where the decrease of the adhesion forces can be observed, especially between day 1 and day 7 of the study. Moreover, in day 1, treated UHMWPE stored under aqueous solution exhibited smaller adhesion forces than treated UHMWPE stored in air. This result suggested that residual electrostatic charges remaining in the sample following the ASPN treatment were lost to the surrounding environment between day 1 and day 7. In this case, it is clear that the cell attachment was not influenced by any residual charges on the surface due to the treatment.

Generally, cells do not attach on a bare surface. First, adsorption of adhesion proteins on the materials surface takes place and then these proteins are recognized by the integrin receptors found on the ECM of the cells. *In vitro* cell attachment on materials surfaces is mediated by glycoproteins (fibronectin and vitronectin) of which the attachment on a surface is dependent on the substrate properties and specifically on the substrate chemistry which controls the nature of the protein layer [204]. It has been reported, that nitrogen containing plasma surfaces have adsorptive characteristics that attract fibronectin and vitronectin, suggesting that the presence of amine groups on a substrate enhances the cell attachment [205].

Cell seeding was conducted for a total duration of 28 days. An initial observation showed that cells attachment was almost the same no matter the duration of the treatment (Figures 3.55-3.57) only the 60 min treated UHMWPE sample was used to evaluate the cells behaviour. For the 60 min treated UHMWPE and for days 0, 14 and 28 of seeding, qualitative analysis using SEM showed that cells were attached and became confluent. During observation at day 0 it was shown, that cells were interconnected and exhibited a cylindrical or stellate shape. Cytoplasmic extensions were observed and the filopodia of adjacent cells were conjoined (Figure 3.82). A morphological alteration of the cell layer was observed between day 0 and days 14 and 21 (Figures 3.83-3.84) as cells could not be distinguished formed a flat layer being firmly attached to one another. Days 14 and 28 showed that fibroblasts were spread at almost the same degree.

Additionally to SEM, interferometric analysis revealed that the thickness of the cellular layer was highest on day 0 and lowest on day 28. Since cells attached on the treated UHMWPE surface, the more they spread the more they proliferated and their contact area with the surface increased. Therefore, their body volume decreased. The distances, however among them became more firm forming layers with minimum gaps in between. Such a result appears

reasonable given that there will be a maximum possible rate of diffusion of nutrients into the layers from the solution, and this may set an upper bound on the total possible number of layers which can be viably maintained as the fibroblasts grow and develop, requiring increased levels of nutrients as they do so.

The AFM adhesion force measurements revealed that F_{peak}/R between the SiO_2 AFM cantilever tip and the fibroblast cell surface increased from day 0 to day 14. As the cells matured, they released proteins that collectively formed the extracellular matrix (ECM) [206]. At day 28, there was a reduction in F_{peak}/R which corresponded to a change in the proteins present at the fibroblast external surface due to cellular maturation and variation in the composition of the extracellular matrix over this time.

3.3.3 Summary

The ASPN technique was used to modify the surface of UHMWPE in an atmosphere of 20/80 H_2/N_2 ratio. The treatment was found to have a positive effect on the fibroblasts seeded on the treated polymeric surfaces enhancing the proliferation, attachment and adhesion of cells. The materials surface characterization showed that the mechanical properties, adhesion forces and surface roughness of UHMWPE did not change significantly due to treatment in contrast with the results presented in section 3.2 where the H_2/N_2 ratio was 75/25. The chemistry of the surface however changed as after the treatment, nitrogen containing bonds were introduced on the surface. Therefore, this study has revealed, that the improved cell compatibility of UHMWPE surface treated by ASPN was mainly caused due to the successful modification of the polymer surface chemistry.

CHAPTER 4 : CONCLUSIONS AND FUTURE WORK

4.1 Ionomer Glass

The active screen plasma nitriding technique was applied to inorganic and organic polymeric biomaterials such as an ionomer glass composition and UHMWPE. After the treatment, both materials revealed changes on their surface characteristics and showed a significantly improved cellular compatibility.

The ASPN surface treatment of the ionomer glass resulted in increased hardness and elastic modulus and decreased surface roughness. The surface chemistry was also modified and incorporation of 1.5 % nitrogen of the total elemental composition of the surface was observed and formation of Si-N bonds was recorded. Despite the surface treatment was performed at 400^{o}C, a glassy amorphous structure was retained and observed by XRD. Also compatibility tests using 3T3 fibroblasts showed that after the treatment cellular compatibility was induced on the glass surface. We believe that the main reason that affected the fibroblasts behaviour was the introduction of the nitrogen onto the materials surface. The technique was proved beneficial concerning the introduction of cellular compatibility on the glass.

More work should be carried out in order to optimise the technique and also to understand better the cellular reaction on the plasma treated surfaces. Thus first, different conditions of the treatment should be used and second more detailed cell experiments should be conducted to identify the exact reasons of the improved cellular behaviour.

Specifically, the following future work can be suggested:

1. Different durations of the treatment should be conducted in order to examine if the time of treatment affects the percentage of nitrogen incorporation onto the glass surface.

2. A systematic study using different gas mixtures containing nitrogen and hydrogen should be conducted in order to examine which of the environmental conditions is the optimum for the glass surface and what is the exact nature of the new bonds that are formed after the treatment.

3. Further characterization methods such as contact angle measurements should be employed to study whether the plasma modified surfaces become more hydrophobic or hydrophilic.

4. More detailed cell experiments should be conducted involving dead live staining, MTT assays, Interferometry and AFM so that the number of cells and their morphology will be tested over a specific period of time (e.g: 1 month).

5. Apart from the fibroblasts, other cell lines could be used to seed the glass surface such as osteoblasts.

4.2 UHMWPE

Samples of a flat UHMWPE sheet were treated under two different environmental conditions (75/25 and 20/80 H_2/N_2). All the parameters of the plasma treatment were kept the same apart from the temperature and the gas mixture. For the first treatment that was conducted at 120^oC, in a gas mixture of 25% N_2 and 75% H_2 results showed that both the surface characteristics and the cellular compatibility of the polymer were affected. Both surface hardness and elastic modulus increased after the treatment without being affected by the duration of the treatment whereas the surface roughness did not change significantly. The more significant changes on the surface of UHMWPE were observed on the surface chemistry of the polymer due to the introduction of new chemical bonds containing nitrogen (C-N bonds). The incorporation of nitrogen was ~6-7 % and the duration of the treatment did not affect the nitrogen content of the treated surface. Finally, the fibroblasts seeding on the untreated and plasma treated surfaces showed that the cellular compatibility was improved with the time of treatment. The cell culture study showed clearly that the treatment was beneficial for the cell attachment and proliferation on the plasma treated surfaces.

The next series of treatments conducted at 90^oC, in a gas mixture of 80% N_2 and 20% H_2 showed slightly different results. Here, the mechanical properties, electrostatic forces and surface roughness of UHMWPE did not change significantly due to treatment. It is believed that the effect of the treatment depends significantly on the gas mixture used and specifically whether the gas mixture is rich in nitrogen or hydrogen. This work showed clearly, that a surface treatment in a hydrogen rich atmosphere will increase the mechanical properties of the surface whereas a nitrogen rich atmosphere will not have significant effect on the mechanical properties of the surface. The surface chemistry was significantly affected by the surfaces treatment observed by the formation of new bonds very similar to the bonds found in

the first treatment. The amount of nitrogen found on the surface was increased for about 3% compared to the first treatment, probably due to the increased amount of nitrogen in the gas mixture during the treatment. However, this slight difference in nitrogen % seemed to affect significantly the cellular behaviour on the plasma treated surfaces. This was revealed only after 24 hours of the fibroblast seeding showing great response of the cells on the surface with very high proliferation, attachment and adhesion rates. A more detailed analysis of the cellular behaviour revealed that the treatment successfully modified the surface of UHMWPE, since layers of cells attached and were viable for a month on to the treated surfaces. According to the results obtained from both treatments it is clear that the more nitrogen in the gas mixture the more the fibroblasts are attracted to the treated surface.

Further work should be conducted in order to optimize the process of plasma treatment, and identify the most appropriate combination of plasma gas that will modify successfully a surface.

The following recommendations can be made:

1. A systematic study of the treatment duration would be very beneficial in order to identify the optimum minimum treatment duration when the surface nitrogen content reaches saturation.

2. Contact angle measurements should be carried out, since cells viability is highly affected by this parameter.

3. A more systematic work on cell culture experiments is suggested, this should contain protein expression experiments in order to identify specific proteins that are triggered due to the plasma treatment.

LIST OF REFERENCES

1.Kostov KG, Ueda M, Lepiensky M, Soares Jr PC, Gomes GF, Silva MM, et al. Surface modification of metal alloys by plasma immersion ion implantation and subsequent plasma nitriding. *Surf Coat Technol* 2004; **186**: 204-208

2.Damborenea J. Surface modification of metals by high power lasers. *Surf Coat Technol* 1998; **100-101**: 377-382

3.Oehr C. Plasma surface modification of polymers for biomedical use. *Nucl Instrum Methods B* 2003; **208**: 40-47

4.Hoffman AS. Surface modification of polymers: physical, chemical, mechanical and biological methods. *Macromol Symp* 1996; **101**: 443-454

5.Theppakuttai S, Chen S. Nanoscale surface modification of glass using a 1064 nm pulsed laser. *Appl Phys Lett* 2003; **83**: 758-760

6.Ratner BD. New ideas in biomaterials science-a path to engineered biomaterials. J *Biomed Mater Res* 1993; **27**: 837-850

7.Oliva A, Ragione FD, Salerno A, Riccio V, Tartaro G et *al.* Biocompatibility studies on glass ionomer cements by primary cultures of human osteoblasts. *Biomaterials* 1996; **17**: 1351-1356

8.Peppas NA, Langer R. New challenges in Biomaterials. *Mater Sci* 1996; **262**: 1715-1720

9.Boyan BD, Hummert TW, Dean DD, Schwartz Z. Role of material surfaces in regulating bone and cartilage cell response. *Biomaterials* 1996; **17**: 137-146

10.Cao W, Hench LL. Bioactive materials. *Ceram Int* 1996; **22**: 493-507

11.Anderson JM. Biological responses to materials. *Annu Rev Mater Res* 2001; **31**: 81-110

12.Chu PK, Chen JY, Wang LP, Huang N. Plasma-surface modification of biomaterials. *Mater Sci Eng R* 2002; **36**: 143-206

13.Wong JY, Leach JB, Brown XQ. Balance of chemistry, topography and mechanics at the cell-biomaterial interface: Issues and challenges for assessing the role of substrate mechanics on the cell response. *Surf Sci* 2004; **570**: 119-133

14.Ratner BD. Surface modification of polymers: chemical, biological and surface analytical challenges. *Biosens Bioelectron* 1995; **10**: 797-804

15.Sodhi RNS. Appication of surface analytical and modification techniques to biomaterial research. *J. Electron. Spectrosc. Relat. Phenom.* 1996; **81**: 269-284

16.BD Ratner. Surface properties and surface characterization of materials. In: BD Ratner, AS Hoffman, FJ Schoen, JE Lemons, editors. *Biomaterials Science*. Academic press Elsevier; 2004; p 40-58.

17.Yasuda H, Gazicki M. Biomedical applications of plasma polymerization and plasma treatment of polymer surfaces. *Biomaterials*. 1982; **3**: 68-77.

18.Ratner BD, Chilkoti A, Lopez GP. Plasma deposition and treatment for biomaterial applications. In: D'Agostino R, editor. Plasma deposition, treatment, and etching of polymers. San Diego: Academic Press, Inc; 1990; p 471-510

19.Chu PK. Plasma-treated biomaterials. *IEEE T Plasma Sci.*2007; **35**: 181-187

20.Cui FZ, Luo ZS. Biomaterials modification by ion-beam processing. *Surf Coat Techno.* 1999; **112**: 278-285

21.Hoffman *et al*. US Patent 5,034.265 No. 19

22.Aronson BO, Lausmaa J, Kasemo B. Glow discharge plasma treatment for surface cleaning and modification of metallic biomaterials. *J Biomed Mater Res.* 1997; **35**: 49-73

23.Ratner BD. Plasma deposition for biomedical applications: a brief review. *J. Biomater. Sci. Polymer.* 1992; **4**: 3-11

24.Boudou JP, Paredes JI, Cuesta A, Martinez-Alonsi A, Tascon JMD. Oxygen plasma modification of pitch-based isotropic carbon fibres. *Carbon* 2003; **41**: 41-56

25.Inagaki N, Tasaka S, Kawai H, Kimura Y. Hydrophilic surfaces modification of polyethylene by NO-plasma treatment. *J. Adhesion Sci. Technol*. 1990; **4**: 99-107

26.Badey JP, Espuche-Urbaczewski E, Jugnet Y, Sage D, Duc TM, Chabert B. Surface modification of polytetrafluoroethylene by microwave plasma downstream treatment. *Polymer*. 1994; **35**: 2472-2479

27.Hegemann D, Brunner H, Oerh C. Plamsa treatment of polymers for surface and adhesion improvement. *Nucl Instrum Methods* 2003; **208**: 281-286

28.Ozdemir Y, Hasirci N. Oxygen plasma modification of polyurethane membranes. *J Mater Sci – Mater M* 2002; **13**: 1147-1152

29.Yuan S, Szakalas-Gratzl G, Ziats NP, Joacobsen K, Kottke-Marchant K, Marchant RE. Immobilization of High-affinity herapin oligosaccharides to radio frequency plasma-modified polyethylene. *J. Biomed. Mat. Res*. 1993; **27**: 811-819

30.Smetana K. Cell biology of hydrogels. *Biomaterials* 1993; **14**: 1046-1050

31.Sheu MS, Hoffmann AS, Feuen J. A glow discharge treatment to immobiolize poly (ethylene oxide)/poly (propylene oxide surfactants for wettable and non-fouling biomaterials. *J. Adhesion Sci. Technol*. 1992; **6**: 995-1009

32.France RM, Short RD. Effects of energy transfer from an argon plasma on the surface chemistry of poly(styrene), low density poly (ethylene), poly (propylene) and poly (ethylene terephthalate). *J. Chem. Soc. Faraday Trans* 1997; **93**: 3173-3178

33.Zhao C, Wang LY, Han L. Active screen plasma nitriding of AISI 316L austenitic stainless steel at different potentials. *Surface Eng.* 2008; **24**: 188-192

34.Menthe E, Rie KT. Plasma nitriding and plasma nitrocarburizing of electroplated hard chromium to increase the wear and the corrosion properties. *Surf Coat Techno.* 1999; **112**: 217-220

35.Rei KT, Stucky T, Silva RA, Leitao E, Bordii K et al. Plasm surface treatment and PACVD on Ti alloys for surgical implants. *Surf Coat Techno.* 1995; **74-75**: 973-980

36.Menthe E, Rie KT, Schultze JW, Simson S. Structure and properties of plasma-nitrided stainless steel. *Surf Coat Techno.* 1995; **74-75**: 412-416

37.Shen YZ, Oh KH, Lee DN. Nitriding of steel in potassium nitrate salt bath. *Scripta Mater*. 2005; **53**: 1345-1349

38.Zhao C, Li CX, Dong H, Bell T. Study on the active screen plasma nitriding and its nitriding mechanism. *Surf Coat Techno.*2006; **201**: 2320-2325

39.Li CX, Bell T. Sliding wear properties of active screen plasma nitride 316 austenitic stainless steel. *Wear* 2004; **256**: 1144-1152

40.Alves C, Araujo FO, Ribiero KJB, Costa JAP, Sousa RRM et al. Use of cathodic cage in plasma nitriding. *Surf Coat Techno.*2006; **201**: 2450-2454

41.Ahangarani S, Mahboubi F, Sabour AR. Effects of various parameters on active screen plasma nitriding behaviour of low-alloy steel. *Vacuum* 2006; **80**: 1032-1037

42.Ahangarani S, Sabour AR, Mahboubi F. Surface modification of 30CrNiMo8 low-alloy steel by active screen setup and conventional plasma nirtiding methods. *Appl Surf Sci.* 2007; **254**: 1422-1435

43.Li CX, Georges J, Li XY. Active screen plasma nitriding of austenitic stainless steel. Plasma Metal S.A. L-1817 Luxembourg. 1-7.

44.Li CX, Dong H, Bell T. A feasibility study of plasma nitriding of steel with an oxide layer on the surface. *J Mater Sci* 2006; **41**: 6116-6118

45. Georges J. Nitriding process and nitriding furnace therefor. Patent No: 5.989.363. 1999

46.Li CX, Bell T. Corrosion properties of active screen plasma nitride 316 austenitic stainless steel. *Corros Sci.* 2004; **46**: 1527-1547

47. Li CX, Bell T, Dong H. A study of active screen plasma nitriding. *Surface Eng.* 2002; **18**: 174-181

48.Shuvaee HA, Hosseini HRM, Lotfabad EM, Roostaie S. Study of nanocrystallization in FINEMET alloy by active screen plasma nitriding. *J Alloy Compd*. 2010; **491**: 487-494

49.Cleugh D. Plasma species analysis for in situ assessment of surface treatments. *Surface Eng*. 2002; **18**: 133-139

50.Gallo SC, Dong H. Study of active screen plasma processing conditions for carburising and nitriding austenitic stainless steel. *Surf Coat Techno.* 2009; **203**: 3669-3675

51.Hubbard P, McCulloch DG, Doyle ED, Dowey SJ, Georges JN. A fundamental contribution to a study of the active screen plasma nitriding process. *BHM* 2006; **11**: 441-445

52.Wang L, Li Y, Wu X. Plasma nitriding of low alloy steels at floating and cathodic potentials. *Appl Surf Sci.* 2008; **254**: 6695-6600

53.Jagielski J, Turos A, Bielinski D, Abdul-Kader AM, Piatowska A. Ion-beam modified polymers for biomedical applications. *Nucl Instrum Methods B*. 2007; **261**: 690-693

54.Kang ET, Neoh KG, Shi JL, Tan KL, Liaw DJ. Surface modification of polymers for adhesion improvement. *Polym. Adv. Technol*. 1999; **10**: 20-29

55.Ikada Y. Surface modification of polymers for medical applications. *Biomaterials*. 1994; **15**: 725-736

56. Strobel M, Walzak MJ, Hill JM, Lin A, Karbashewski E et al. A comparison of gas-phase methods of modifying polymer surfaces. *J. Adhesion Sci Technol*. 1995; **9**: 365-383

57.Chan CM, Ko TM, Hiraoka H. Polymer surface modification by plasmas and photons. *Surf Sci Rep*. 1996; **24**: 1-54

58.Zhang J, Cui CQ, Lim TB, Kang ET, Neoh KG. Adhesion improvement of a poly(tetrafluoroethylene)-copper laminate by thermal graft copolymerization. *J Adhesion Sci Technol*. 1998; **12**: 1205-1218

59. Harth K, Hibst H. Suarface modification of polypropylene in oxygen and nitrogen plasmas. *Surf Coat Techno.* 1993; **59**: 350-355

60.Ozdemir M, Sadikoglu H. A new and emerging technology: lasr-induced surface modification of polymers. *Trends Food Sci Tech*. 1998; **9**: 159-167

61.Kudetoshi H, Kusunoki T, Kobayashi T. Surface modification of polymers by thermal ozone treatments. *J Mater*. 2007; **3**: 1-10

62.Ujvari T, Toth A, Bertoti I, Nagy PM, Juhasz *A. Mater Res Soc Symp P*. 2001; **141-142**: 225-229

63.Teodoru S, Kusano Y, Rozlosnic N, Michelsen PK. Continuous plasma treatment of ultra-high molecular weight polyethylene (UHMWPE) fibres for adhesion improvement. *Plasma Process. Polym*. 2009; **6**: 1-7

64.Favia P, D'Agistino R, Palumbo F. Grafting of chemical groups onto polymers by means of RF plasma treatments: a technology for biomedical applications. *J Phys IV France.* 1997; **7**: 199-208

65.Kauling AP, Soares GV, Figueroa CA, Oliviera RVB, Baumvol IJR et al. Polypropylene surface modification by active screen plasma nitriding. *Mater Sci Eng*. 2009; **29**: 363-366

66.Gengenback TR, Griesser HJ. Post-deposition ageing reactions differ markedly between plasma polymers deposited from siloxane and silazane monomers. *Polymer.* 1999; **40**: 5079-5094

67.Liston EM, Martinu L, Wertheimer MR. Plasma surface modification of polymers for improved adhesion: a critical review. *J. Adhesion Sci. Technol*. 1993: **7**: 1091-1127

68.Guruvrnket S, Rao GM, Komath M, Raichur AM. Plasma surface modification of polystyrene and polyethylene. *Appl Surf Sci.* 2004; **236**: 278-284

69.Gancarz I, Bryjak J, Bryzak M, Pozniak G, Tylus W. Plasma modified polymers as a support for enzyme immobilization 1. Allyl alcohol plasma. *Eur Polym J.* 2003; **39**: 1615-1622

70.Manso M, Valsesia A, Ceccone G, Rossi F. Activation of PCL surface by ion beam treatment to enhance protein adsorption. *J Bioact Compat Pol*. 2004; **19**: 287-300

71.Ren TB, Weigel T, Groth T, Lendlein A. Microwave plasma surface modification of silicone elastomer with allylamine for improvement of biocompatibility. *J Biomed Mater Res A*. 2007; 209-219.

72.Kurtz SM. *The UHMWPE Handbook.* Academic press Elsevier; 2004; p 1-36.

73.Shi W, Li XY, Dong H. Improved wear resistance of ultra-high molecular weight polyethylene by plasma immersion ion implantation. *Wear* 2001; **250**: 544-552

74.Dong H, Bell T, Blawert C, Mordike BL. Plasma immersion ion implantation of UHMWPE. *J Mater Sci Lett* 2000; **19**: 1147-1149

75.Li CX, Bell T. Potential of plasma nitriding of polymer for improved hardness and wear resistance. *J Mater Process Tech* 2005; **168**: 219-224

76.Kostov KG, Ueda M, Tan IH, Leite NF, Beloto AF et *al.* Structural effect of nitrogen plasma-based ion implantation on ultra-high molecular weight polyethylene. *Surf Coat Techno* 2004; **186**: 287-290

77.Hench LL, Best S. Ceramics, glasses and glass-ceramics. In: Ratner BD, Hoffman AS, Schoen FJ, Lemons JE. Editors. Biomaterials Science. Elsevier Academic Press; 2004; p 153-155

78.Hench LL. The history of Bioglass. *J Mater Sci Mater Med.* 2006; **17**: 967-978

79.Hill RG, Stamboulis A, Law RV, Clifford A, Towler MR, Crowler C. The influence of strontium substitution in fluorapatite glasses and glass-ceramics. *J Non-Cryst Solids.* 2004; **336**: 223-229

80.Rafferty A, Clifford A, Hill R, Wood D, Sammeva B, Dimitrova-Lukacs M. Influence of fluorine content in apatite-mullite glass-ceramics. *J Am Ceram Soc*. 2000; **83:** 2833-2838

81.Stamboulis A, Matsuya S, Hill R, Law RV, Udoh K, Nakagawa M, Matsuya Y. MAS-NMR spectroscopy studies in the setting reaction of glass ionomer cements. *J Dent*. 2006; **34**: 574-581

82.Stamboulis A, Law R, Hill R. Characterisation of commercial ionomer glasses using magic angle nuclear magnetic resonance (MAS-NMR). *Biomaterials*. 2004; **25**: 3907-3913

83.Stamboulis A, Hill R, Law R. Characterization of the structure of calcium alumina-silicate and calcium fluoro-alumino-silicate glasses by magic angle spinning nuclear magnetic resonance (MAS-NMR). *J Non-Cryst Solids*. 2004; **333**: 101-107

84.Matsuya S, Stamboulis A, Hill R, Law R. Structural characterization of ionomer glasses by multinuclear solid state MAS-NMR spectroscopy. *J Non-Cryst Solids*. 2007; **353**: 237-243

85.Hill R, Calver A, Stamboulis A, Bubb N. Real-time nucleation and crystallization studies of a fluorapatite glass-ceramics using small-ngle neutron scattering and neutron diffraction. *J Am Ceram Soc*. 2000; **3**: 763-768

86.Freeman CO, Brook IM, Johnson A, Hatton PV, Hill RG, Stanton KT. Crystallization modifies osteoconductivity in an apatite-mullite glass-ceramic. *J Mater Sci-Mater M*. 2003; **14**: 985-990

87.Qin M, Hou S, Wang L, Feng Xi, Wang R et al. Tow methods for glass surface modification and their application in protein immobilization. *Colloid Surface B*. 2007; **60** 243-249

88.Cech V, Prikryl R, Balkova R, Grycova A, Vanek J. Plasma surface treatment and modification of glass fibers. *Composites*. 2002; **33** 1367-1372

89.Hubbell J. Biomaterials in tissue engineering. *Nature*. 1995; **13**: 565-575

90.Jager M, Zilkens C, Zanger K, Krauspe R. Significance of Nano and Microtopography for cell-surface interactions in orthopaedic implants. *J Biomed Biotechnol.* 2007; 69036: pp19

91.Doyan BD, Hummert TW, Dean DD, Schawartz Z. Role of material surface in regulating bone and cartilage cell response. *Biomaterials*. 1996; **17**: 137-146

92.Kasemo B. Biological surface science. *Surf Sci*.1998; **3**: 451-459

93.Anselme K. Osteoblast adhesion on biomaterials. *Biomaterials*. 2000; **21**: 667-681

94.Carre A, Lacarriere V. How substrate properties control cell adhesion. A physical-chemical approach. *J Adhes Sci Techolog*. 2010; **24**: 815-830

95.Dewez JL, Detrait E, Berger V, Dupont-Gillain CC, Vincent LM et al. Adhesion of mammalian cells to polymer surfaces: from physical chemistry of surfaces to selective adhesion on defined patterns. *Biomaterials*. 1998; **19**: 1441-1445

96.Kasemo B, Lausmaa J. Matreial-tissue interfaces: the role of surface properties and processes. *Environ Health Persp*. 1994; **102**: 41-45

97.Anselme K, Ploux L,Ponch A. Cell/material interfaces: influence of surface chemistry and surface topography on cell adhesion. *J Adhes Sci Technol*. 2010; **24**: 831-852

98.Kowalczynska HM, Nowak-Wyrzykowska M. Modulation of adhesion, spreading and cytoskeleton organization of 3T3 fibroblasts by sulfonic groups present on polymer surfaces. *Cell Biol Int*. 2003; **27**: 101-114.

99.Zhu X, Chian KS, Chang-Park Mbe, Lee ST. Effect of argon-plasma treatment on proliferation of human-skin-derived fibroblast on chitosan membrane in vitro. *Wiley interScience*. 2005; 10.1002; 264-274

100.Pu FR, Williams PL, Markkula TK, Hunt JA. Effects of plasma treated PET AND PTFE on expresion of adhesion molecules by human endothelial cells in vitro. *Biomaterials*. 2002; **23**: 2411-2428

101.Griesser HJ, Chatekier RC, Gengenbach TR, Johnson G, Steele JG. Growth of human cells on plasma polymers: putative role of amine and amide groups. *J Biomater Sci Polymer Edn.* 1994; **5**: 531-554

102.Agrawa L CM, Ray RB. Biodegradable polymeric scaffolds for musculoskeletal tissue engineering. *John Wiley & Sons*. Inc. 2001; 141-150

103. Anderson AS, Backhed F, Euler A, Richter-Dahlfors, Sutherland D, Kasemo B. Nanoscale features influence epithelial cell morophology and cytokine production. *Biomaterials*. 2003; **24**: 3427-3436

104. Curtis A, Wilkinson C. Topographical control of cells. *Biomaterials*. 1997; **18**: 1573-1583

105. Folch A, Toner M. Microengineering of cellular interactions. *Annu Rev. Biomed. Eng*. 2000; **2**: 227-256

106. Condie R, Bose S, Bandyopadhyaya. Bone cell-material interaction on Si microchannels with bioinert coatings. *Acta Biomater*. 2007; **3**: 523-530

107. Price RL, Haberstroh KM, Webster TJ. Improved osteoblasts viability in presence of smaller nanometre dimensional carbon fibres. *Nanonechnology*. 2004; **15**: 892-900

108. Rosa AL, Beloti MM, Noort R. Osteoblastic differentiation of cultured rat bone marrow cells on hydroxyapatite with different surface topography. *Dent Mater*. 2003; **19**: 768-772

109. Andersson AS, Brink J, Lidberg U, Sutherland DS. Influence of systematically varied nanoscale topography on the morphology of epithelial cells. *Transactions on nanobiosciences*. 2003; **2**: 49-57

110. Badami AS, Kreke MR, Thompson MS, Riffle JS, Goldstein AS. Effect of fiber diameter on spreading, proliferation and differentiation of osteoblastic cells on electrospun poly (lactic) substrates. *Biomaterials*. 2006; **27**: 596-606.

111. Hervy M. Modulation of cell structure and function in response to substrate stiffness and external forces. *J Adhes Sci Technol*. 2010; **24**: 963-973

112. Engler AJ, Sen S, Sweeney HL, Discher DE. Matrix elasticity directs stem cell lineage specification. *Cell*. 2006; **126**: 677-689

113. Choquet D, Felsenfeld DP, Sheetz MP. Extracellular matrix rigidity causes strengthening on integrin-cytoskeleton linkages. *Cell*. 1997: **88**: 30-48

114.Geetha M, Singh AK, Asokamani R, Gogia AK. Ti based biomaterials, the ultimate choice for orthopaedic implants. *Prog Mater Sci*.2009; **54**: 397-425

115.Hallab N, Merritt K, Jacobs JJ. Metal sensitivity in patients with orthopaedic implants. *J Bone Joint Surg Am*. 2001; **83**: 428-426

116.He W, Gonsalves KE, Batina N, Poker DB, Alexander E et al. Micro/nanomachining of Polymer surface for promoting osteoblasts cell adhesion. *Biomed Microdevices*. 2003; **5**: 101-108

117.Comes ME, Reis RL, Cunha AM, Blitterswijk CA, Bruijn JD. Cytocompatibility and response of osteoblastic-like cells to starch-based polymers: effect of several additives and processing conditions. *Biomaterials*. 2001; **22**: 1911-1917

118.Yang XB, Roach HI, Clarke NMP, Quirk R, Shakesheff KM et al. Human osteoprogenitor growth and differentiation on synthetic biodegradable structures after surface modification. *Bone*. 2001; **29**: 523-531

119.Yang J, Shi G, Bei, J, Wang S, Cao Y et al. Fabrication and surface modification of macroporous poly(L-lactic acid) and poly (L-lactic-co-glycolic acid) (70/30) call scaffolds fir human skin fibroblast cell culture. *Wiley Periodical Inc*. 2002; 439-446

120.Chu CR, Monosov AZ, Amiel D. In situ assessment of cell viability within biodegradable polylactic acid polymer matrices. *Biomaterials*.1995; **16**: 1381-1384

121.Sarasam A, Madihally SV. Characterization of chitosan-polycaprolactone blends for tissue engineering applications. *Biomaterials.* 2005; **26**: 5500-5508

122.El-Amin SF, Lu HH, Khan Y, Burems J, Mitchell J et al. Extracellular matrix production by human osteoblasts cultured on biodegradable polymers applicable for tissue engineering. *Biomaterials*. 2003; **24**:1213-1221

123.Calandrelli L, Immirzi B, Orsello G, Volpe MG, Ragione FD et al. Biocompatibility studies on biodegradable polyester-based composites of human osteoblasts: A preliminary screening. *John Wiley & Sons*. 2001; 611-617

124.Mo XM, Xu CY, Kotaki M, Ramakrishna S. Electrospun P(LLA-PC) nanofiber: a biomimetic extracellular matrix for smooth muscle cell and endothelial cell proliferation. *Biomaterials*. 2004; **25**: 1883-1890

125.Ma L, Gao C, Mao Z, Zhou J, Shen J et al. Collagen/chitosan porous scaffolds with improved biostability for skin tissue engineering. *Biomaterials*. 2003; **24**: 4833-4841

126.Garric X, Garreau, Vert M, Moles JP. Behaviours of keratinocytes and fibroblasts on films of PLA-PEO-PLA triblock copolymers with various PLA segment lengths. *J Mater Sci Mater Med*. 2008; **19**: 1645-1651

127.Yoon JJ, Song SH, Lee DS, Park TG. Immobilization of cell adhesive RGD peptide onto the surface of highly porous biodegradable polymer scaffolds fabricated by a gas foaming/salt leaching method. *Biomaterials*. 2004; **25**: 5613-5620

128.Kooten TG, Spijker HT, Busscher HJ. Plasma-treared polystyrene surfaces: model surfaces for studying cell-biomaterial interactions. *Biomaterials*. 2004; **25**; 1735-1747

129.Kweon HY, Yoo MK, Park IK, Kim TH, Lee HC. A novel degradable polycaprolactone networks for tissue engineering. *Biomaterials*. 2003; **24**: 801-808

130.Ducheyne P, Qui Q. Bioactive ceramis: the effect of surface reactivity on bone formation and bone cell function. *Biomaterials*.1999; **20**: 2287-2303

131.El-Ghannam A, Ducheyne P, Shapiro IM. Porous bioactive glass and hydroxyapatite ceramic effect bone cell function in vitro along different lines. *J Biomed Mater Res.*1997; **36**: 167-180

132.Oliva A, Salerno A, Locardi B, Riccio V, Ragione FD, Iardino P. Behaviour of human osteoblasts cultured on bioactive glass coatings. *Biomaterials*. 1998; **19**: 1019-1025

133.Price N, Bendall SP, Fronoza C, Jinnah RH, Hungerford DS. Human osteoblasts-like cells (MG63) proliferate on a bioactive glass surface. *John Wiley & Sons*. 1997; 395-400

134.Garcia AJ, Ducheyne P, Boettiger D. Effetc of surface reaction stage on fibronectin-mediated adhesion of ostoblast-like cells to bioactive glass. *John Wiley & Sons.* 1998; 48-56

135.Matsuda T, Davies JE. The in vitro response of osteoblasts to bioactive glass. Biomaterials. 1987; 8; 275-284

136.Webster TJ, Ergun C, Doremus RH, Siegel R, Bizios R. Specific proteins meiate enhanced osteoblasts adhesion on nanophase ceramics. *John Wiley & Sons*.2000;476-483

137.Pecheva E, Pramatarova L, Altankov G. Fibroblast interaction with different material surface. *Eur Cells Mater*.2004; **7**: 76

138.Geurtsen W, Spahl W, Leyhausen G. Residual monomer/additive release and variability in cytotoxicity of light-curing glass-ionomer cements and compomers. *J Dent Res*. 1998; **77**: 2012-2019

139.Vance RJ, Miller DC, Thapa A, Haberstroh KM, Webster TJ. Decreased fibroblast cell density on chemically degraded poly-lactic-co-glycolic acid, polyurethane and polycaprolactone. *Biomaterials*. 2004;**25**: 2095-2103

140.Silva SS, Luna SM, Comes ME, Benesch J, Pashkuleva I et al. Plasma surface modification of chitosan membranes: characterization and preliminary cell response studies. *Macromol Biosci*. 2008; **8**: 568-576

141.Pharr GM, Oliver WC. Measurement of thin film mechanical properties using Nanoindentation. *MRS Bulletin*. 1992; **17**: 28-33

142.Oliver WC, Pharr GM. Measurement of hardness and elastic modulus by instrumented indentation: Advances in understanding and refinements to methodology. *J Mater Res*. 2004; **19**: 3-20

143. Li X, Bhushan B. A review on Nanoindentation continuous stiffness measurements technique and its applications. *Mater Charact*. 2002; **48**: 11-36

144.Kim SW, Kim GH. Thickness-profile measurement of transparent thin-film layers by white-light scanning Interferometry. Applied Opt. 1999; **38**: 5968-5973

145.Cao G, Wang Y. *Nanostructure and nanomaterials.* World scientific publishing, Co Pte Ltd. 2011; p 435-436

146.Peter J. Larkin. *IR and Raman spectroscopy: principles and spectra interpretation.* Elsevier Inc. 2011; p 7-27, 73-80

147.Wagner JM. *X-Ray photoelectron spectroscopy: chemical engineering methods and technology*. PublisherNova Science Pub Inc. 2010

148.Bowen J, Cheneler D, Walliman D, Arkless SG, Zhang Z et al. On the calibration of rectangular atomic force microscope cantilevers modified by particle attachment and lamination. *Meas Sci Technol*. 2010; **21**: 1-9

149.Stamboulis A, Hill RG, Law RV. Characterization of the structure of calcium alumino-silicate and calcium fluoro-alumino-silicate glasses by magic angle spinning nuclear magnetic resonance (MAS-NMR). *J Non-Cryst Solids*. 2003; **333**: 101-107

150.Hill RG, Stamboulis A, Law RV. Characterisation of fluorine containing glasses by ^{19}F, ^{27}Al, ^{29}Si and ^{31}P MAS-NMR spectroscopy. *J Dent. 2006*; **34**: 525-532

151.Conrad JR, Radtke JL, Dodd RA, Worzala FJ, Tran NC. Plasma source ion-implantation techniques for surface modification of materials. *J Appl Phys*. 1987; **62**: 4591-4596

152.Karakan M, Alsaran A, Celik A. Effects of various gas mixtures on plasma nitriding behaviour of AISI 5140 steel. Mater Charact. 2003

153.Schrimpf C, Frischat. Some properties of nitrogen-containing Na_2O-CaO-SiO_2 glasses. *J Non-Cryst Solids.* 1982; **52**: 479-485

154.Grande T, Holloway JR, McMillan PF, Angell CA. Nitride glasses obtained by high-pressure synthesis. Nature. 1994; 369: 43-45

155. Wang F. Cation substitution in ionomer glasses: effect on glas structure and ctystallisation. PhD thesis. 2009: pp 70-89

156.Cvelbar U, Pejovnik S, Mozetie M, Zalar A. Increased surface roughness by oxygen plasma treatment of graphite/polymer composite. *App Surf Sci.* 2003; **210**: 255-261

157. McMillan P. Structural studies of silicate glass and melts-applications and limitations of Raman spectroscopy. *Am Mineral*. 1984; **69**: 622-644

158. Bandet J, Despax B, Caumont M. Nitrogen bonding environments and local order in hydrogenated amorphous silicon nitride films studied by Raman spectroscopy. *J Appl Phys*.1999; **85**: 7899-7904

159. Hench LL, Splinter RJ, Allen WC, Greenlee TK. Bonding mechanisms at the interface of ceramic prosthetic materials. *J Biomed Mater Res*. 1972; **2**: 117-141

160. Kurtz SM. *The UHMWPE Handbook.* Academic press Elsevier; 2004; p 13-32

161. Reggiani M, Tinti A, Taddei P, Visentin M, Stea S, De Clerico M, Fagnano C. Phase transformation in explanted highly crystalline UHMWPE acetabular cups in vivo wear. *J Mol Struct*. 2006; **785**: 98-105

162. Reis M, Pruitt L. Effect of cross-linking on the microstructure and mechanical properties of ultra-high molecular weight polyethylene. *Clin Orthop Relat Res*. 2005; **440**: 149-156

163. Billmeyer FW. Textbook of Polymer Science. 3rd Edn: *New York: Wiley*.1984; pp 343-7

164. Goldman M, Pruitt L. Comparison of the effects of gamma radiation and low temperature hydrogen peroxide gas plasma sterilization on the molecular structure, fatige resistance, and wear behaviour of UHMWPE. CCC 0021-9304/98/030378-07. 1998: 379-384

165. Moon SI, Jang J. The effect of the oxygen-plasma treatment of UHMPWE fiber on the transverse properties of UHMWPE-fiber/vinylester composites. *Compos Sci Technol*. 1999: **59**: 487-493

166. Arefi-Khonsari F, Tatoulian M, Kurdi J, -Ben-Rejeb S, Amouroux J. Study of the surface properties and stability of polymer films treated by NH_3 plasma and its mixtures. *J Photopolym Sci Tec*. 1998; **11**: 277-292

167. Dong H, Bell T. State-of –the-art overview: ion beam surface modification of polymers towards improving tribological properties. *Surf Coat Tech*. 1999; **111**: 29-40

168. Toth A, Mohai M, Ujvari T, Bertoti I. Hydrogen plasma immersion ion implantation of ultra-high molecular weight polyethylene. *Surf Interface Anal*. 2006; **38**: 898-902

169. Sanchis MR, Blanes V, Blanes M, Garcia D, Balart R. Surface modification of low density polyethylene (LDPE) film by low pressure O_2 plasma treatment. *Eur Polym J*. 2006; **42**: 1558-1568

170. Sanchis MR, Calvo O, Fenollar O, Garcia D, Balart R. Characterization of the surface changes and the aging effects of low-pressure nitrogen plasma treatment in a polyurethane film. *Polym Test.* 2008; **27**: 75-83

171. Zhao CX, Zhang WD. Preparation of waterborne polyurethane nanocomposites: Polymerization from functionalized hydroxyapatite. *Eur Polym J*. 2008; **44**: 1988-1995

172. Yu YK, Mckellop HA, Salovey R. Hydroperoxide Formation in irradiated Polyethylene. *J Polym Sci Pol Chem*. 1999;37:3309-3316

173. G. Beamson, D. Briggs, High Resolution XPS of Organic Polymers: The Scienta ESCA300 Database, 1992

174. Marcondes AR, Ueda M, Kostov KG, Beloto AF, Leite NF. Improvements of Ultra-High-Molecular Weight Polyethylene mechanical properties by nitrogen plasma immersion ion implantation. *Braz J Phys*. 2004; 34:1667-1672

175. Gancarz I, Bryjak J, Pozniak G, Tylus W. Plasma modified polymers as a support for enzyme immobilization. *Eur Polym J*.2003; 39: 2217-2224

176. Arefi-Khonsari F, Tatoulian M, Kurdi J, Ben-Rejeb S, Amouroux J.N. Study of the surface properties and stability of polymer films treated by NH_3 plasma and its mixtures. *J Photopolym Sci Tec*.1998; **11**: 277-292

177. Vesel A, and Mozetic M. Modification of PET surface by nitrogen plasma treatment. *J. Phys.: Conf Ser.* 100 012027 2008

178.Arpagaous C, Rohr R. Short-time plasma surface modification of HDPE powder in a Plasma Dawner Reactor-process, wettability improvement and ageing effects. *Appl Surf Sci.* 2005; **252**: 1581-1595

179.Wilson DJ, Williams RL, Pond RC. Plasma modification of PTFE surfaces. *Surf Interface Anal*. 2001; **31**: 385-396

180. Lommatzsch U, Pasedag D, Baalmann A, Ellighorst G, Wanger HE. Atmospheric pressure plasma jet treatment of polyethylene surfaces for adhesion improvement. *Plasma Process. Polym.* .2007; **4***:* 1041-1045

181.Kurtz SM. *The UHMWPE Handbook.* Academic press Elsevier; 2004; p 245-61

182. Junkar I, Vesel A, Cvelbar U, Mozetic M, Strnad Simona. Influence of oxygen and nitrogen plasma treatment on polyethylene terephthalate (PET) polymers. *Vacuum* 2010; 84: 83-85

183.Toth A, Bertoti I, Szilagyi E, Dong H, Bell T. Surface characterization of ultra high molecular weight polyethylene after nitrogen ion implantation. *Surf Interface Anal* 2000; **30**: 434-438

184.Ujvari T, Toth A, Mohai M, Szepvolgyi J, Bertoti I. Composition and chemical structure characteristics of CN_x layers prepared by different plasma assisted techniques. *Solid State Ionics*.2001; **141-142**; 63-69

185.Bertoti I. Characterization of nitride coatings by XPS. *Surf Coat Tech*. 2002; **151-152:** 194-203

186.Wagner AJ, Fairbrither DH, Reniers F. A comparison of PE surfaces modified by plasma generated neutral nitrogen species and nitrogen ions. *Plasma Polym.* 2003; **8**:119-134

187.Ma Z, Mao Z, Gao C. Surface modification and property analysis of biomedical polymers used for tissue engineering. *Colloid Surface B*. 2007; **60**: 137-157

188.Griesser HJ, Chatelier RC, Gengenbach TR, Johnson G, Steele JG. Growth of human cells on plasma polymers: Putative role of amine and amide groups. *J Biomater Sci Polymer.* 1994; **5**: 531-554

189.Parhi P, Gola A, Vogler E. Role of proteins and water in the initial attachment of mammalian cells to biomedical surfaces: A review. *J Adhes Sci Technol*. 2010; **24:** 853-888

190.Kooten TG, Spijker HT, Busscher HJ. Plasma-treated polystyrene surfaces: model surfaces for studying cell-biomaterial interactions. *Biomaterials*. 2004; **25:** 1735-1747

191.Ramsey WS, Hertl W, Nowlan ED, Binkowski NJ. Surface treatments and cell attachment. *In Vitro*. 2983; **20**: 802-808

192.Schroder K, Finke B, Jesswein H, Luthen F, Diener A. *J Adhes Sci Technol*. 2010; **24**: 905-923

193.Tamada Y, Ikada Y. Cell adhesion to plasma-treated polymer surfaces. *Polymer*. 1993; **34**: 2208-2212

194.Ramires PA, Mirenghi L, Romano AR, Palumbo F, Nicolardi G. Plasma-treated PET surfaces improve the biocompatibility of human endothelial cells. 2000; *John Wiley & Sons, Inc*. 535-539

195.Tseng DY, Edelman ER. Effects of amide and amine plasma-treated ePTFE Vascular Grafts on Endothelial Cell Lining in an Artificial Circulatory System. CCC 0021-9304/98/020188-11. 1998; 189-198

196. Ertel SI, Chilkoti A, Horbett TA, Ratner BD. Endothelial cell growth on oxygen-containing films deposited by radio-frequency plasmas: the role of surface carbonyl groups. *J Biomater Sci Polymer*. 1991; **3**: 163-183

197.Ho PYJ, Nosworthy NJ, Bilek MMM, Gan BK, McKenzie DR. *Plasma Process Polym*. 2007;**4**: 583-590

198.Kaklamani G, Mehrban N, Chen J, Bowen J, Dong H, Grover L et al. Effect of plasma surface modification on the biocompatibility of UHMWPE. *Biomed Mater* 2010; **5**: 054101

199.Toth A, Mohai M, Ujvari T, Bertoti I. Hydrogen plasma immersion ion implantation of ultra-high molecular weight polyethylene. *Surf Interface Anal* 2006; **38**: 898-902

200. Hervy M. Modulation of cell structure and function in response to substrate stiffness and external forces. *J Adhesion Sci Technol* 2010; **24**: 963-973

201. Curtis A, Wilkinson C. Topographical control of cells. *Biomaterials* 1997; **18**: 1573-1583

202. Gerenser LJ. XPS studies of in situ plasma-modified polymer surfaces. *J Adhesion Sci Technol*. 1993; **7**: 1019-1040

203. O'Kell S, Henshaw T, Farrow G, Aindow M, Jones C. Effects of low-power plasma treatment on polyethylene surfaces. *Surface & Interface analysis*. 1995; **23**: 319-327

204. Schoen FJ, Mitchell NR. Tissues, the extracellular matrix, and cell-biomaterial interactions. In: Ratner BD, Hoffman AS, Schoen FJ, Lemons JE, editors. Biomaterials Science. London: Elsevier Inc; 2004, p 260-281.

205. Steele JG, Johnson G, McFarland C, Dalton BA, Gengenbach TA, Chatelier RC et al. Roles of serum vitronectin and fibronectin in initial attachment of human vein endothelial cells and dermal fibroblasts on oxygen- and nitrogen-containing surfaces made by radiofrequency plasmas. *J Biomater Sci Polym Edn* 1994; **5**: 511–532.

206. Yoon JH, Halper J. Tendon proteoglycans: biochemistry and function. *J Musculoskeletal Neuronal Interact* 2005; **5**: 22-34.

APPENDIX

CONFERENCES

1. IC4N 2008: Halkidiki, Greece, Poster Presentation:
Active Screen Plasma Nitriding Of Ultra High Molecular Weight Polyethylene
G. Kaklamani, H. Dong and A. Stamboulis
Best poster award

2. IC4N 2009: Rhodes, Greece, Oral presentation:
Active Screen Plasma Nitriding of an Ionomer Glass
G. Kaklamani, H. Dong and A. Stamboulis

3. THERMEC 2009: Berlin, Germany, Poster Presentation:
Effect of plasma surface modification on the biocompatibility of an ionomer glass
G. Kaklamani, L. Grover, H. Dong and A. Stamboulis
Abstract student award

4. ISSIB-II 2010: Hong Kong, China, Oral presentation:
Effect of Active Screen Plasma Nitriding on the biocompatibility of UHMWPE Surfaces
G. Kaklamani, N. Mehrban, J. Bowen, L.Grover, H. Dong and A. Stamboulis

5. ELEMBIO 2010: Ioannina, Greece, Oral presentation:
Plasma Surface Modification of Biomaterials
G.Kaklamani and A.Stamboulis

6. UKSB 2010: Glasgow, Scotland, Poster Presentation:
Effect of plasma surface modification on the biocompatibility of UHMWPE
G. Kaklamani, N.Mehrban**,** J. Chen, J.Bowen, H. Dong, L.Grover and A. Stamboulis

7. ESB 2010: Finland, Tampere, Poster Presentation:
Effect of Plasma Surface Modification on the Biocompatibility of an Ionomer Glass
G. Kaklamani, N. Mehrban, J.Bowen, H. Dong, L. Grover And A. Stamboulis

8. 4th International Conference on Tissue Engineering 2011: Chania, Greece, Oral Presentation:
Effect of Active Screen Plasma Nitriding Surface Modification on the Cellular Compatibility of an Ionomer Glass and a Polymeric Modified Surface
G. Kaklamani, J. Bowen, N. Mehrban, L. Grover, H. Dong and A. Stamboulis
Best oral presentation award

9. Thermec 2011: Quebec, Canada: Oral Presentation
Improvement of Surface Properties and Cellular Compatibility of Biomaterials by Plasma Treatment
G. Kaklamani, N. Mehrban, J. Bowen, L.Grover, H. Dong and A. Stamboulis
Abstract student award

Publications in Peer Reviewed Journals

Kaklamani G, Mehrban N, Chen J, Bowen J, Dong H, Grover L, Stamboulis A.
Effect of Plasma Surface Modification on the Biocompatibility of UHMWPE
Biomed. Mater 2010; **5 054101 (10pp)**].
[Published]

Kaklamani G, Bowen J, Grover L, Mehrban N, Dong H and Stamboulis A.
Active Screen Plasma Nitriding Enhances Cell Attachment to Polymeric Surfaces.
[Under preparation]

Kaklamani G, Bowen J, Grover L, Mehrban N, Dong H and Stamboulis A.
Effect of Plasma Surface Modification on the Biocompatibility of an Ionomer Glass
[Under preparation]